# Plasma Instability

- MHD instabilities
  - Basic MHD instabilities and stability analysis
  - Tokamak instability theory
  - Beta limit
- Experimental Tokamak instabilities
  - Basic MHD instabilities
  - Disruptions
  - Other instabilities
- Micro-instabilities : finite Larmor radius and kinetic dissipation effects, where wavelength comparable to ion gyro radius
  - Drift wave instabilities
  - Trapped particle instabilities
  - Micro-tearing modes

# MHD Instability

- Basic destabilizing forces
  - Current gradients
  - Pressure gradients combined with adverse magnetic field curvature
- Resulting instabilities
  - Ideal modes : instabilities even with perfectly conducting plasmas
  - Resistive modes : dependent on the finite resistivity of the plasma

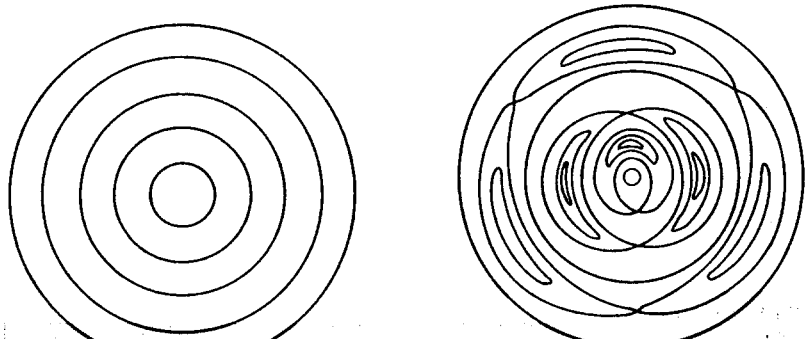

**Magnetic Islands (Tearing Modes)**

# Stabilizing Effects

- Magnetic field line bending / compression
  - stronger stabilizing effect for high-m modes
  - high-m modes are localized around a resonance surface of rational surface on which $m=nq$
  - limited $q$ operation excludes most global low-m modes
- Good magnetic field curvature
  - the center of curvature being in the opposite direction to the pressure gradient

**Fig. 6.1.1** Magnetic field line bending and magnetic field compression are stabilizing for mhd modes. The magnetic field curvature is stabilizing if the negative pressure gradient is in the direction of the centre of curvature.

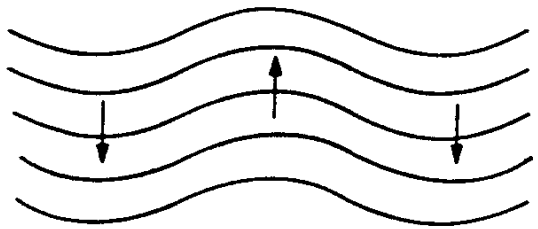

Bending of magnetic field lines

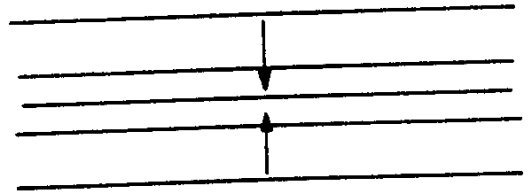

Compression of magnetic field

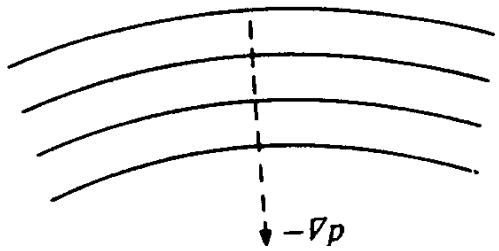


**Fig. 6.1.2** Showing how exclusion of resonant surfaces from the tokamak plasma reduces the number of potential modes of instability. These modes are restricted to $q_0 < m/n \lesssim q_a$ and are indicated by asterisks. At low $\beta$, high $m$-modes are stabilized by line bending and by good average field line curvature.

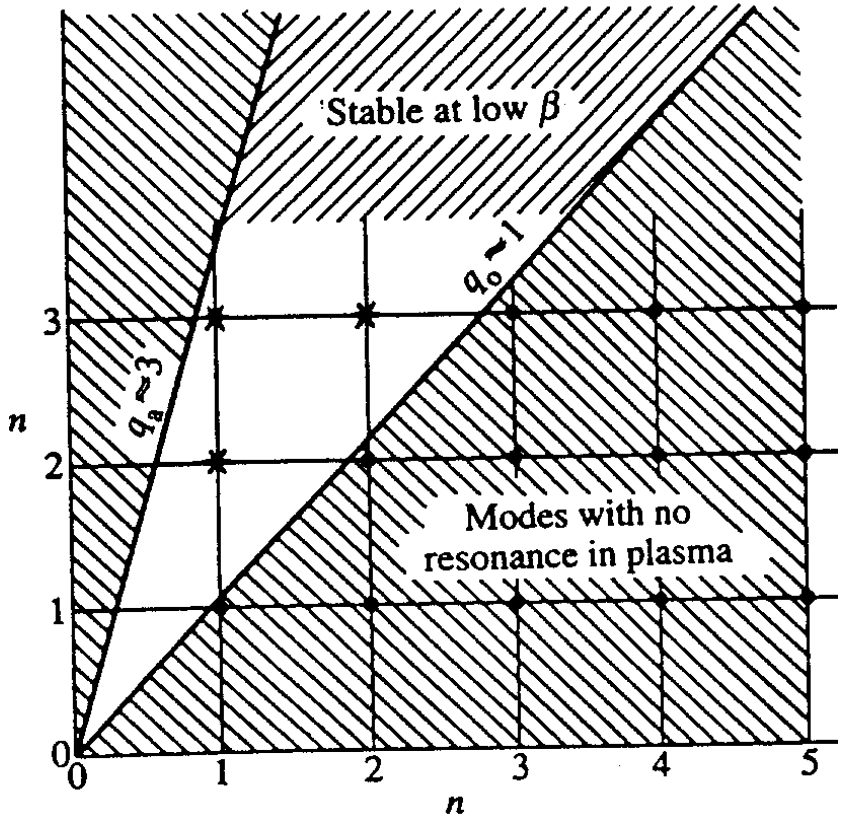

# Theoretical Stability Analyses

- Normal mode analysis
  - calculation of the eigenfunctions and corresponding eigenvalues for the frequency $\omega$ --> sign of $Im(\omega)$
- Marginal stability equation
  - solution of the marginal stability equation : $Im(\omega)=0$
- Energy principle
  - potential energy change resulting from a plasma displacement is examined

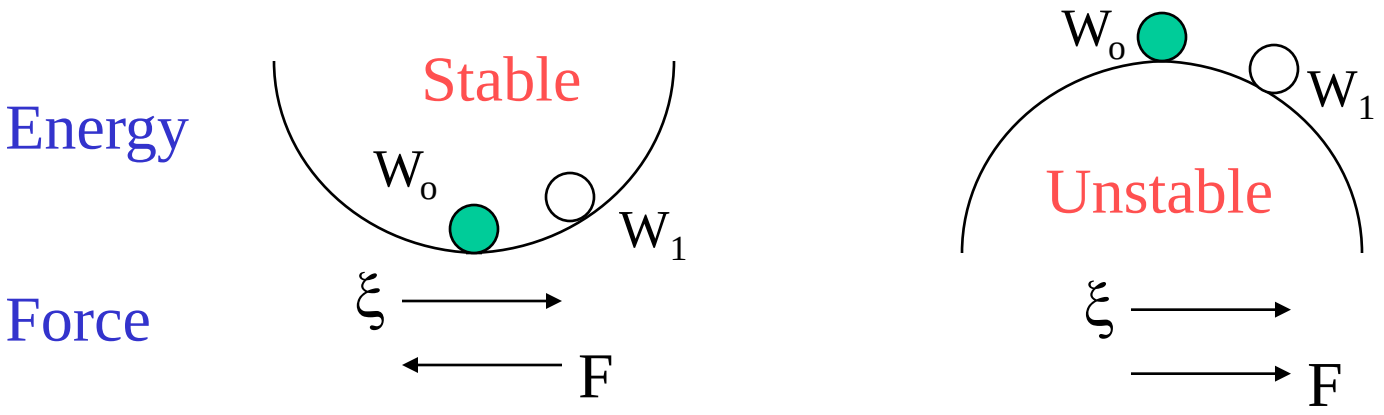

# Single Fluid Equations : MHD

**Mass density** $\rho_m = \sum_s m_s n_s \approx n m_i$ **Charge density** $\rho = \sum_s e_s n_s \approx 0$

Quasi neutrality

**Current density** $\vec{j} = \sum_s e_s n_s \vec{u}_s \approx ne(\vec{u}_i - \vec{u}_e)$

**Center of mass velocity** $\vec{v} = \frac{\sum_s n_s m_s \vec{u}_s}{\sum_s n_s m_s} \approx \frac{m_i \vec{u}_i + m_e \vec{u}_e}{m_i + m_e} \approx \vec{u}_i + \frac{m_e}{m_i}\vec{u}_e$

**Equation of mass/charge conservation** $\frac{\partial \rho_m}{\partial t} + \nabla \cdot (\rho_m \vec{v}) = 0$ $\frac{\partial \rho}{\partial t} + \nabla \cdot \vec{j} = 0$

**Equation of motion** $\rho_m (\frac{\partial \vec{v}}{\partial t} + \vec{v} \cdot \nabla \vec{v}) = -\nabla p + \vec{j} \times \vec{B} + \rho \vec{E}$

**Ideal MHD**

**Ohm's law** $\vec{E} + \vec{v} \times \vec{B} = \eta \vec{j} + \frac{1}{en}(\vec{j} \times \vec{B} - \nabla p_e)$ → $\vec{E} + \vec{v} \times \vec{B} = 0$

**Conservation of entropy** $\frac{d}{dt}(p \rho_m^{-\gamma}) = 0$ or $\frac{dp}{dt} + \gamma p \nabla \cdot \vec{v} = 0$

**Maxwell's equations** $\nabla \times \vec{E} = \nabla \times (\vec{v} \times \vec{B}) = -\frac{\partial \vec{B}}{\partial t}$ $\nabla \times \vec{B} = \mu_o \vec{j}$

# Linear Stability Theory : perturbation theory

Linearize ideal MHD equations about a static equilibrium

$$p = p_0 + p_1 \quad \rho_m = \rho_0 + \rho_1 \qquad \vec{v} = \vec{v}_1 \qquad \vec{B} = \vec{B}_0 + \vec{B}_1$$

$$\frac{\partial \rho_1}{\partial t} + \nabla \cdot (\rho_0 \vec{v}_1) = 0 \qquad \rho_0 \frac{\partial \vec{v}_1}{\partial t} = -\nabla p_1 + (\nabla \times \vec{B}_1) \times \vec{B}_0 + (\nabla \times \vec{B}_0) \times \vec{B}_1$$

$$\frac{\partial p_1}{\partial t} + \vec{v}_1 \cdot \nabla p_0 + \gamma p_0 \nabla \cdot \vec{v}_1 = 0 \qquad \nabla \times (\vec{v}_1 \times \vec{B}_0) = -\frac{\partial \vec{B}_1}{\partial t}$$

Introduce Lagrangian displacement vector $\xi$, $\quad \vec{v}_1 = \frac{\partial \vec{\xi}}{\partial t}$

$$\rho_1 = -\nabla \cdot (\rho_0 \vec{\xi}) \qquad \vec{B}_1 = -\nabla \times (\vec{\xi} \times \vec{B}_0)$$

$$p_1 = -\vec{\xi} \cdot \nabla p_0 - \gamma p_0 \nabla \cdot \vec{\xi}$$

$$\vec{F}(\vec{\xi}) = \rho_0 \frac{\partial^2 \vec{\xi}}{\partial t^2} = -\nabla p_1 + (\nabla \times \vec{B}_1) \times \vec{B}_0 + (\nabla \times \vec{B}_0) \times \vec{B}_1$$

# Normal Mode Analysis

- Eigenmode analysis

  Perturbations in normal modes $\vec{\xi}(\vec{r},t) = \hat{\xi}(\vec{r})e^{-i\omega t}$

  --> an eigenvalue problem $\vec{F}(\hat{\xi}) = -\rho_0\omega^2\hat{\xi}$

  eigenvvector

  eigenvalue

  stable $\omega^2 > 0$ unstable $\omega^2 < 0$

- Marginal stability equation $\vec{F}(\hat{\xi}) = 0$

$$\beta \equiv 2\mu_o p / B^2$$

$$q_1 \sim 1/I_p$$

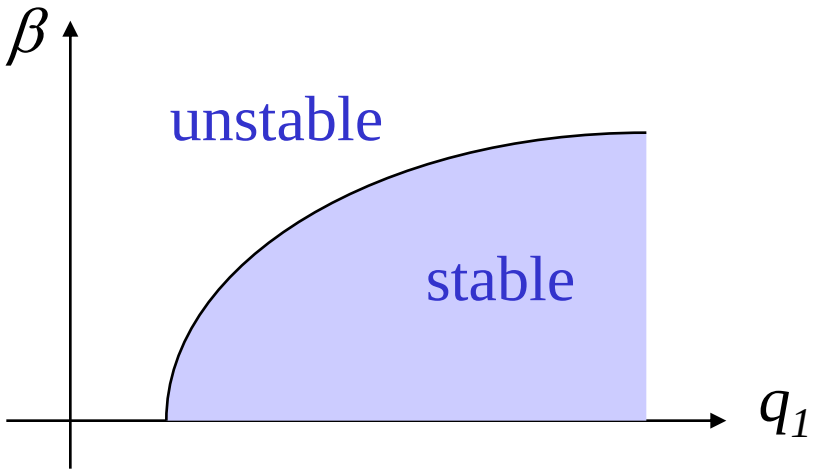


- Full dynamics

$$\vec{F}(\vec{\xi}) = \rho_0 \frac{\partial^2 \vec{\xi}}{\partial t^2} \longleftarrow L = K - \delta W = \int \frac{1}{2}\rho_0\omega^2\xi^2 d\tau + \int \frac{1}{2}\vec{\xi}\cdot\vec{F}d\tau$$

# Energy Principle

Potential energy change due to an arbitrary displacement $\xi$

$$\delta W = -\int \frac{1}{2}\vec{\xi}\cdot\vec{F}d\tau \qquad \text{unstable} \quad \delta W < 0$$

Linearized force $\vec{F}(\vec{\xi}) = -\nabla p_1 + (\nabla\times\vec{B}_1)\times\vec{B}_0 + (\nabla\times\vec{B}_0)\times\vec{B}_1$

with $\vec{B}_1 = -\nabla\times(\vec{\xi}\times\vec{B}_0) \qquad p_1 = -\vec{\xi}\cdot\nabla p_0 - \gamma p_0\nabla\cdot\vec{\xi}$

$$\delta W = -\frac{1}{2}\int\left(\begin{array}{l}\vec{\xi}\cdot\nabla(\vec{\xi}\cdot\nabla p_0 + \gamma p_0\nabla\cdot\vec{\xi}) \\ +\frac{1}{\mu_o}\vec{\xi}\cdot\left[(\nabla\times\nabla\times(\vec{\xi}\times\vec{B}_0))\times\vec{B}_0 + (\nabla\times\vec{B}_0)\times\nabla\times(\vec{\xi}\times\vec{B}_0)\right]\end{array}\right)d\tau$$

$$\delta W = \frac{1}{2}\int\left((\vec{\xi}\cdot\nabla p_0)\nabla\cdot\vec{\xi} + \gamma p_0(\nabla\cdot\vec{\xi})^2 + \frac{1}{\mu_o}B_1^2 - \frac{1}{\mu_o}\nabla\times\vec{B}_0\cdot(\vec{B}_1\times\vec{\xi})\right)d\tau$$

$$+\frac{1}{2}\int(p_1 + \frac{1}{\mu_o}\vec{B}_0\cdot\vec{B}_1)\vec{\xi}\cdot d\vec{S}$$

**for conducting boundary** $\vec{\xi}\cdot\hat{n} = 0$

$$\delta W = \frac{1}{2}\int_{plasma}\left((\vec{\xi}\cdot\nabla p_0)\nabla\cdot\vec{\xi} + \gamma p_0(\nabla\cdot\vec{\xi})^2 + \frac{B_1^2}{\mu_o} - \vec{j}_o\cdot(\vec{B}_1\times\vec{\xi})\right)d\tau + \int_{vacuum}\frac{B_v^2}{\mu_o}d\tau$$

# Tokamak Instabilities

- Ideal modes occur even if the plasma is perfectly conducting
- For ideal MHD stable plasmas, resistive modes can be unstable
- Ideal and resistive modes are paired usually
- Tokamak MHD instabilities
  - Kink instabilty : driven at low $\beta$ by the current gradient, at high $\beta$ by pressure gradient as well
  - Tearing mode : the resistive form of the kink instability
  - Internal kink : m=1, plasma core where q<1, driven by the pressure gradient at that region
  - Resistive m=1 instability : similar to internal kink affecting the plasma core, but with a different energy source
  - Ballooning modes : localized, driven by the pressure gradient
  - Vertical instability : arising from plasma elongation

# Large Aspect-Ratio Tokamak

- Analytic calculation for MHD stability using large aspect-ratio approximation instead of numerical one --> still contains some toroidal effects
- Tokamak ordering
  - large aspect-ratio limit with $q \sim 1 : B_\theta / B_\phi \sim a / R \equiv \varepsilon$
  - low $\beta$ approximation $p \sim B_\theta^2 / 2\mu_o$ $\beta_p \sim 1$

$$q \sim 1 \qquad B_\theta \sim \varepsilon B_\varphi \qquad \beta \sim \varepsilon^2$$

$$\frac{dp}{dr} + \frac{d}{dr}\frac{B_\phi^2}{2\mu_o} + \frac{B_\theta}{\mu_o r}\frac{d}{dr} r B_\theta = 0 \qquad \frac{dB_\phi}{dr} \sim \frac{\mu_o}{B_\phi}\frac{dp}{dr} \sim \beta \frac{B_\phi}{a} \sim \varepsilon^2 \frac{B_\phi}{a}$$

$$j_\theta = (j_\phi B_\theta - \frac{dp}{dr}) / B_{\phi o} \sim j_\phi B_\theta / B_{\phi o} \sim \varepsilon j_\phi \qquad j_\theta \sim \varepsilon j_{\varphi o}$$

$$\longrightarrow \qquad \delta W(\varepsilon)$$

# Sausage and Kink Modes

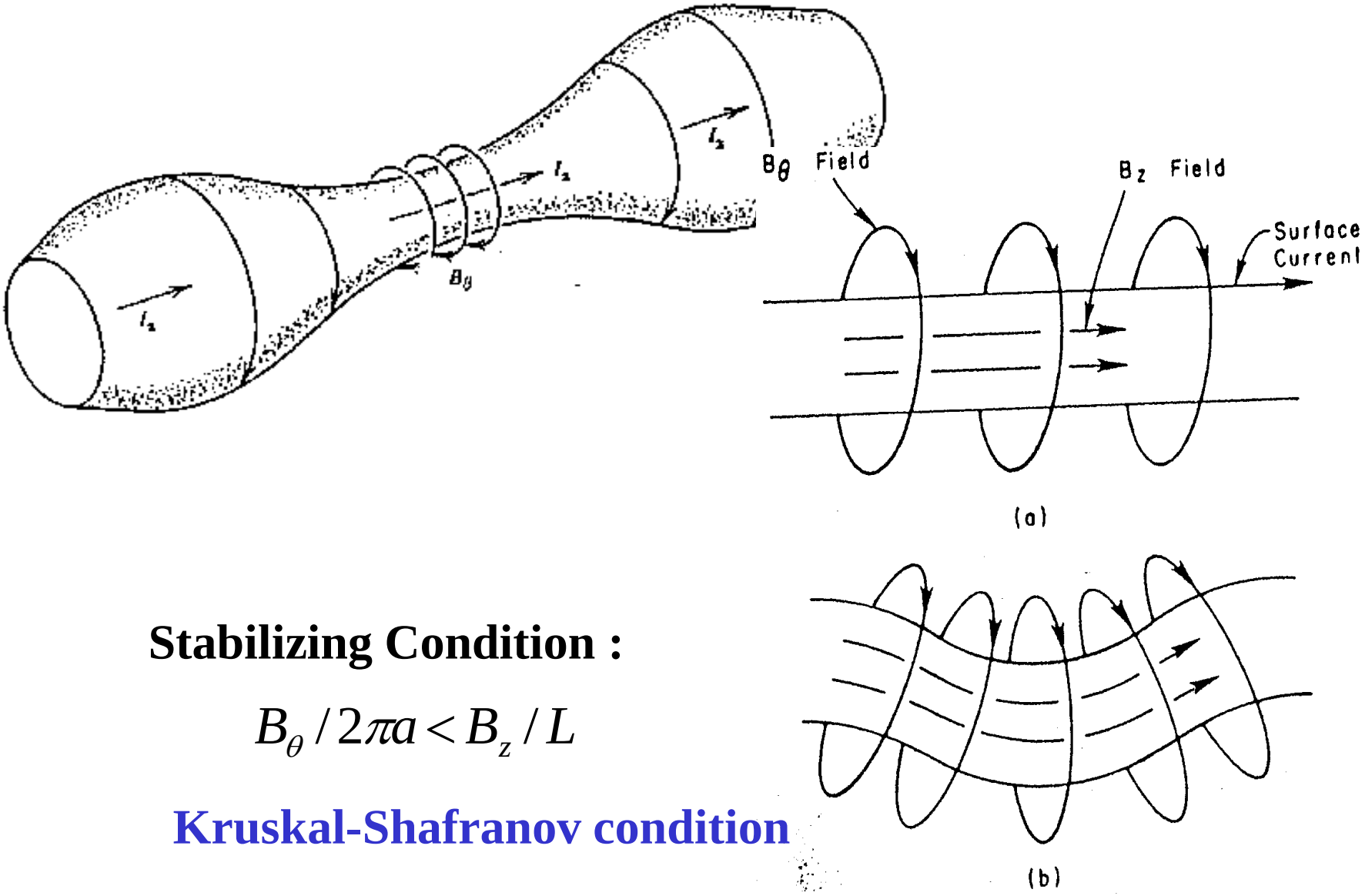


**Stabilizing Condition :**

$$B_\theta / 2\pi a < B_z / L$$

**Kruskal-Shafranov condition**

# Kink Instabilities

$$\delta W = \frac{1}{2}\int_{plasma}\left((\vec{\xi}\cdot\nabla p_0)\nabla\cdot\vec{\xi} + \gamma p_0(\nabla\cdot\vec{\xi})^2 + \frac{B_1^2}{\mu_o} - \vec{j}_o\cdot(\vec{B}_1\times\vec{\xi})\right)d\tau + \int_{vacuum}\frac{B_v^2}{\mu_o}d\tau$$

For a circular, large aspect-ratio tokamak with low beta,

$$\partial/\partial r \sim (1/r)\partial/\partial\theta >> (1/R)\partial/\partial\phi \quad \nabla\cdot\vec{\xi} = 0 \quad \xi_r \sim \xi_\theta >> \xi_\phi \quad B_{r1} \sim B_{\theta 1} >> B_{\phi 1}$$

$$\delta W = \delta W_p + \delta W_v = \pi R\int_0^a\left(\frac{B_1^2}{\mu_o} - j_{zo}(B_{r1}\xi_\theta - B_{\theta 1}\xi_r)\right)d\theta r dr + \pi R\int_a^b\frac{B_v^2}{\mu_o}d\theta r dr$$

Perturbations in a Fourier analyzed in the form of $e^{i(m\theta - n\phi)}$

$$\nabla\cdot\vec{\xi} = 0 \rightarrow \xi_\theta = -\frac{i}{m}\frac{d}{dr}(r\xi_r)$$

$$\vec{B}_1 = -\nabla\times(\vec{\xi}\times\vec{B}_0) \longrightarrow \begin{cases} B_{r1} = -\dfrac{imB_\phi}{R}\left(\dfrac{n}{m} - \dfrac{1}{q}\right)\xi_r \\ B_{\theta 1} = \dfrac{B_\phi}{R}\dfrac{d}{dr}\left[\left(\dfrac{n}{m} - \dfrac{1}{q}\right)r\xi_r\right] \end{cases}$$

$$\delta W_p = \frac{\pi^2 B_\phi^2}{\mu_o R}\int_0^a \left\{ \begin{array}{l} m^2(\frac{n}{m}-\frac{1}{q})^2\xi_r^2 + \left(\frac{d}{dr}\left[(\frac{n}{m}-\frac{1}{q})r\xi_r\right]\right)^2 \\ +\frac{1}{r}\frac{d}{dr}(rB_\theta)\frac{R}{B_\phi}\left[(\frac{n}{m}-\frac{1}{q})\xi_r\frac{d}{dr}(r\xi_r)+\frac{d}{dr}\left[(\frac{n}{m}-\frac{1}{q})r\xi_r\right]\xi_r\right] \end{array} \right\} rdr$$

$$\delta W_p = \frac{\pi^2 B_\phi^2}{\mu_o R}\int_0^a \left\{(r\frac{d\xi}{dr})^2 + (m^2-1)\xi^2\right\}(\frac{n}{m}-\frac{1}{q})^2 rdr$$

$$+\left[\frac{2}{q_a}(\frac{n}{m}-\frac{1}{q_a})+(\frac{n}{m}-\frac{1}{q_a})^2\right]a^2\xi_a^2$$

flux function

$$B_{r1} = -(1/r)\partial\psi/\partial\theta \qquad B_{\theta 1} = \partial\psi/\partial r \qquad B_v^2 = B_{r1}^2 + B_{\theta 1}^2 = \frac{m^2}{r^2}\psi^2 + (\frac{d\psi}{dr})^2$$

$$\delta W_v = \frac{\pi^2 R}{\mu_o}\int_a^b B_v^2 rdr = \frac{\pi^2 R}{\mu_o}\left\{\int_a^b\left[\frac{m^2}{r^2}\psi^2 - \frac{\psi}{r}\frac{d}{dr}(r\frac{d\psi}{dr})-\right]rdr + (r\psi\frac{d\psi}{dr})\Big|_a^b\right\}$$

$$= \frac{\pi^2 R}{\mu_o}(r\psi\frac{d\psi}{dr})\Big|_a^b$$

0

$$\nabla\cdot\vec{B} = 0 \longrightarrow \frac{1}{r}\frac{d}{dr}(r\frac{d\psi}{dr}) - \frac{m^2}{r^2}\psi = 0$$

$$\nabla\cdot\vec{B}=0 \longrightarrow \frac{1}{r}\frac{d}{dr}\left(r\frac{d\psi}{dr}\right)-\frac{m^2}{r^2}\psi=0 \qquad \psi=\alpha r^m+\beta r^{-m}$$

boundary conditions

$$B_{r1}(r=a)=-\frac{imB_\phi}{R}\left(\frac{n}{m}-\frac{1}{q_a}\right)\xi_a=-\frac{1}{a}\frac{\partial\psi}{\partial\theta}=-\frac{im}{a}\psi_a$$

$$\psi_a=\frac{aB_\phi}{R}\left(\frac{n}{m}-\frac{1}{q_a}\right)\xi_a=B_{\theta a}\left(\frac{nq_a}{m}-1\right)\xi_a \qquad \psi(r=b)=0$$

$$\longrightarrow \quad \psi=B_{\theta a}\left(\frac{nq_a}{m}-1\right)\frac{\left(\frac{r}{b}\right)^m-\left(\frac{b}{r}\right)^m}{\left(\frac{a}{b}\right)^m-\left(\frac{b}{a}\right)^m}\xi_a$$

$$\delta W_v=\frac{\pi^2B_\phi^2}{\mu_o R}m\lambda\left(\frac{n}{m}-\frac{1}{q_a}\right)^2a^2\xi_a^2 \qquad \lambda=\frac{1+(a/b)^{2m}}{1-(a/b)^{2m}}$$

$$\delta W=\delta W_p+\delta W_v=\frac{\pi^2B_\phi^2}{\mu_o R}\left\{\int_0^a\left[\left(r\frac{d\xi}{dr}\right)^2+(m^2-1)\xi^2\right]\left(\frac{n}{m}-\frac{1}{q}\right)^2rdr\right.$$

$$\left.+\left[\frac{2}{q_a}\left(\frac{n}{m}-\frac{1}{q_a}\right)+(1+m\lambda)\left(\frac{n}{m}-\frac{1}{q_a}\right)^2\right]a^2\xi_a^2\right\}$$

For conducting wall $\xi_a=0$

$\delta W>0$ stable

# Growth Rate for Various Modes

For any conducting wall at b>a, stable $\delta W > 0$ for $m/n < q_a$

Since q ~ $r^2$, modes with resonance rational surface outside the plasma has $m/n > q_a$ ⟶ can be unstable !

For growth rate, the eigenmode equation need to be solved

$$\frac{d}{dr}\left[(\rho\omega^2 - F^2) r \frac{d}{dr}(r\xi)\right] - \left[m^2(\rho\omega^2 - F^2) - r\frac{dF^2}{dr}\right]\xi = 0$$

$$F = (m - nq) B_\theta / r\mu_o^{1/2}$$

BC's

$$\frac{d}{dr}(r\xi) = \frac{m(m-nq_a)^2}{(\mu_o\rho\omega^2 a^2 / B_\theta^2) - (m-nq_a)^2}\left(\lambda - \frac{2}{m-nq_a}\right)\xi$$

$\xi \propto r^{m-1}$

r=0 r=a

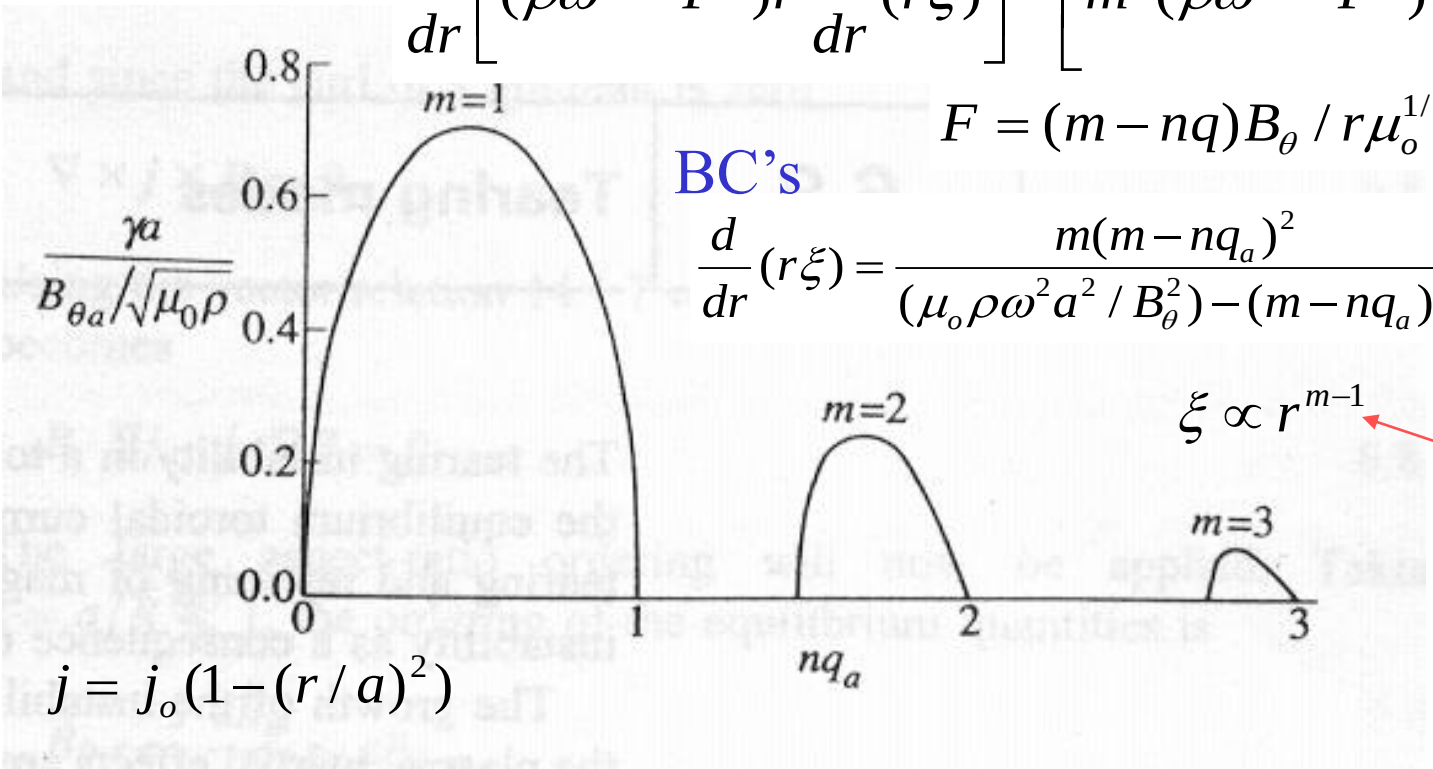

# Stability Diagram for External Kink Modes

$$j = j_o(1-(r/a)^2)^\nu$$

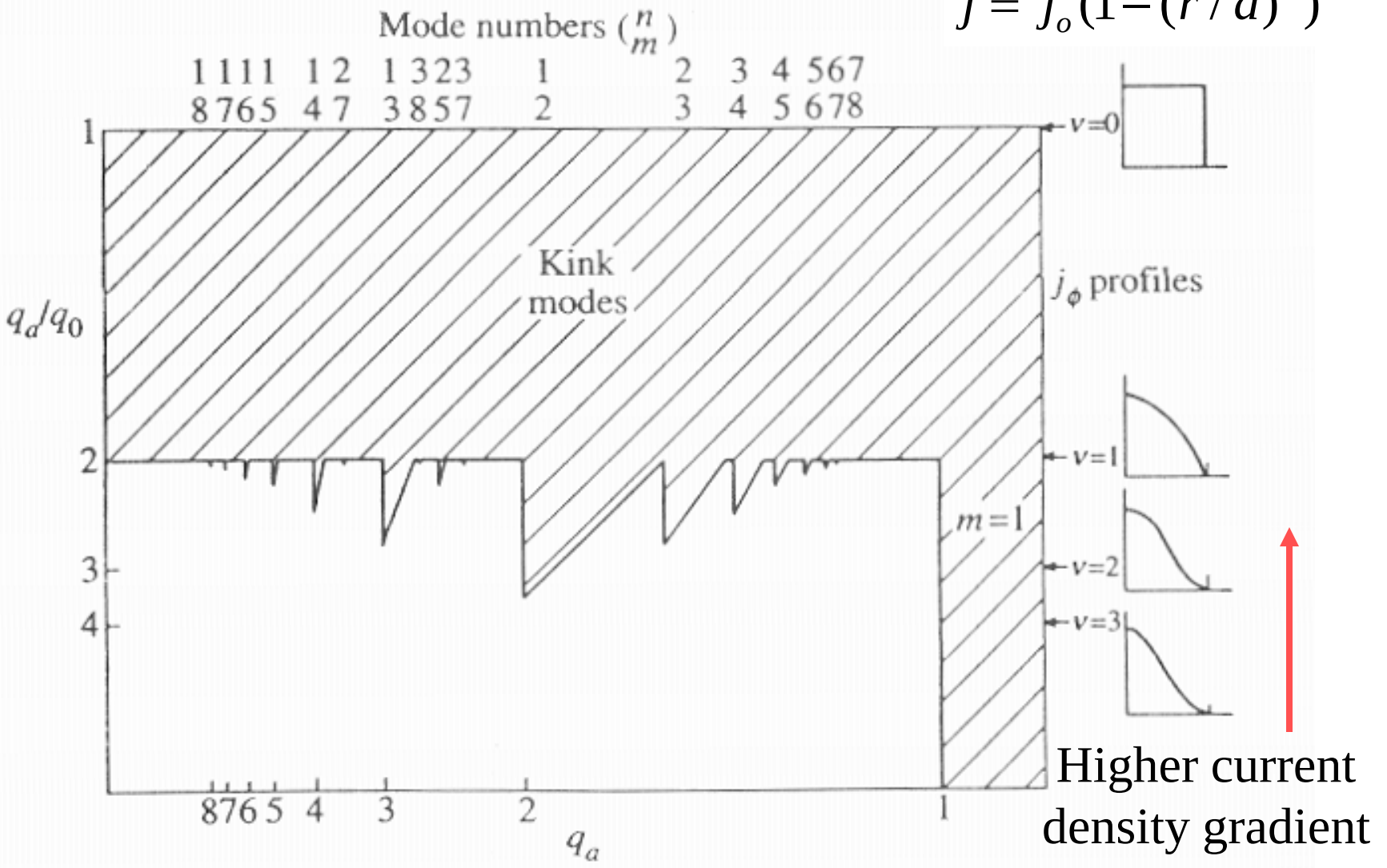


Higher current density gradient at plasma surface

# Internal Kink Mode

- Resonant surface : q = 1 from m=1/n=1 mode
- Sufficient condition for stability : $q_o > 1$
- Potential energy for large aspect-ratio approximation

$$\delta W = \frac{\pi^2 B_\phi^2}{\mu_o R}\int_0^a \left\{ (r\frac{d\xi}{dr})^2 + (m^2-1)\xi^2 \right\} (\frac{n}{m}-\frac{1}{q})^2 r dr + O(\varepsilon^2)$$

$$\xi_a = 0 \longrightarrow \text{no surface term}$$

$$\xi(r<r_1) = const. \quad \xi(r>r_1) = 0 \quad q(r=r_1) = 1$$

leading order : marginally stable

$$\delta W \sim \int_{r_o-\delta}^{r_o} (\frac{\xi}{\delta})^2 (q'x)^2 dx \to 0 \quad \text{as} \quad \delta \to 0$$

then

$$\delta W = O(\varepsilon^2) = (1-\frac{1}{n^2})\delta W_C + 2\pi^2 R \xi_o^2 \frac{B_\phi^2}{\mu_o}(\frac{r_1}{R})^4 \delta\tilde{W}_T$$

n=1

$$\delta\tilde{W}_T = 3(1-q_o)\delta(\frac{13}{144}-\beta_{p1}^2) \qquad \beta_{p1} = \frac{\int_0^{r_1}(p-p_1)2rdr}{(B_{\theta 1}^2/2\mu_o)r_1^2}$$

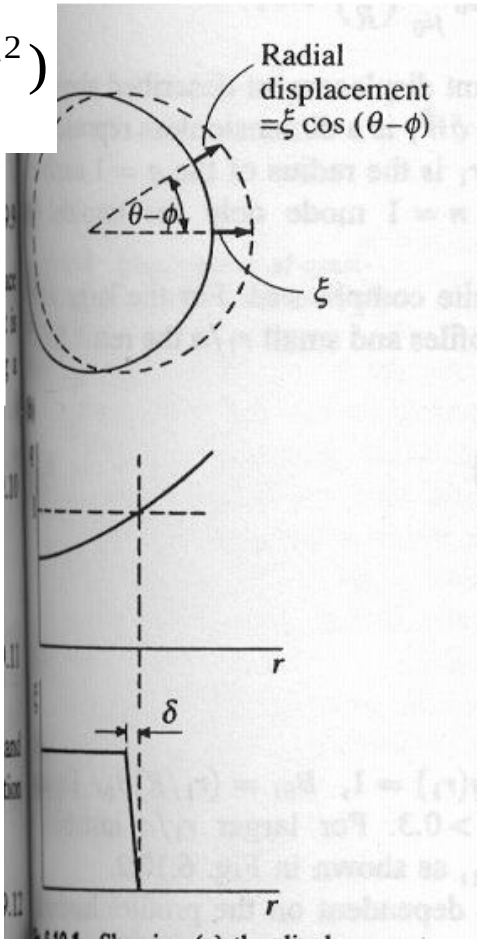

# Tokamak Stability Diagram for Ideal Kinks

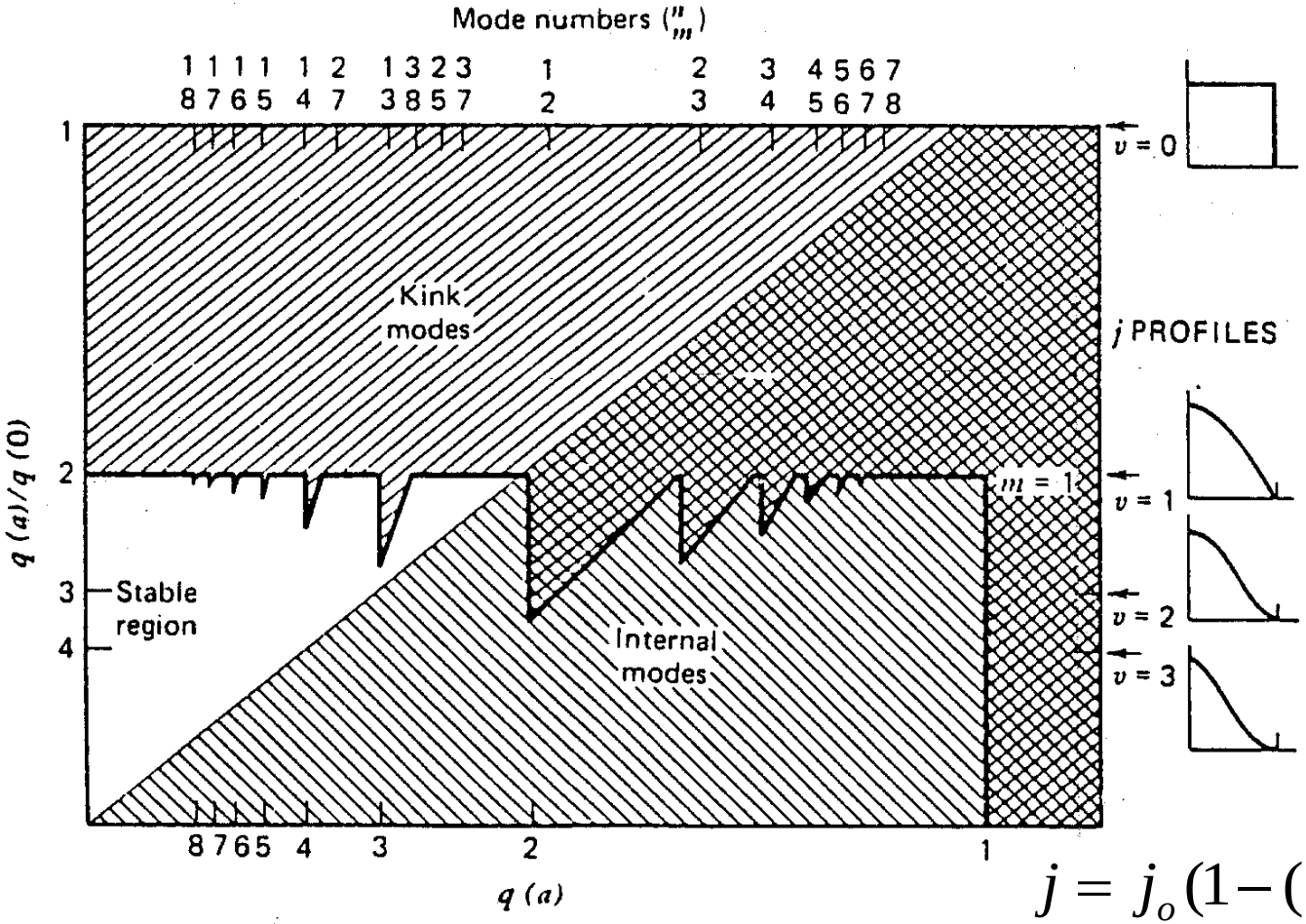


**FIGURE 5.7.** Stability diagram for ideal kink and internal modes of a large-aspect-ratio circular cross-section tokamak. The current distribution is $j_\phi(r) = j_\phi(0)[1 - r/a)^2]^\nu$. Complete stability against kink modes may be obtained for any $q(a) > 1$ by sufficient peaking of the current profile (larger value of $\nu$). The maximum stable current for this model is obtained with a parabolic current distribution with $q(0) = 1$ and $q(a) = 2$. (Data from J.A. Wesson [17].)

*Rayleigh-Taylor instability* : It occurs when a heavy incompressible fluid is supported against the force of gravity by a light incompressible fluid.

*Plasma analogy* :

plasma <----------> "heavy" fluid

magnetic field <----------> "light" fluid

general plasma forces <----------> gravity

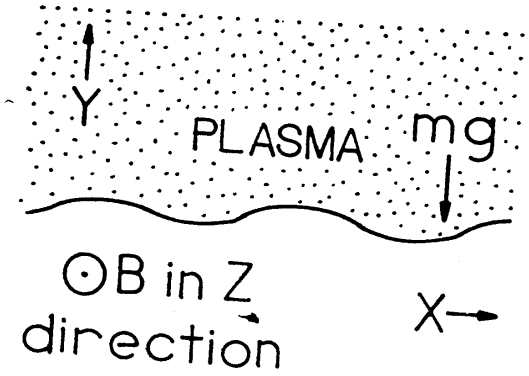


Fig. 8D3. The case of a plasma suspended against gravity by a uniform magnetic field.

$\nabla p \uparrow\downarrow \overline{F}orce$ : ***Unstable !***

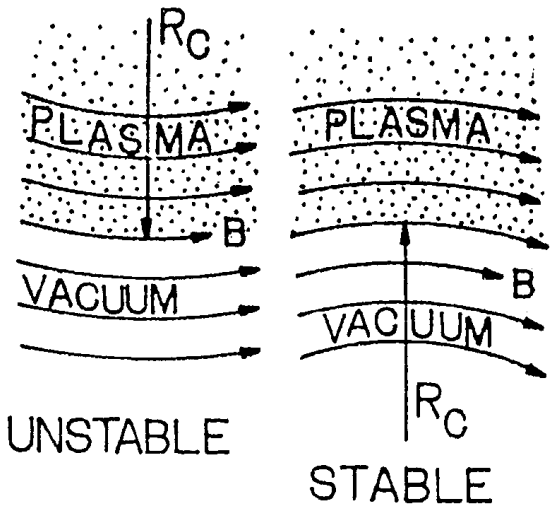


Fig. 8D4. Plasma supported by magnetic field with magnetic field radius of curvature $R_c$ outwards (unstable) and inwards (stable).

**Minimum-B configuration for stable condition**

# Interchange (Flute) Mode in a Simple Mirror

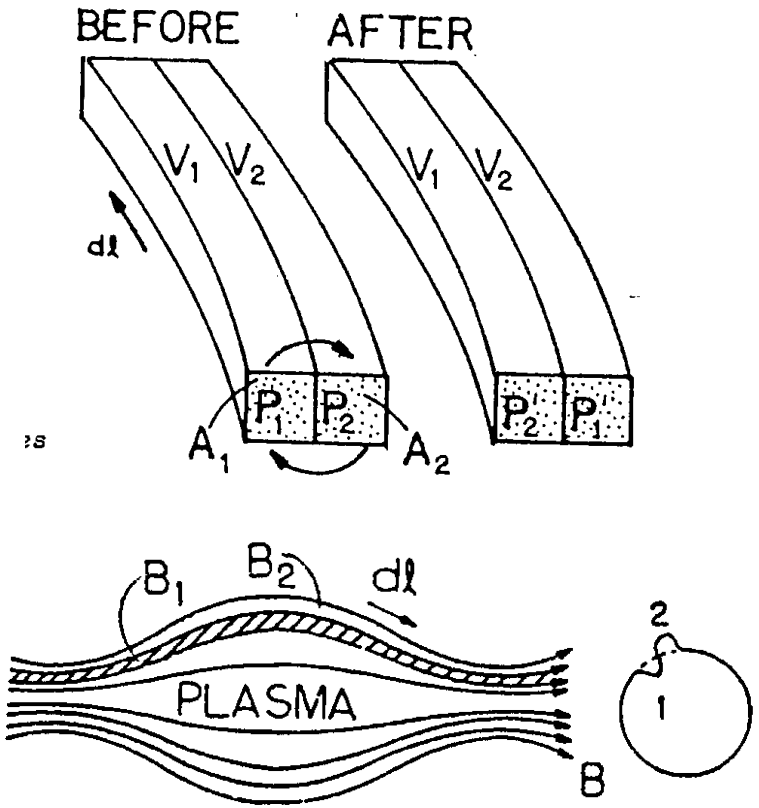


*Fig. 8D6. Outward displacement of a flux tube in a magnetic mirror. In the central region B decreases with radius. When flux tube 1 interchanges with flux tube 2 containing vacuum, the surface becomes rippled and the potential energy decreases ($\delta W < 0$).*

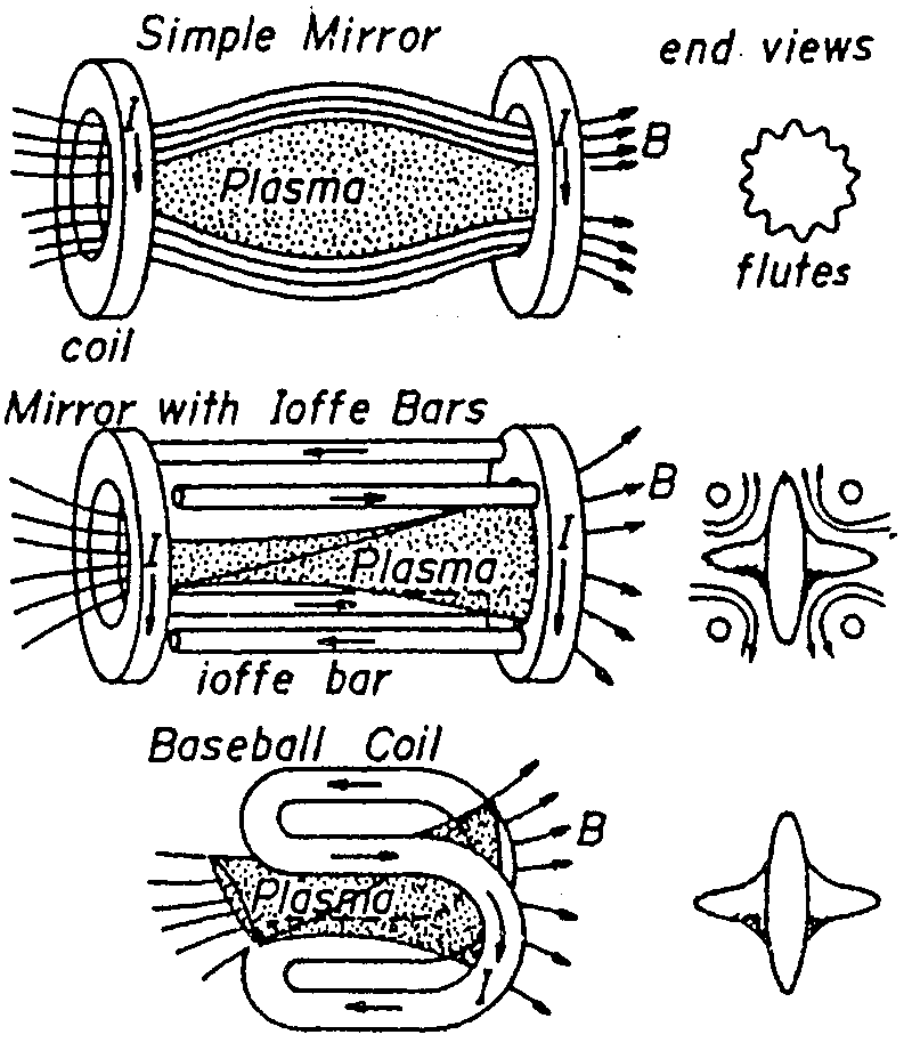

# Localized High-n Modes

Relevant part of the potential energy in a cylindrical plasma

$$\delta W = \pi \int \frac{1}{k^2}\left[\frac{1}{2\mu_o}(\vec{k}\cdot\vec{B}\frac{d\xi_r}{dr})^2 + \frac{k_z^2}{r}\frac{dp}{dr}\xi_r^2\right] r dr$$

**stabilize high-n modes**

$$\vec{k} = (m/r)\hat{\theta} + k_z\hat{z}$$

0 at resonant surface (q=m/n) → localized high-n modes

- Suydam criterion $\frac{rB_z^2}{8\mu_o}(\frac{q'}{q})^2 > (-p')$ $\frac{q'}{q} = \frac{(B_z/rB_\theta)'}{B_z/rB_\theta}$ magnetic shear
- Mercier criterion for large aspect-ratio circular tokamak

$$\frac{rB_\phi^2}{8\mu_o}(\frac{q'}{q})^2 > (-p')(1-q^2)$$

**Stabilizing contribution of the average curvature of the toroidal magnetic field**

- Mercier criterion is only a necessary stability condition

→ Complete treatment of the destabilizing bad curvature on the outer side of the torus → Ballooning modes

# Balooning Modes (high-n modes)

Destabilizing energy available from the pressure gradient

$$\delta W_d \sim \frac{-dp/dr}{R_c}\xi^2$$

Energy required for line bending

$$\delta W_s \sim k_{//}^2 (B_\phi^2/\mu_o)\xi^2$$

$$k_{//} \sim 1/qR \qquad R_c \sim R_o$$

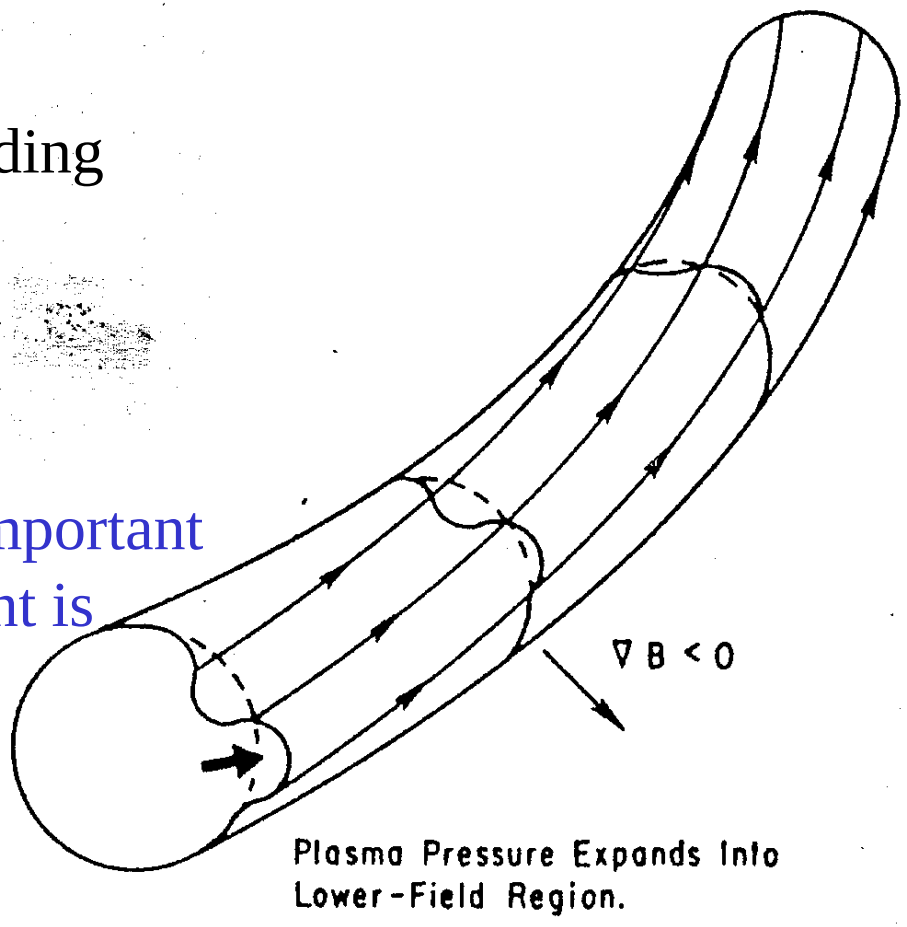


• Ballooning modes become important only when the pressure gradient is sufficiently large that

$$-\frac{dp}{dr} \sim \frac{B_\phi^2/\mu_o}{q^2 R_o} \rightarrow \beta \sim \frac{\varepsilon}{q^2}$$

• Infernal Mode : low mode number pressure-driven instability at low magnetic shear region close to rational surface with low mode number

# Balooning Modes

Potential energy in the limit of large mode number in an orthogonal coordinate system ($\psi$, $\chi$, $\phi$) : Eq. (6.13.1)

Minimization leads to an Euler equation of (6.13.2) with

$$X = RB_p\xi_\psi \xrightarrow{\text{Eikonel transform}} X = F\exp\left(-in\int^y JB_\phi / Rd\chi\right)$$

For large aspect-ratio circular tokamak with low beta $\beta \sim \varepsilon^2$

Instability occurs for $-(dp/dr)/(B_\phi^2/\mu_o) \sim a/R$

$$\delta W = \int\left[(1+\Lambda^2)\left(\frac{dF}{d\theta}\right)^2 - \alpha(\Lambda\sin\theta+\cos\theta)F^2\right]d\theta$$

$$\Lambda = s\theta - \alpha\sin\theta \qquad s = \frac{r}{q}\frac{dq}{dr}$$

average magnetic shear

$$\alpha = -\frac{2\mu_o Rq^2}{B^2}\frac{dp}{dr}$$

**stabilizing effect of line bending**

**shear dependent contribution**

**destabilizing effect of the pressure gradient**

$$\frac{d\Lambda}{d\theta} = s - \alpha\cos\theta$$

$$\frac{d}{d\theta}\left[(1+(s\theta-\alpha\sin\theta)^2)\frac{dF}{d\theta}\right] + \alpha\left[(s\theta-\alpha\sin\theta)\sin\theta+\cos\theta\right]F = 0$$

# Balooning Modes

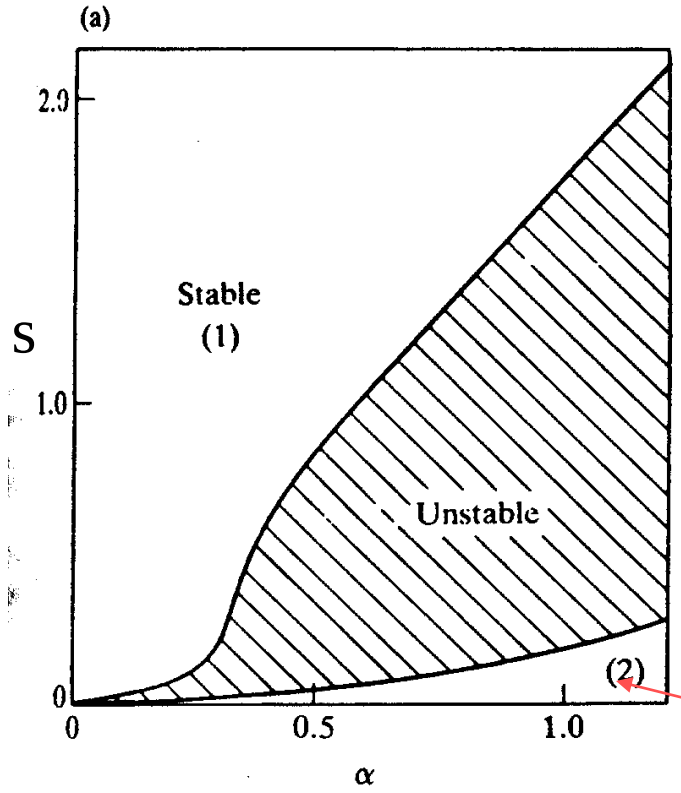


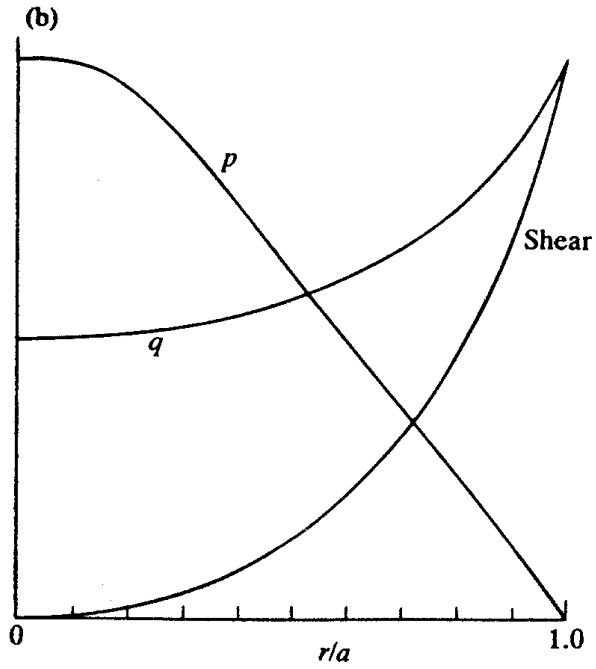


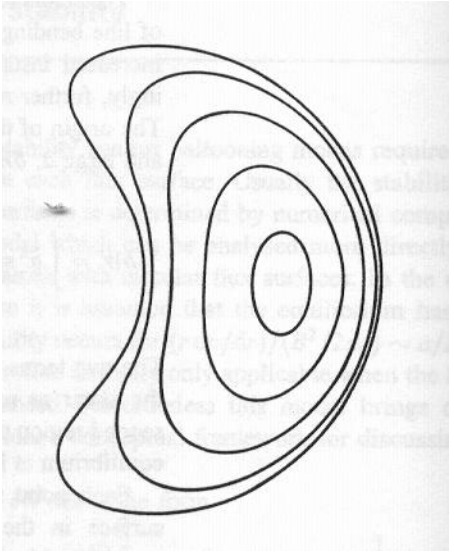

Second stability region

$$s = \frac{r}{q}\frac{dq}{dr}$$ **S-α diagram**

$$\alpha = -\frac{Rq^2}{B^2/2\mu_o}\frac{dp}{dr}$$

$$\delta W = \int \alpha^2 \sin^2\theta \left[ \left(\frac{dF}{d\theta}\right)^2 + F^2 \right] d\theta$$

$$\Lambda = s\theta - \alpha\sin\theta \approx -\alpha\sin\theta$$

- Pressure and q profiles control (DIII-D)
- Bean shaped plasma boundary (PBX-M)

# Axisymmetric Modes

- **Elongated tokamak plasmas are susceptible to an axisymmetric instability (n=0)**
  - circular cylindrical plasmas are neutrally stable to a rigid displacement without conducting wall
  - elongated plasmas are unstable to a motion along the direction of elongation
  - in the presence of conducting wall, there is a critical elongation for instability
  - complicated in reality from toroidal effects and adjacent structural effects
- **Elongation of the plasma due to currents in external conductors**

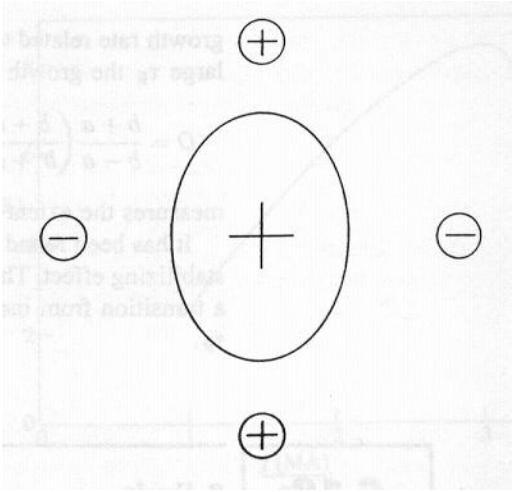

# Stability Criteria of Axisymmetric Modes

**in terms of the equilibrium magnetic field from external currents**

- **circular large aspect-ratio plasmas without stabilizing conductors**

$$n = -\frac{R}{B_z}\frac{dB_z}{dR} > 0$$

- **cylindrical elliptical plasmas with uniform current density surrounded by a perfectly conducting confocal elliptical shell**

$$\frac{b-a}{b+a} > \left(\frac{b+a}{b'+a'}\right)^2$$ : Instability in inertial time-scale

**Otherwise, instability in resistive time-scale**

$$\gamma = (D\tau_R)^{-1} \qquad D = \frac{b+a}{b-a}\left(\frac{b+a}{b'+a'}\right)^2 - 1$$

- **Toroidal stabilizing effect confirmed in numerical calculations**

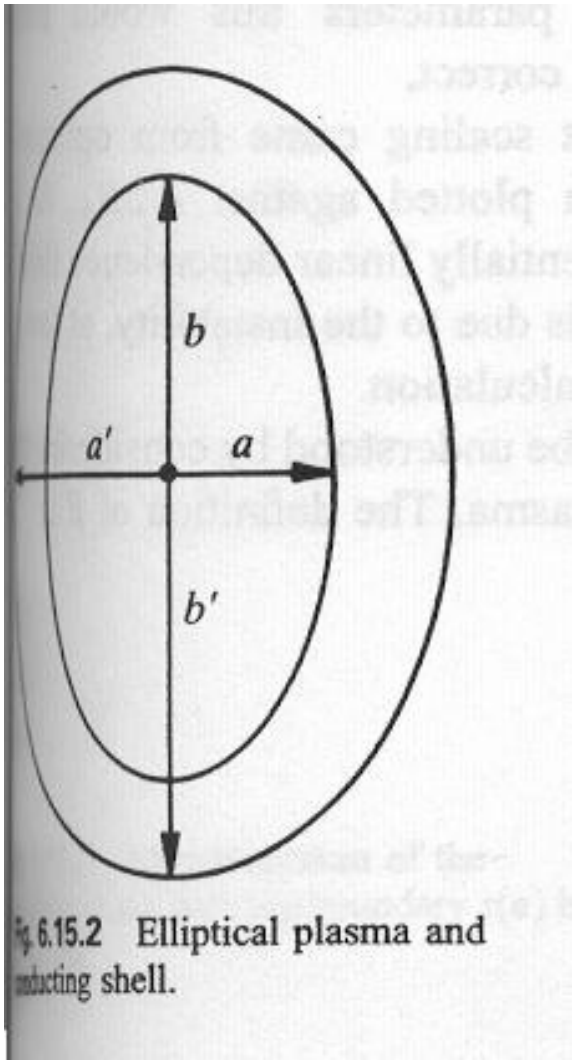

6.15.2 Elliptical plasma and conducting shell.

# Beta Limit

**Basic MHD parameter measuring the confined pressure, related to the MHD stability driven by pressure gradients**

- **Ballooning modes**

$$\beta \sim \frac{\varepsilon}{q^2} \sim (I / aB_\phi)^2 / \varepsilon$$

- Correct scaling from optimized stability calculations for JET

$$\beta \sim I / aB_\phi$$

- turnover at high beta is due to the instability of low-m modes at low q included in the calculations

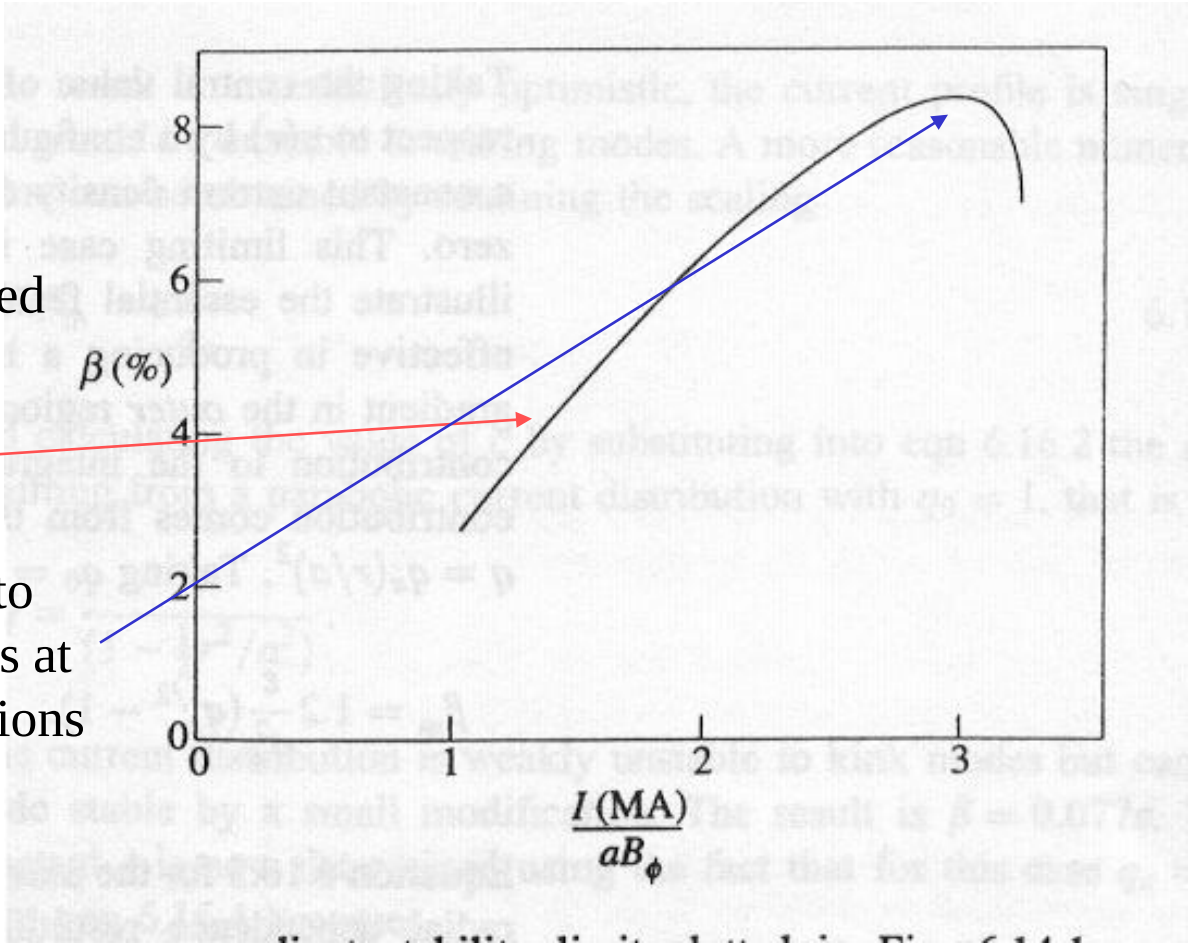

# Approximate Linear Scaling of Beta Limit

**For large aspect-ratio circular plasmas,**

$$\beta = \frac{2\pi\int_0^a prdr}{\pi a^2 (B_\phi^2/2\mu_o)} = \frac{2\mu_o}{a^2 B_\phi^2}\int_0^a -\frac{dp}{dr} r^2 dr$$

$$s \equiv \frac{r}{q}\frac{dq}{dr} = 1.67\alpha = -1.67\frac{2\mu_o R q^2}{B_\phi^2}\frac{dp}{dr}$$

$$\beta = -0.3\frac{1}{Ra^2}\int_0^a \frac{d}{dr}\left(\frac{1}{q^2}\right) r^3 dr$$

$$\beta_m = 1.2\frac{\varepsilon}{q_a^2}(q_a^{1/2} - 1)$$

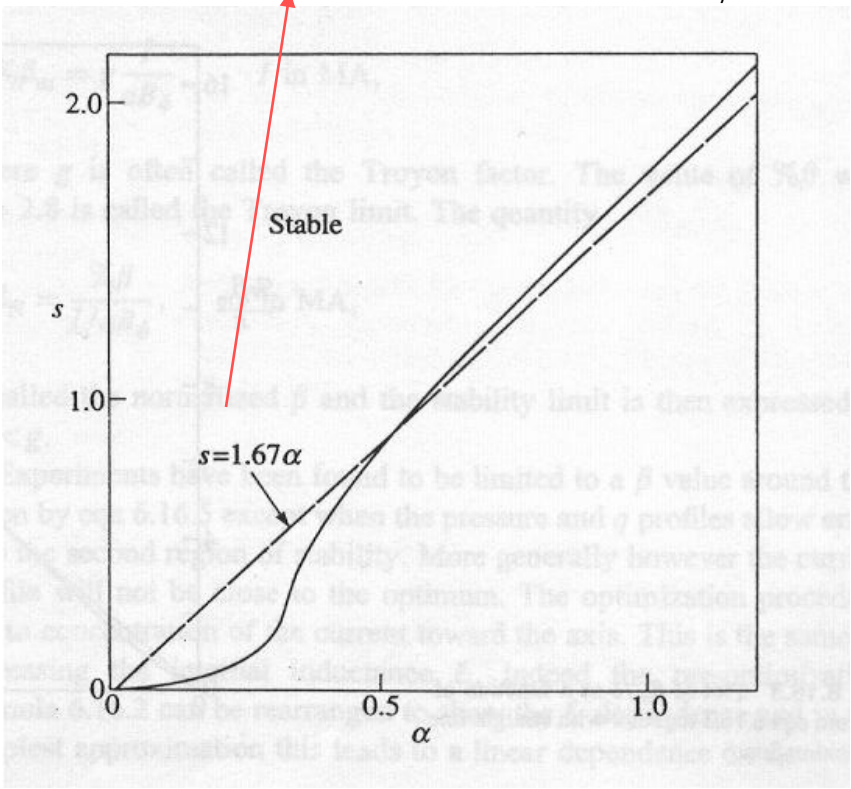


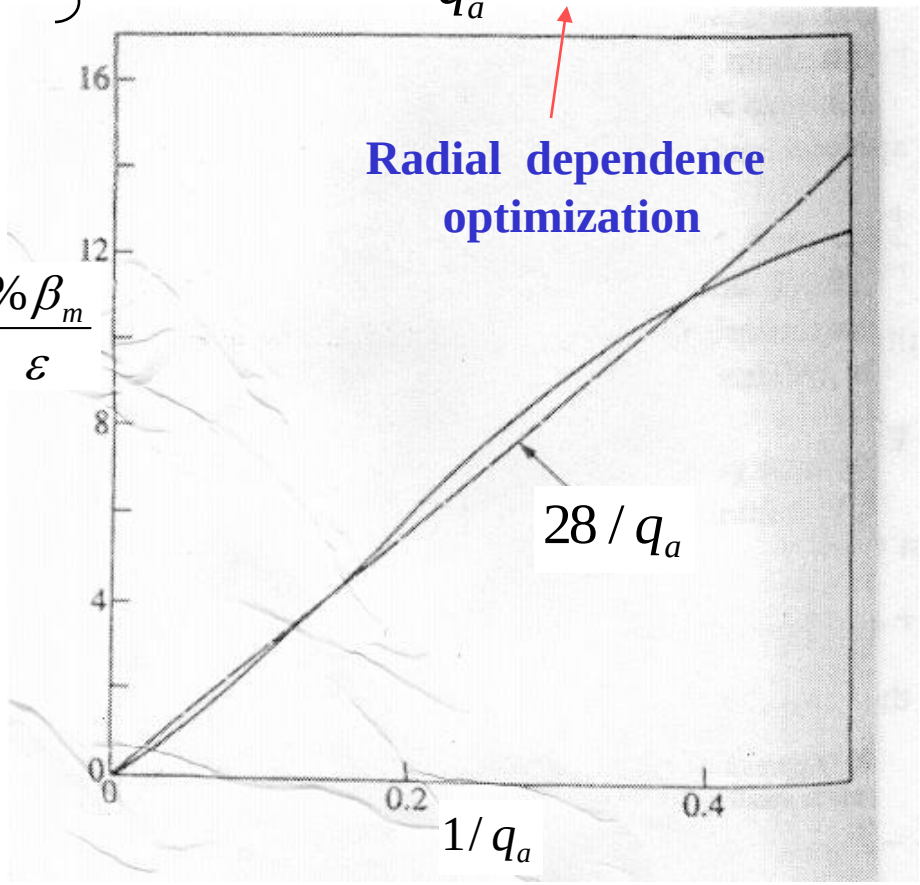

# Troyon Beta Limit

$$\%\beta_m = 28\frac{\varepsilon}{q_a} \quad \text{or} \quad \%\beta_m = 5.6\frac{I[MA]}{aB_\phi}$$

**unrealistically optimistic !**

With $q = \dfrac{1}{(1 - r^2/2a^2)}$ and $q_a \le 2$

$$\%\beta_m = 15\frac{\varepsilon}{q_a} \quad \text{or} \quad \%\beta_m = 3\frac{I[MA]}{aB_\phi}$$

Computer calculation by Sykes and Troyon

$$\%\beta_m = g\frac{I[MA]}{aB_\phi}$$ Troyon factor

$$\beta_N = \frac{\%\beta}{I[MA]/aB_\phi}$$ Normalized β

$$\beta_N < g = 2.8$$ **Troyon limit**

**experiments**

$$\%\beta = 4l_i\frac{I[MA]}{aB_\phi}$$

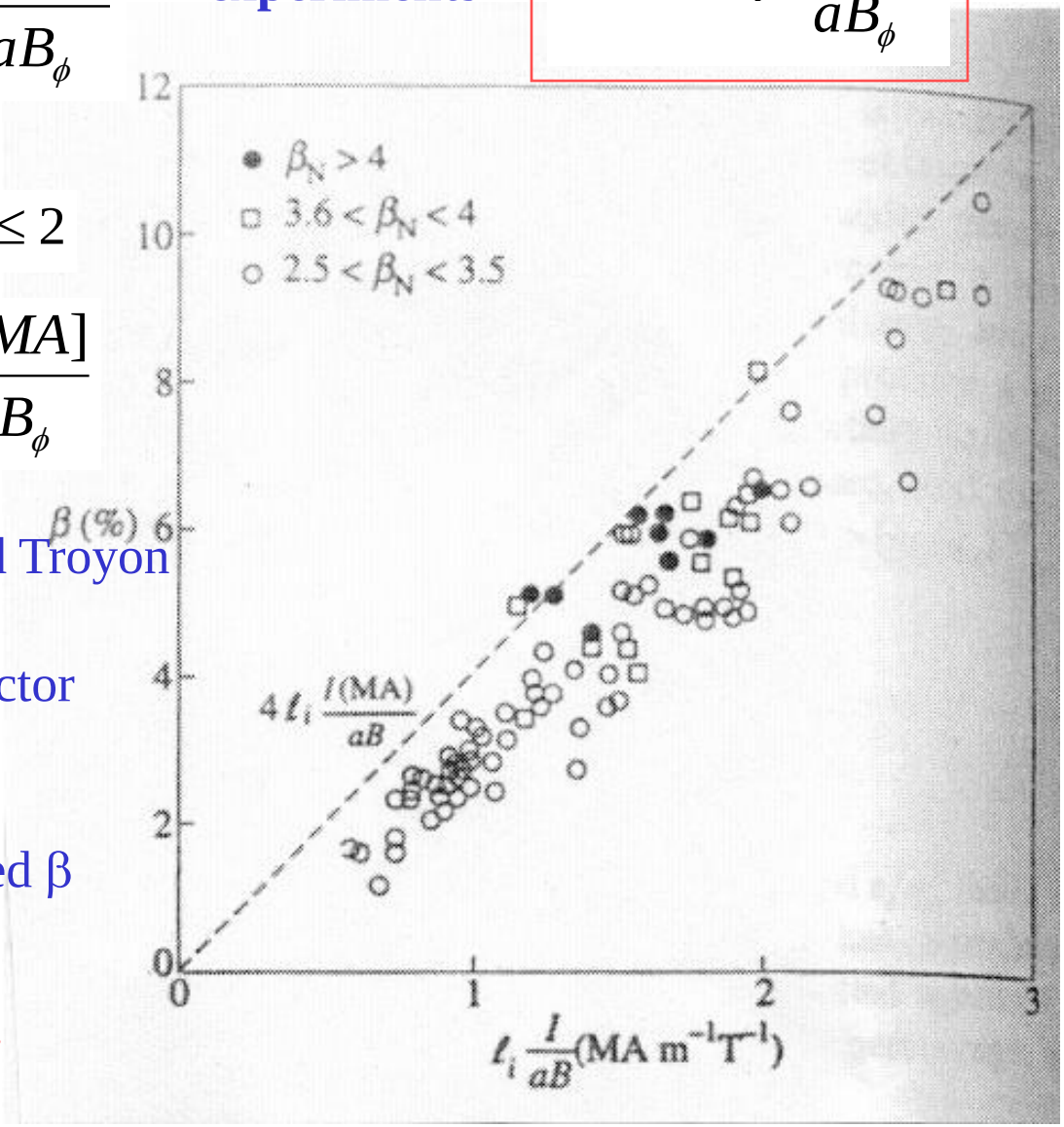

# Tearing Modes

**driven by the radial gradient of the equilibrium toroidal current density**

- **Tearing and rejoining of magnetic field lines due to finite resistivity --> tearing instability**
  - **slow growth : inertial effects negligible**
  - **vxB negligible at the resonance surface**
  - **matching two solutions of both resistive layer and outer layer**

$$E \sim \eta j$$

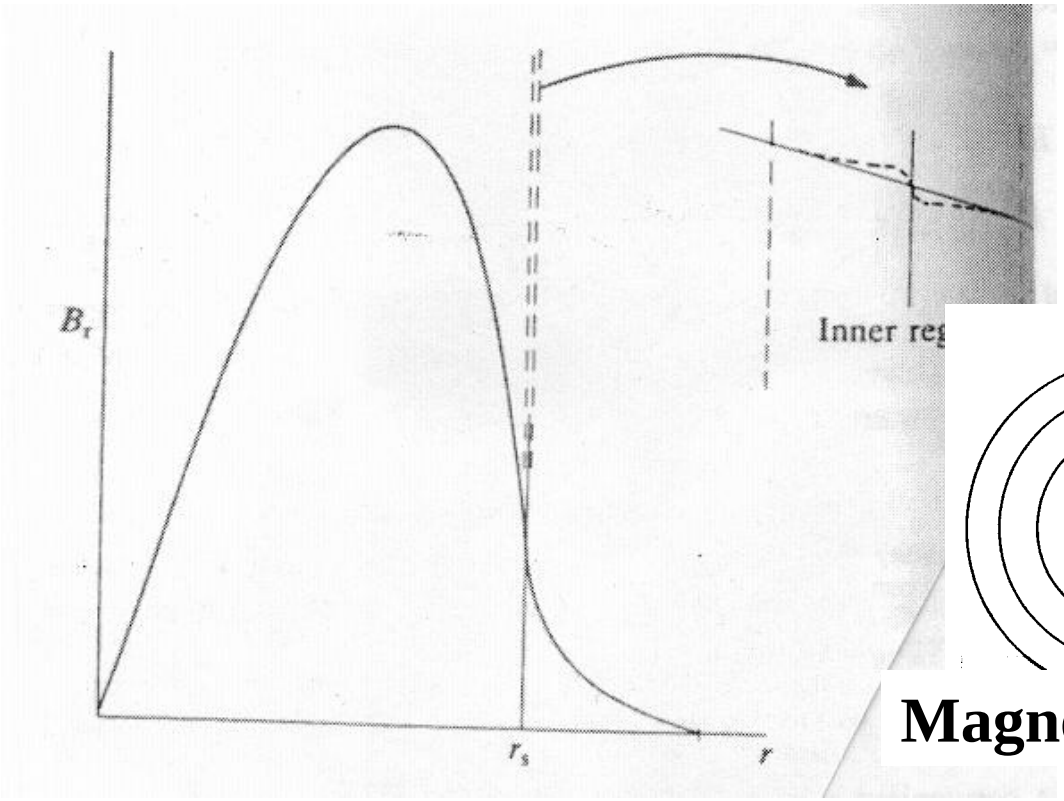


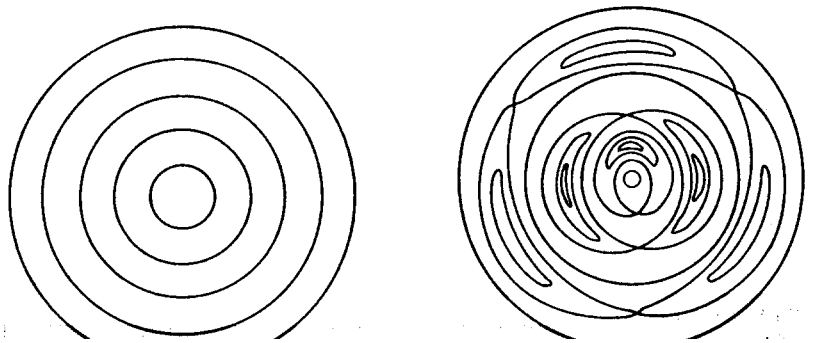

**Magnetic Islands (Tearing Modes)**

# Stability of Tearing Modes

- **Tearing mode stability criterion**

$$\Delta' = \lim_{\varepsilon \to 0} \left. \frac{\psi'}{\psi} \right|_{r=r_s-\varepsilon}^{r=r_s+\varepsilon} > 0 \quad \textbf{unstable}$$

$$\frac{1}{r}\frac{d}{dr}\left(r\frac{d\psi}{dr}\right) - \frac{m^2}{r^2}\psi - \frac{\mu_o dj_\phi / dr}{B_\theta (1 - nq/m)}\psi = 0$$

$$\left(1 - \frac{nq}{m}\right) \to -\left(\frac{q'}{q}\right)_{r_s} (r - r_s)$$

$$\frac{d^2\psi}{dr^2} + \left[\frac{dj_\phi / dr}{B_\theta / \mu_o}\frac{q}{q'}\right]_{r_s} (r - r_s)^{-1}\psi = 0 \qquad k$$

$$\psi = 1 + k(r - r_s)\ln|r - r_s| + \ldots + A^-(r - r_s) + \ldots \quad r < r_s$$

$$\psi = 1 + k(r - r_s)\ln|r - r_s| + \ldots + A^+(r - r_s) + \ldots \quad r > r_s$$

$$\Delta' = A^+ - A^- \quad \text{numerical solutions with b.c.'s}$$

$$\psi(r = 0) = 0 \qquad \psi'(r = a) = \left(-\frac{m}{a} + \gamma\mu_o\sigma\delta\right)\psi(r = a)$$

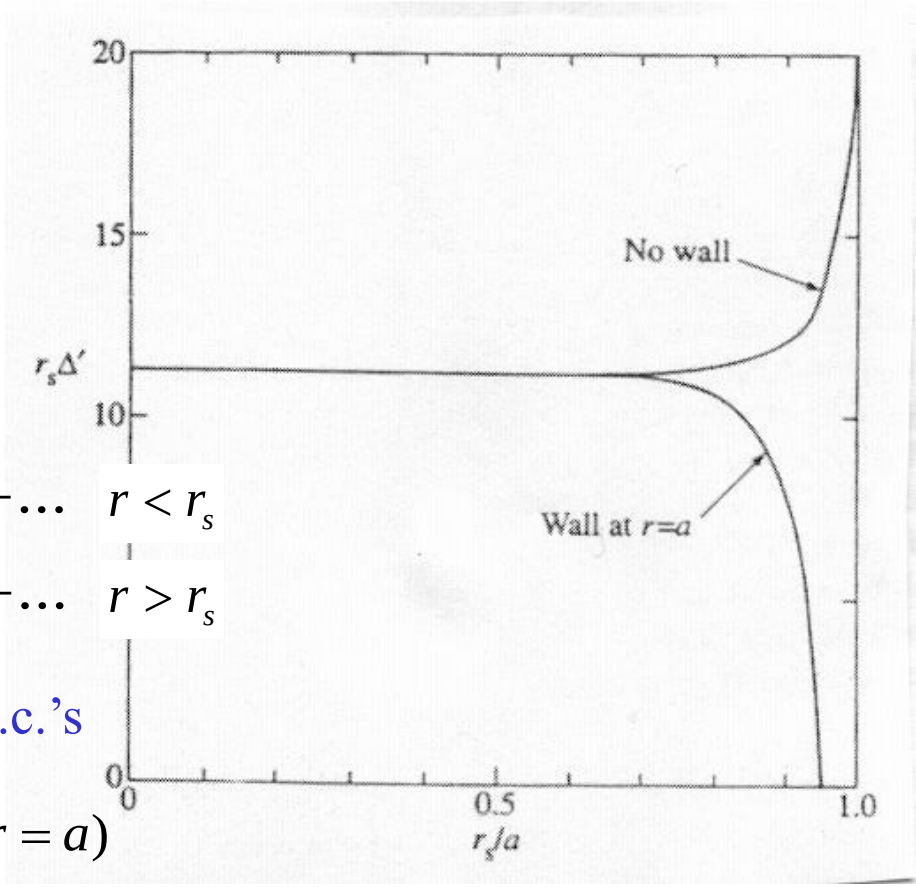

# Stability of Tearing Modes

- **Stability diagram for the m=2 kink and tearing modes for current distributions** $j = j_o(1-(r/a)^2)^\nu$

- **The tearing instability is continuous with the kink instability as the resonant surfaces pass through the plasma boundary**

- **stability for $q_0>2$ results from the absence of a q=2 resonant surface**

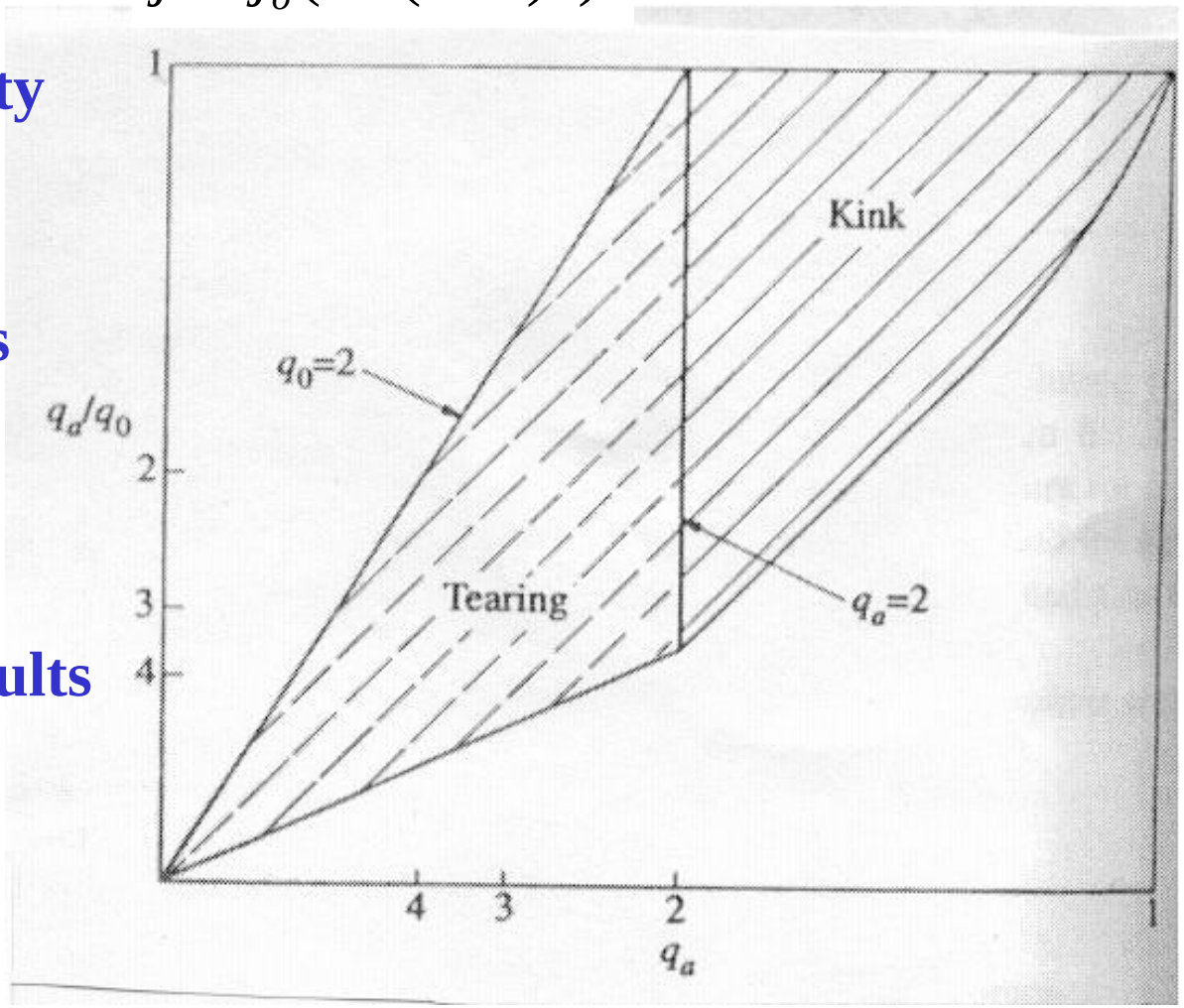

# Conducting Wall Boundary Condition

- **Mode frequency due to either natural frequency or plasma rotation by NBI affects the influence of conducting shell**
  - **low frequency : penetration with resistive time scale** $\tau_s \sim \mu_o \sigma b \delta$
  - **high frequency : no penetration due to eddy current shielding** $\omega \tau_s >> 1$

$$\frac{1}{r}\frac{d}{dr}\left(r\frac{d\psi}{dr}\right) = \frac{m^2}{r^2}\psi$$

vacuum region (a<r<b)

$$\left(\frac{\psi'}{\psi}\right)_a = -\frac{m}{a}\frac{1+f(a/b)^{2m}}{1-f(a/b)^{2m}}$$

$$\frac{1}{r}\frac{d}{dr}\left(r\frac{d\psi}{dr}\right) = \frac{m^2}{r^2}\psi + \mu_o\sigma E_\phi = \frac{m^2}{r^2}\psi + \mu_o\sigma\frac{\partial\psi}{\partial t}$$

shell region (b<r<b+δ)

$$f = \frac{(\psi'/\psi)_b - m/b}{(\psi'/\psi)_b + m/b}$$

$$\left(\frac{\psi'}{\psi}\right)_{b+\delta} - \left(\frac{\psi'}{\psi}\right)_b = \left(\frac{m^2}{r^2} - i\omega\mu_o\sigma\right)\delta$$

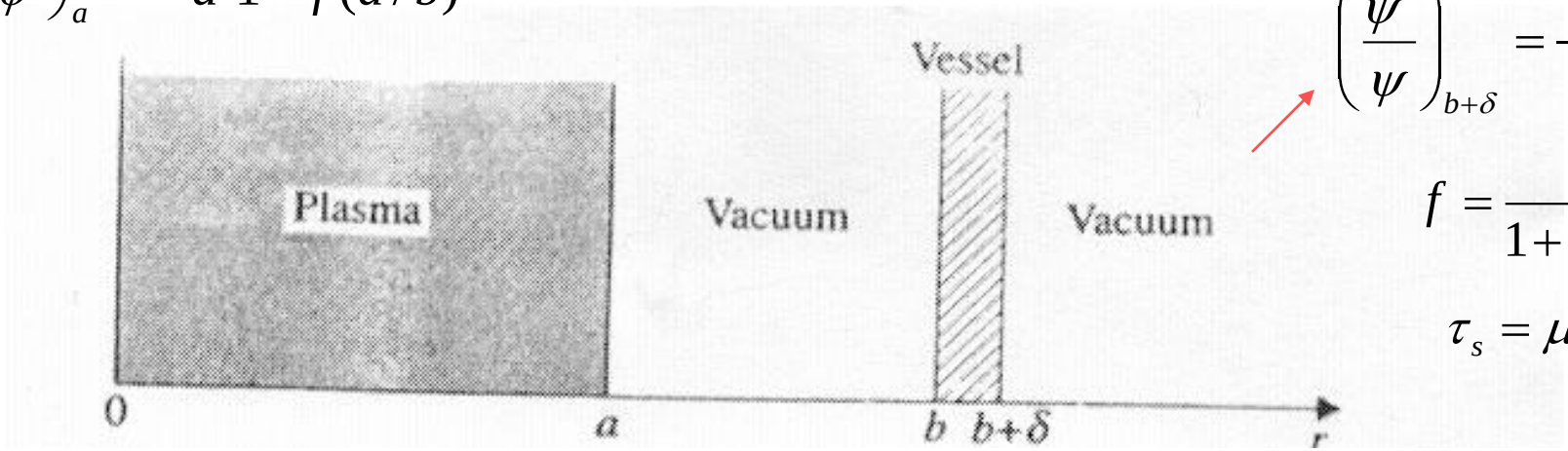


$$\left(\frac{\psi'}{\psi}\right)_{b+\delta} = -\frac{m}{b}$$

$$f = \frac{1}{1+im/\omega\tau_s}$$

$$\tau_s = \mu_o\sigma b\delta/2$$

- **Vacuum vessel lower the frequency of the instability --> at large amplitude the mode locks to the vessel (mode locking), bringing the frequency to zero.**

# Tokamak Macroscopic Instabilities

- Basic MHD instabilities
  - Magnetic islands
  - Tearing modes
  - Mirnov oscillations
  - Sawtooth
- Disruptions
  - Causes of disruptions
  - Physics of disruptions
  - Mode locking,
    error field instability,
    vertical instability, ergodicity
- Other instabilities
  - Fishbone instability, TAE, MARFEs, ELMs

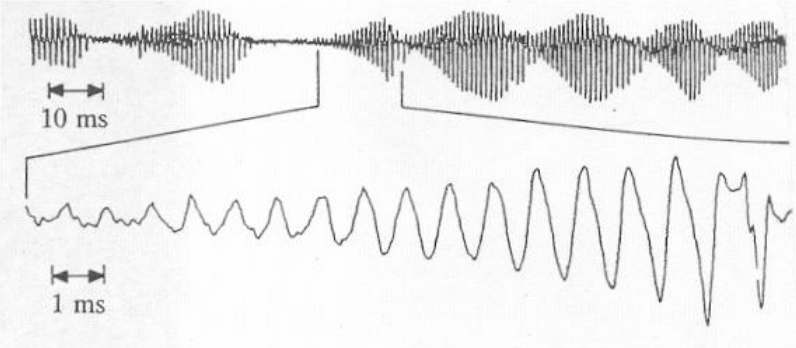


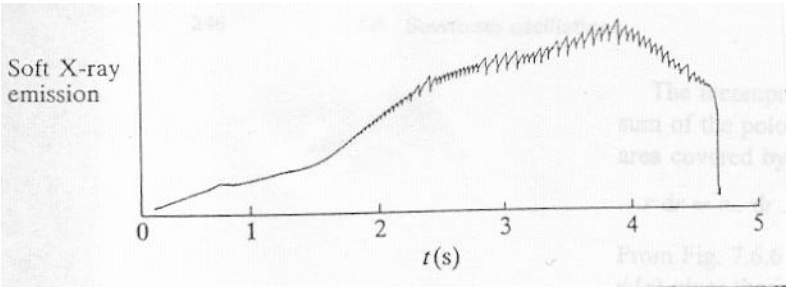


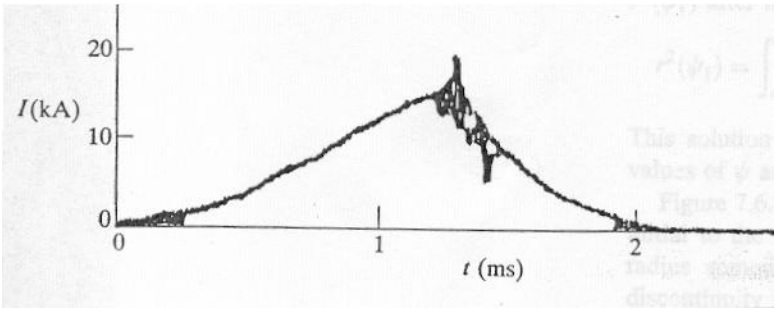

# Magnetic Islands

- Formation of magnetic islands
  - Resistive MHD instability, particularly tearing modes
  - non-linearly developed near the resonant surface in the plasma

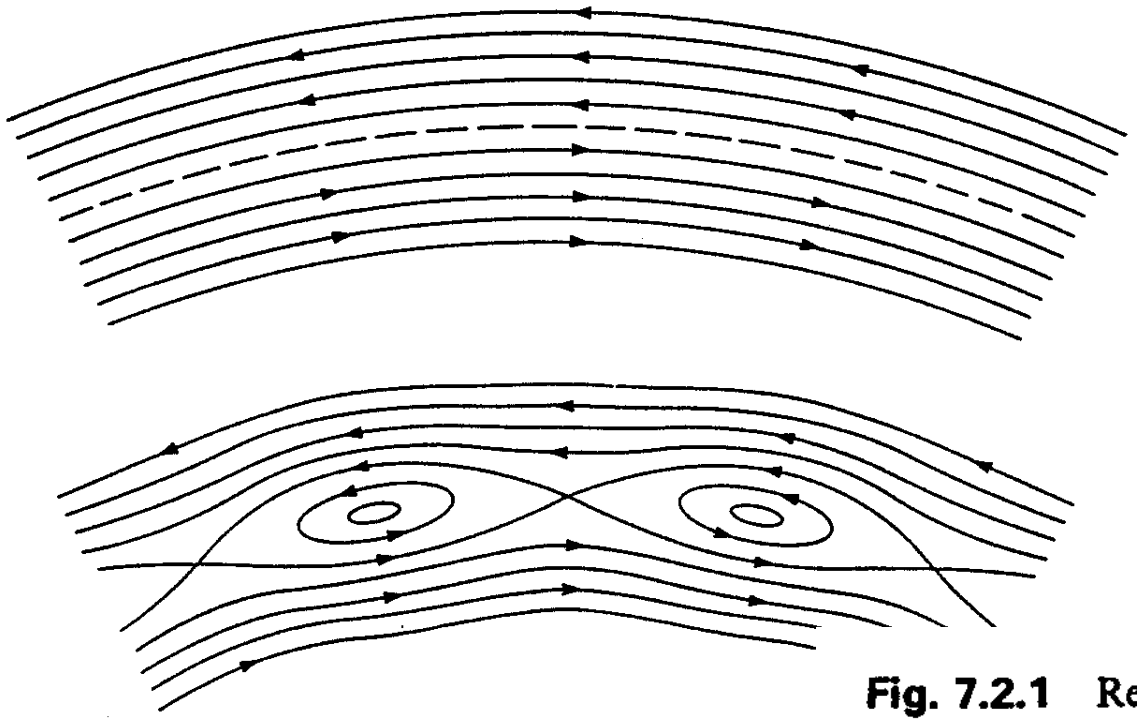

**Fig. 7.2.1** Reconnection of magnetic field producing magnetic islands.

# Geometry of Magnetic Islands

Equilibrium configuration around a resonant surface $q = q_s = m/n$

Resonant perturbation $e^{im\chi}$ $\chi = \theta - \frac{n}{m}\phi$

Angular coordinate orthogonal to the helix

Equilibrium field in this orthogonal direction $B^* = B_\theta(1 - \frac{n}{m} q(r))$ $B^* = -(B_\theta \frac{q'}{q})_s z$ $z = r - r_s$

Magnetic field line equation

$$\frac{dr}{r_s d\chi} = \frac{dz}{r_s d\chi} = \frac{B_r}{B^*} = \frac{\hat{B}_r(r)\sin m\chi}{-(B_\theta q'/q)_s z}$$

integrate

$$z^2 = \frac{w^2}{8}(\cos m\chi - \cos m\chi_o)$$

$$w = 4\left(\frac{rq\hat{B}_r}{mq'B_\theta}\right)_s^{1/2}$$ **: island width**

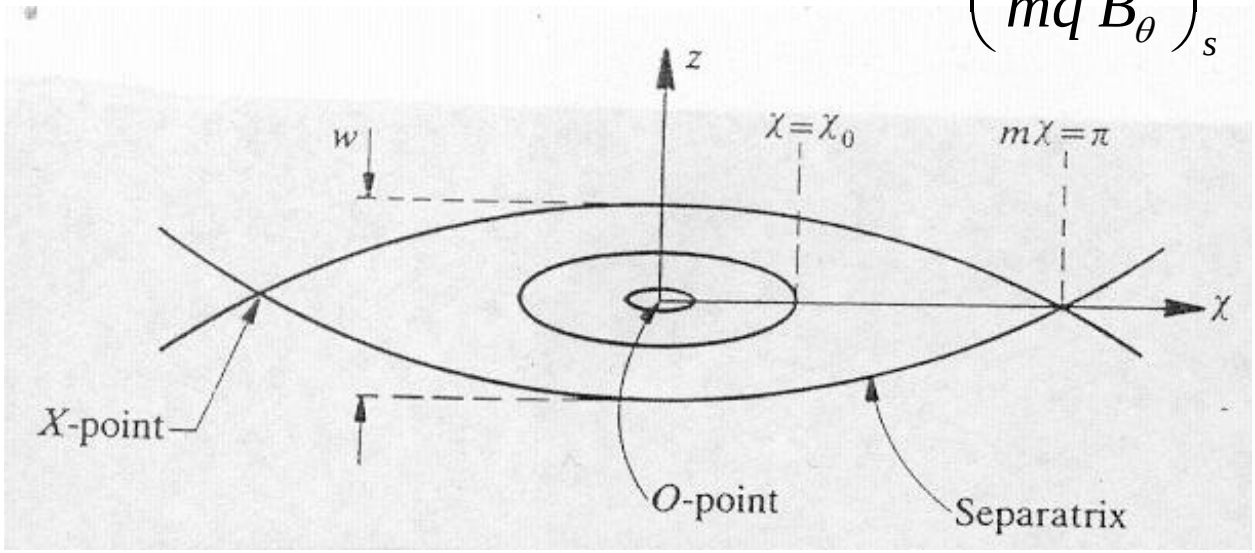

# Tearing Modes

- Growth of islands
  - destabilizing effects from current gradients in the plasma
  - growth rate limited by resistive diffusion
  - island width ~ $B_r$ --> growth rate limited by $B_r$ diffusion

$$\frac{\partial B_r}{\partial t} = \frac{\eta}{\mu_o}\frac{\partial^2 B_r}{\partial r^2}$$

Integrate over the island width with approx. constant $B_r$

$$w\frac{\partial B_r}{\partial t} = \frac{\eta}{\mu_o}\frac{\partial B_r}{\partial r}\bigg|_{r_s-w/2}^{r_s+w/2}$$

$$B_r = w^2$$

$$wdB_r = w^2 dw = B_r dw$$

$$\frac{dw}{dt} \cong \frac{\eta}{2\mu_o}\frac{1}{B_r}\frac{\partial B_r}{\partial r}\bigg|_{r_s-w/2}^{r_s+w/2} = \frac{\eta}{2\mu_o}\frac{\psi'}{\psi}\bigg|_{r_s-w/2}^{r_s+w/2} = \frac{\eta}{2\mu_o}\Delta'(w)$$

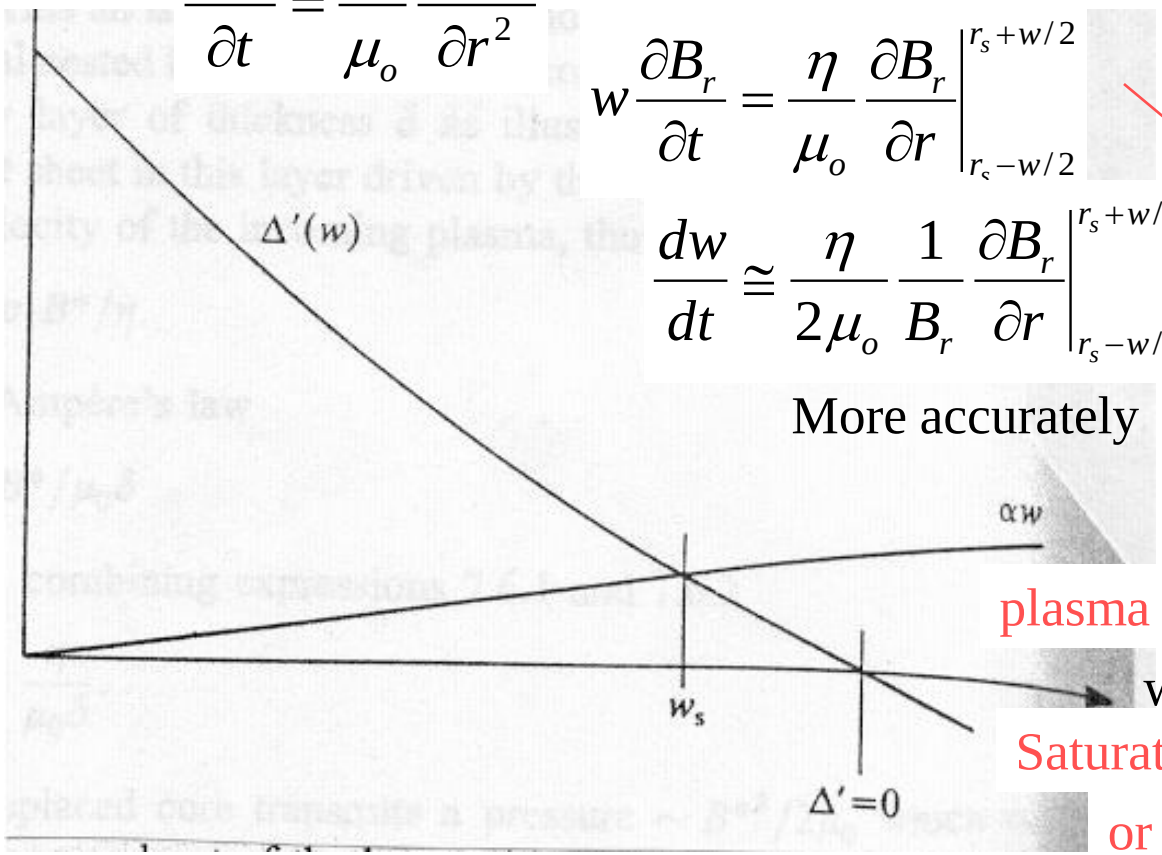


More accurately

$$\frac{dw}{dt} = 1.66\frac{\eta}{\mu_o}(\Delta'(w) - \alpha w)$$

plasma flow effect

detailed treatment of island region

Saturated island size $\Delta'(w_s) = \alpha w_s$

or approximately $\Delta'(w_s) = 0$

# Internally Driven Tearing Modes

- Tearing modes driven inside the islands
  - modified resistivity within the island from enhanced impurity radiation or the effect of an injected pellet
  - modified from the change of bootstrap currents within the island

Faraday's law and Ohm'slaw

$$\frac{\partial \psi}{\partial t} = E_h = (\eta j)_h = \eta_h j + \eta j_h \longrightarrow \quad j_h = -\eta_h j / \eta$$

The associated flux perturbation defines the resulting magnetic island $\nabla^2 \psi = \mu_o j_h$

The resulting reduction of bootstrap current leads to a helical current $\delta j_b$

$$\nabla^2 \psi = \mu_o \delta j_b \qquad j_b = \frac{\varepsilon^{1/2}}{B_\theta}\left(-\frac{dp}{dr}\right)$$

If the pressure gradient were completely remove $\delta j_b = -j_b$ $\rightarrow$ $\frac{d^2\psi}{dr^2} = \mu_o \delta j_b = -\mu_o j_b$

$$\psi \Delta'(w) = \psi'\Big|_{r_s - w/2}^{r_s + w/2} \cong -\mu_o \frac{\varepsilon^{1/2}}{B}\left(-\frac{dp}{dr}\right) w$$

$$\Delta'(w) \cong -16\varepsilon^{1/2} \frac{(-dp/dr)}{B_\theta^2 / 2\mu_o} \frac{q}{q'} \frac{1}{w}$$

# Mirnov Instabilities

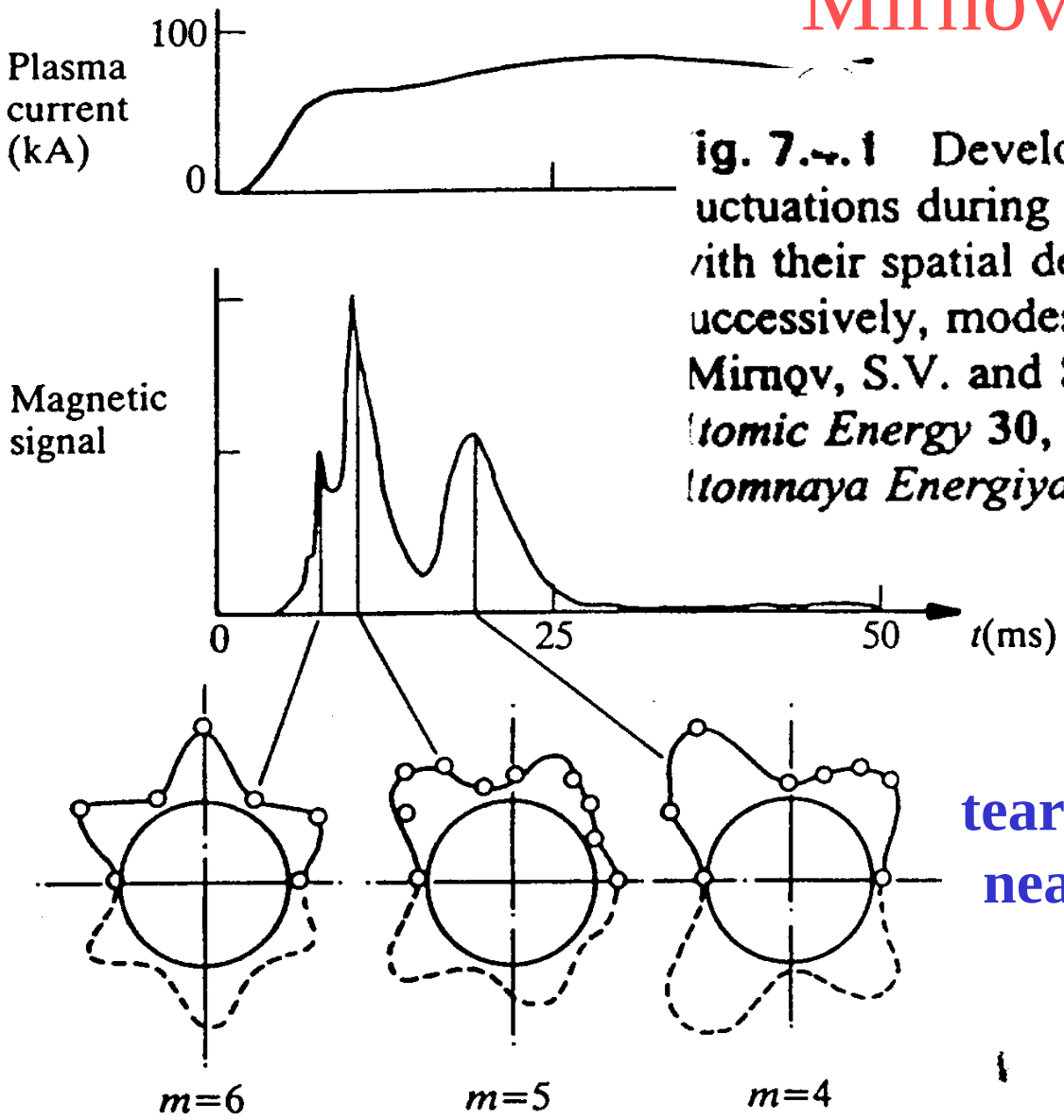


ig. 7.-.1 Development of magnetic uctuations during the current rise, together /ith their spatial dependence indicating, uccessively, modes $m = 6$, 5, and 4. Mirnov, S.V. and Semenov, I.B., *Soviet tomic Energy* **30**, 22 (1971), from tomnaya Energiya **30**, 20 (1971).

**Considered to be tearing modes with m~$q_a$ near the plasma surface**

$$q_a = \frac{aB_\phi}{RB_{\theta a}} = \frac{2\pi a^2 B_\phi}{\mu_o R I}$$

# Characteristics of Mirnov oscillations

- frequency of 1-10kHz typically
- propagation velocity has the sign of electron drift velocity
- tearing mode theory with finite Larmor radius effects
  mode frequency of the electron drift frequency

mode number

$$\omega_{*e} = \frac{mT_e}{eBrn_e}\frac{dn_e}{dr}$$

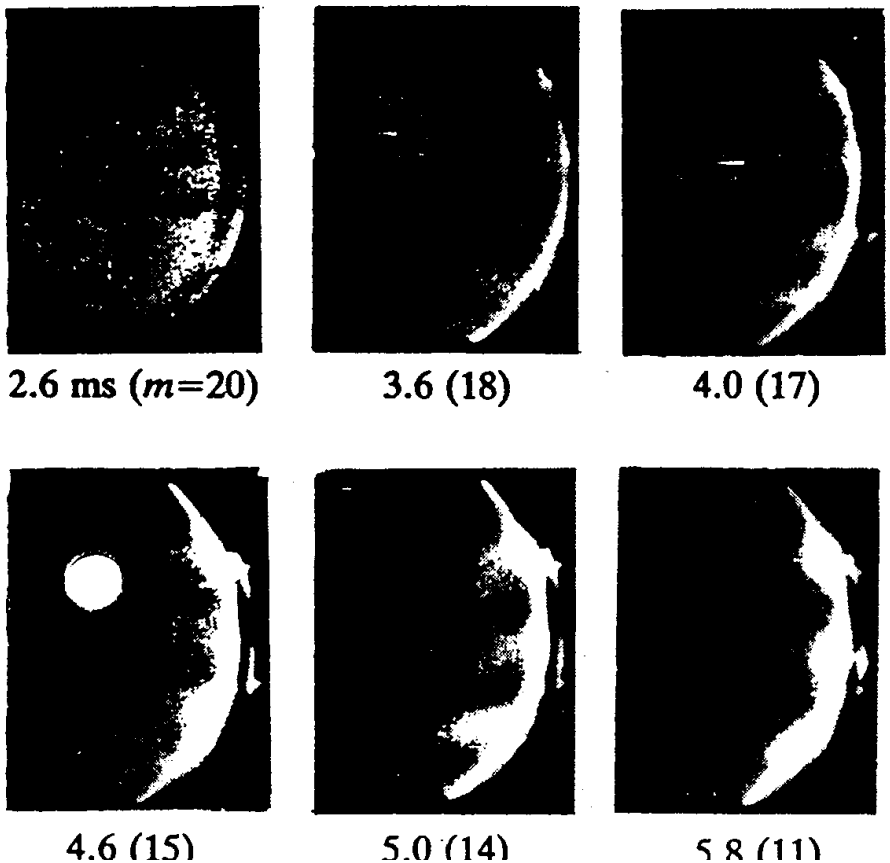


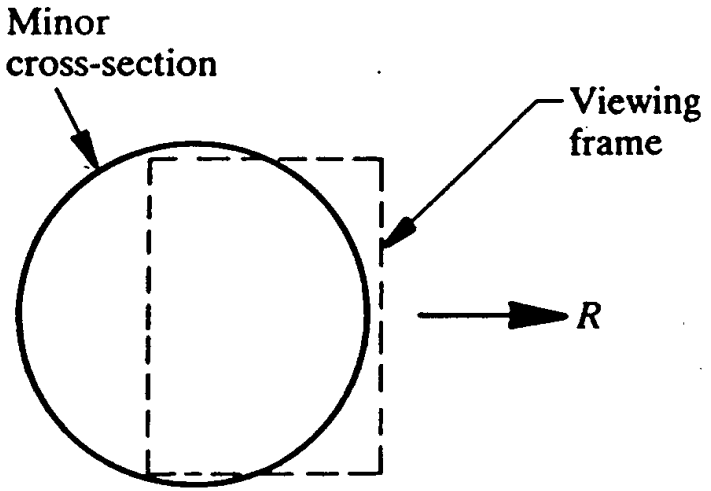


**Fig. 7.4.2** Cine photographs of instability observed during the current rise in the DITE tokamak. The time from the start of the pulse is given together with the poloidal mode number, *m*. (Goodall, D.J.H. and Wesson, J.A. *Plasma Physics* 26, 789 (1984).

# Current Penetration (Double Tearing Mode)

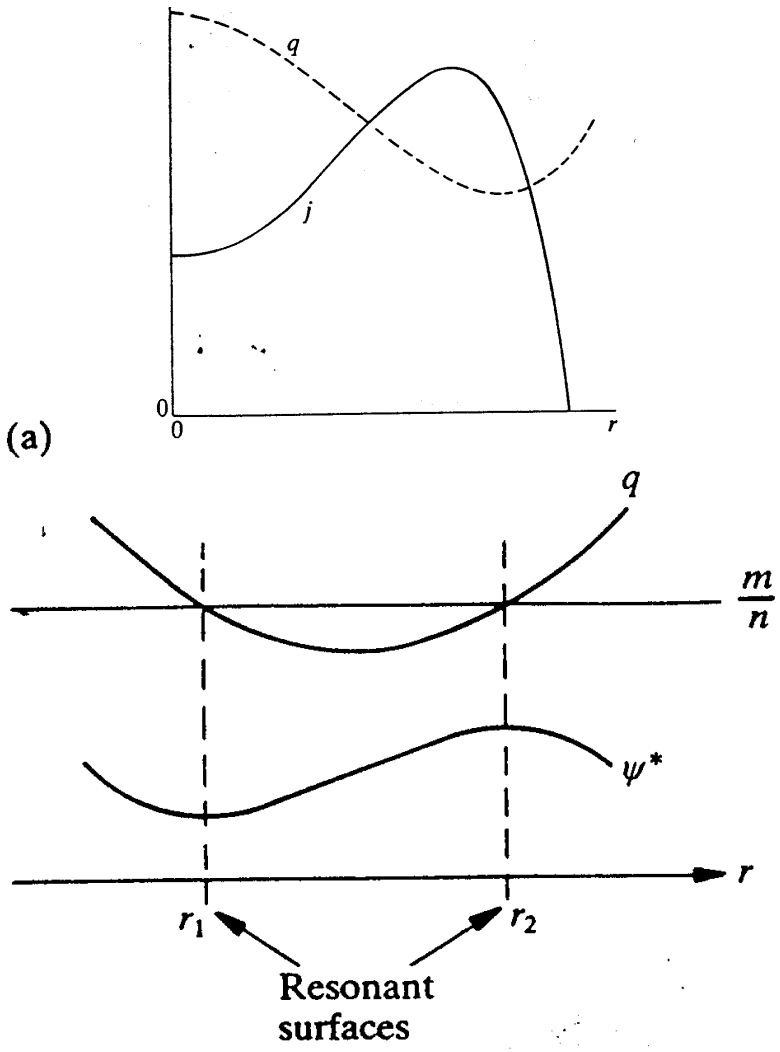


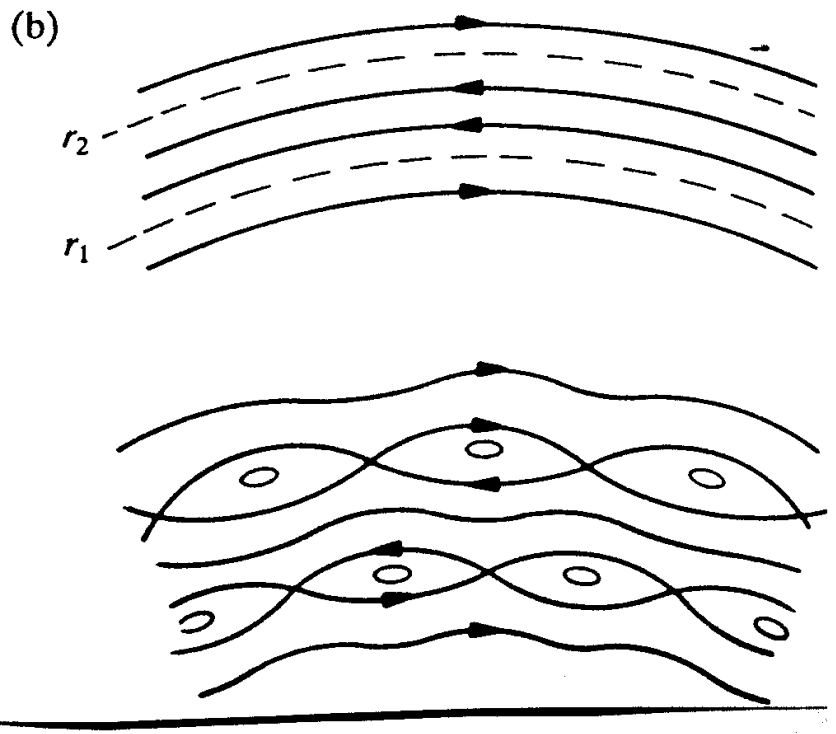


g. 7.5.2 (a) A minimum in $q$ allows o resonant surfaces with the same values $m$ and $n$. $\psi^*$ is the corresponding helical x. (b) The two resonant surfaces lead to o sets of magnetic islands.

g. 7.5.3 Graphs of $q(r)$, $\psi^*(r)$, and $j(r)$ fore the instability (dashed lines) and after e instability (full lines). The instability ttens $q$ and enhances the current netration.

# Current Penetration (Double Tearing Mode)

Tearing mode equation $$\nabla^2\psi - \frac{\mu_o dj_\phi / dr}{B_\theta(1-nq/m)}\psi = 0$$

⟶ The region between the resonances combines a destabilizing current gradient and a small value of *1-nq/m*

Helical flux of the equilibrium configuration associated with the resonance surface $$B^* = B_\theta(1-\frac{n}{m}q(r)) \quad B^* = \frac{d\psi^*}{dr}$$ ⟶ form islands

⟶ Instability flatten the profiles

dashed lines : before the instability
solid lines : after instability

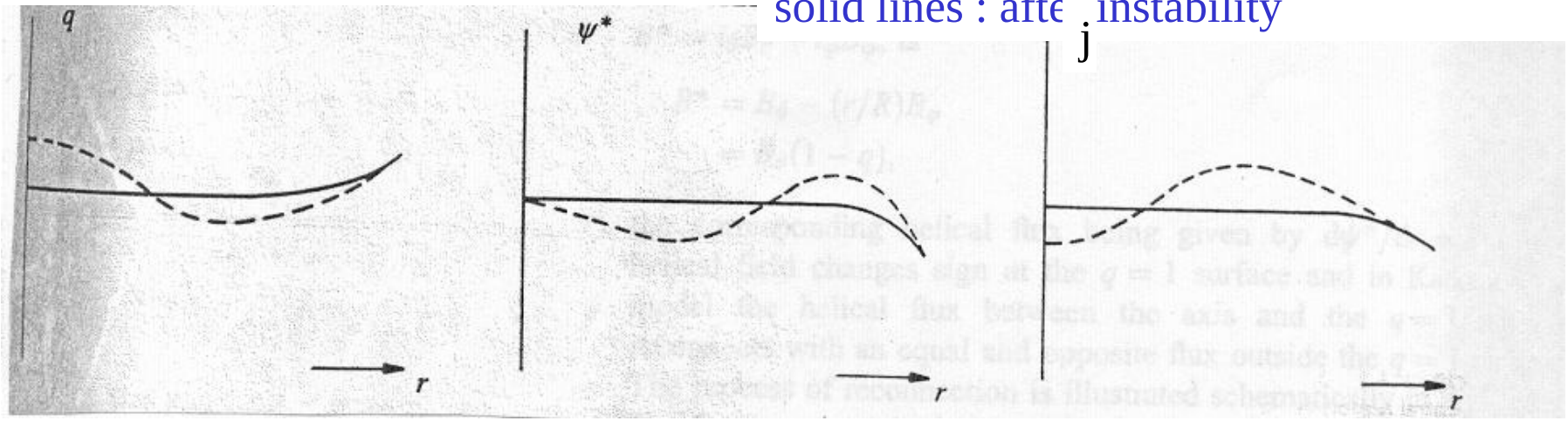

# Sawtooth Oscillations

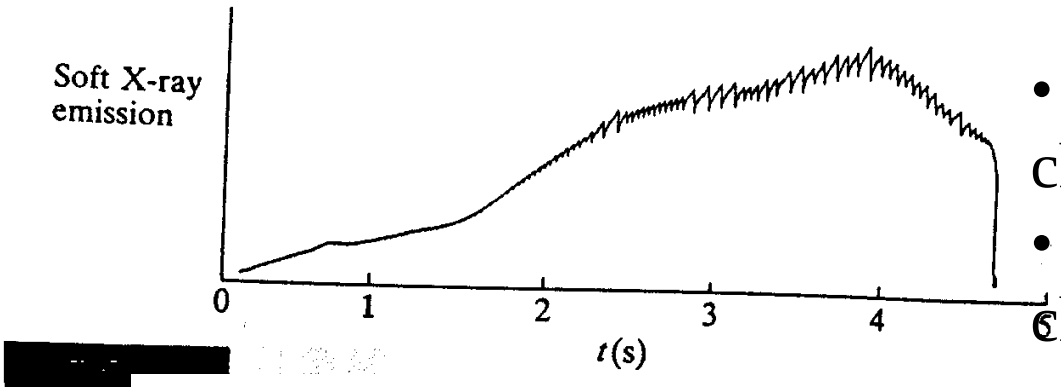


- Density and temperature change typically a few percent
- Much shorter than the characteristic resistive time

**Fig. 7.1.2** Sawtooth oscillations of the soft X-ray emission (JET).

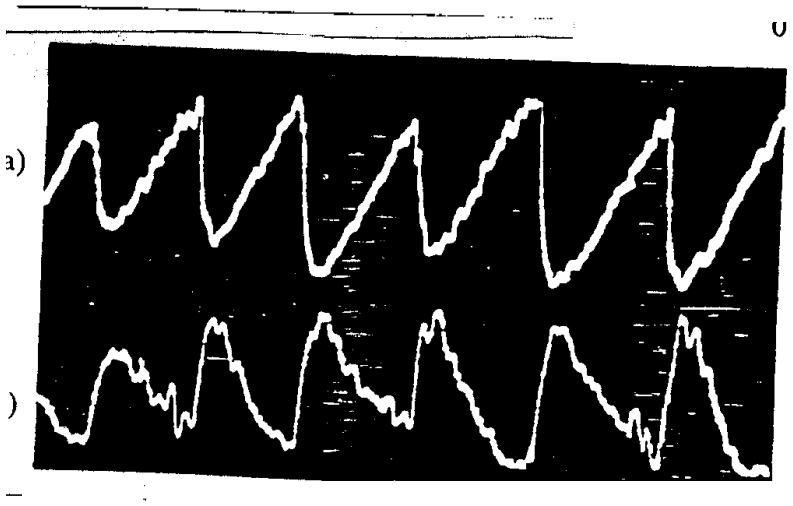

**Fig. 7.6.1** X-ray emission from (a) the central region of the plasma and (b) the outer region. (TFR.)

Heating raises central temperature and makes current profile peaked

$q_o < 1$ m=1/n=1 instability

Central temperature collapses and thermal energy released to the outer region

# Sawtooth Models

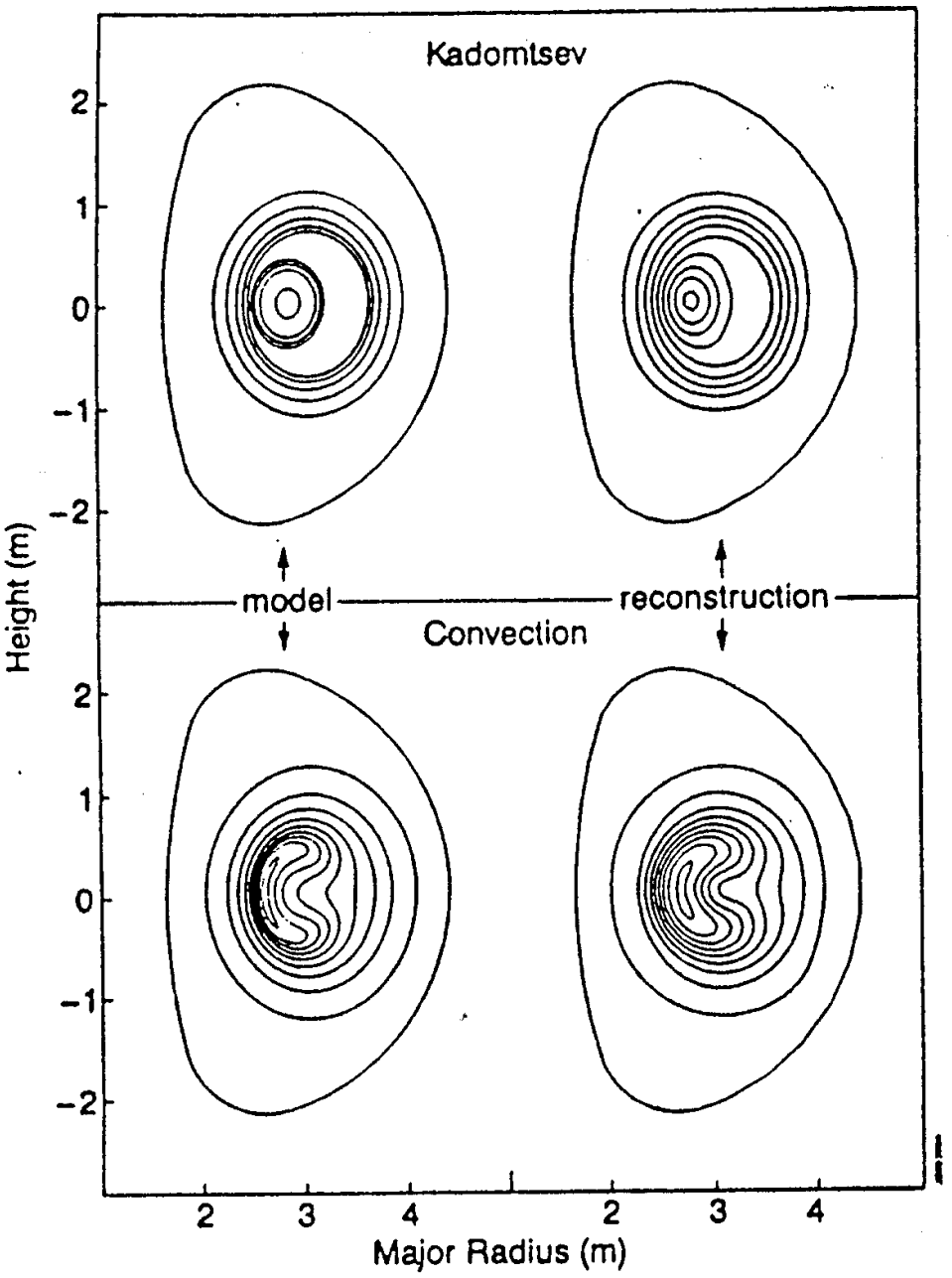


**FIG 1:** *Comparison of simulated soft X−ray analyses of the two most common models for the sawtooth collapse: full−reconnection (Kadomtsev) and 'quasi−interchange' (convection).*

# Kadommtsev's Model

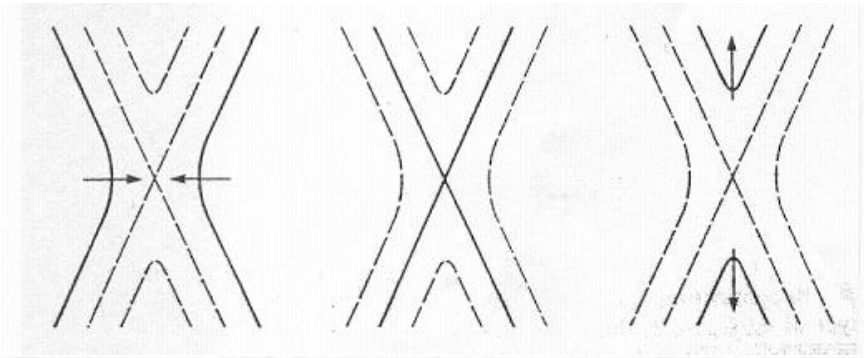

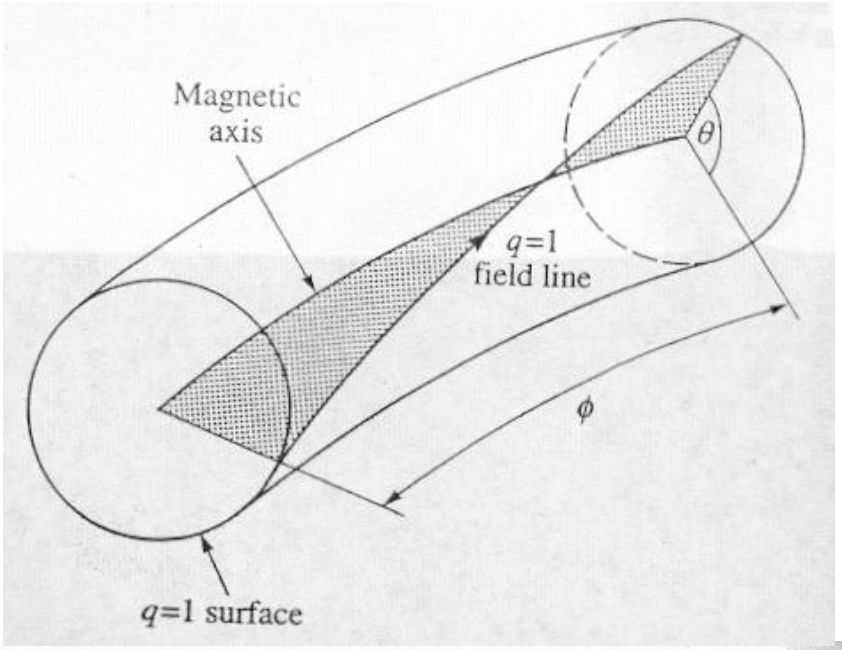


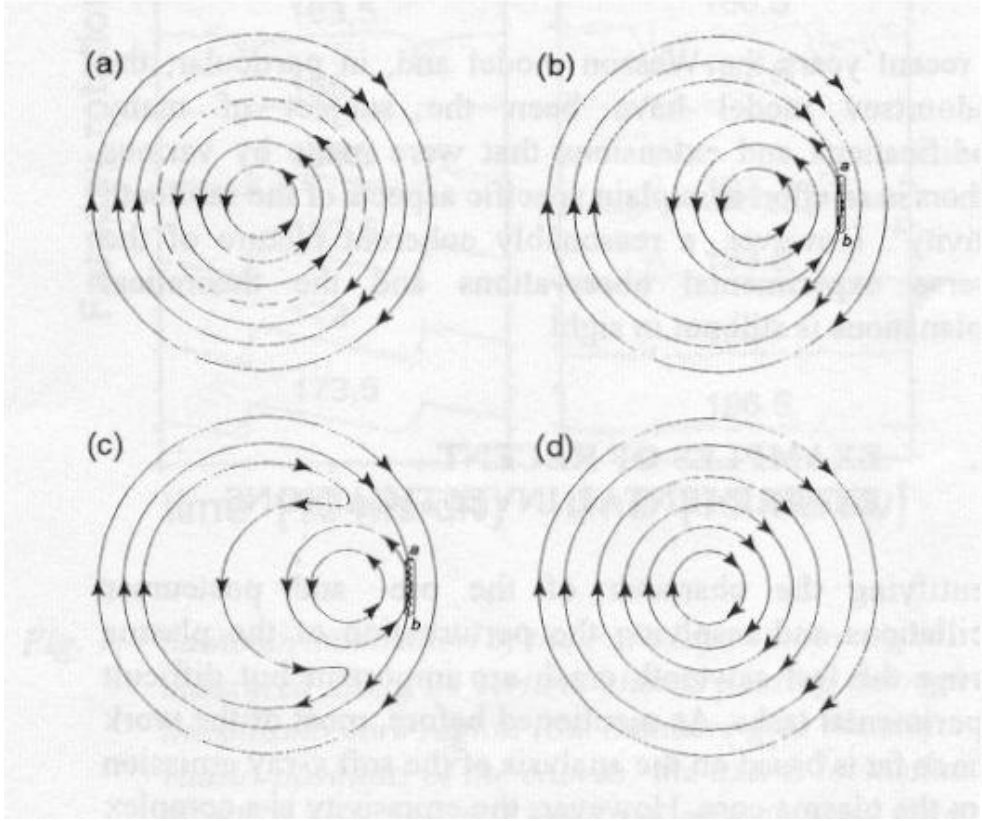


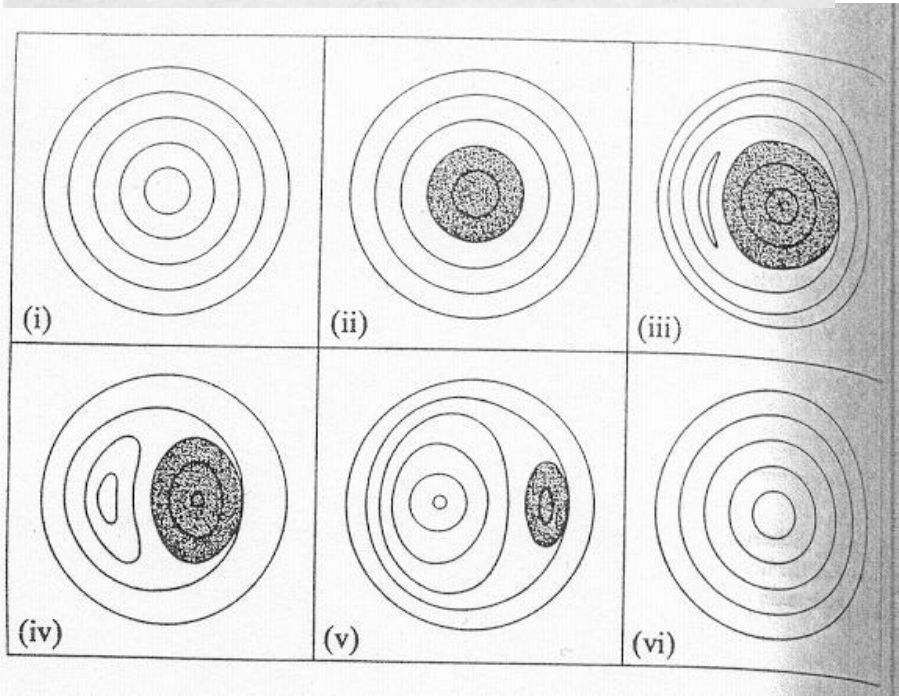

# Collapse Time

Ohm's law

$$j \sim v_1 B^* / \eta \qquad j \sim B^* / \mu_o \delta$$

Ampere's law

$$v_1 = \frac{\eta}{\mu_o \delta}$$

$$\rho v_2^2 \sim \frac{B^{*2}}{2\mu_o}$$

continuity

$$r_1 v_1 \sim \delta v_2$$

$$\delta^2 \sim \frac{\eta}{\mu_o} \frac{\sqrt{\mu_o \rho}}{B^*} r_1 \sim \frac{\tau_A}{\tau_R} r_1^2$$

**Collapse time**

$$\tau_K \sim \frac{r_1}{v_1} \sim (\tau_R \tau_A)^{1/2} \sim r_1^{3/2}$$

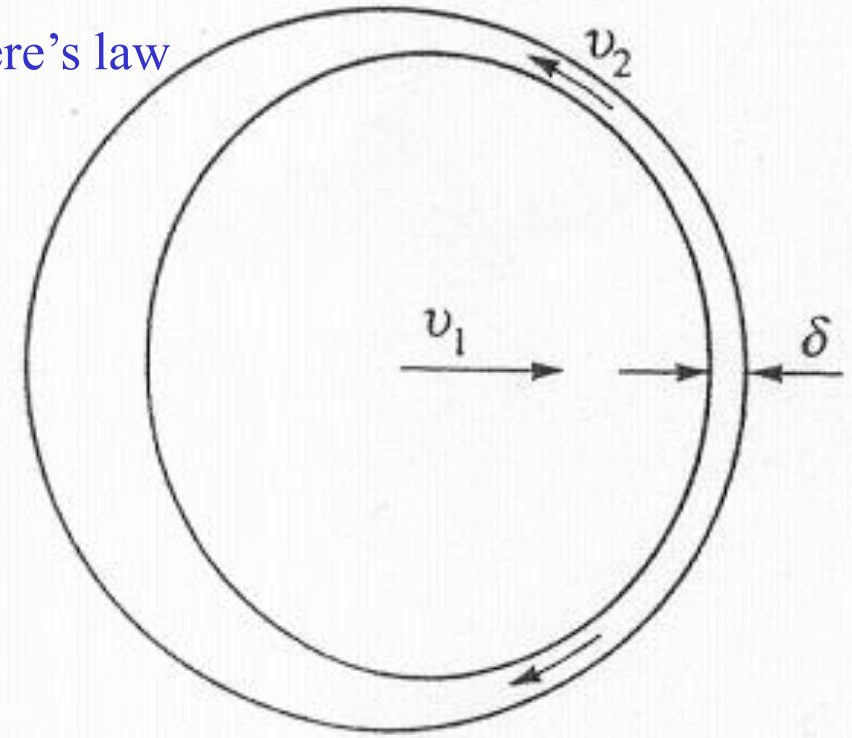


**Fig. 7.6.5** Reconnection takes place in narrow layer of thickness $\delta$, the central core moves into the layer with velocity $v_1$ and the plasma leaves the layer with velocity $v_2$.

# Discrepancy between the Model and Experiments

- Collapse time: the observed collapse time too short

JET *(~10ms vs. ~100$\mu s$)* -->quasi-interchange instability? No $q_o$*~0.7*

- Spontaneous onset: the time for equilibrium change to produce

a configuration having the observed growth rate is very much longer than the sawtooth collapse time (JET: two orders of magnitude)

- $q_o$ remains below zero
- Stability during the ramp phase:

resistive kink unstable at ramp phase expecting growth rate of less than 1 ms based on q' at q=1 surface ($\gamma \sim q'^{2/3}$)

- Thermal collapse: temperature

flattening across whole q<1 region on incomplete magnetic reconnection

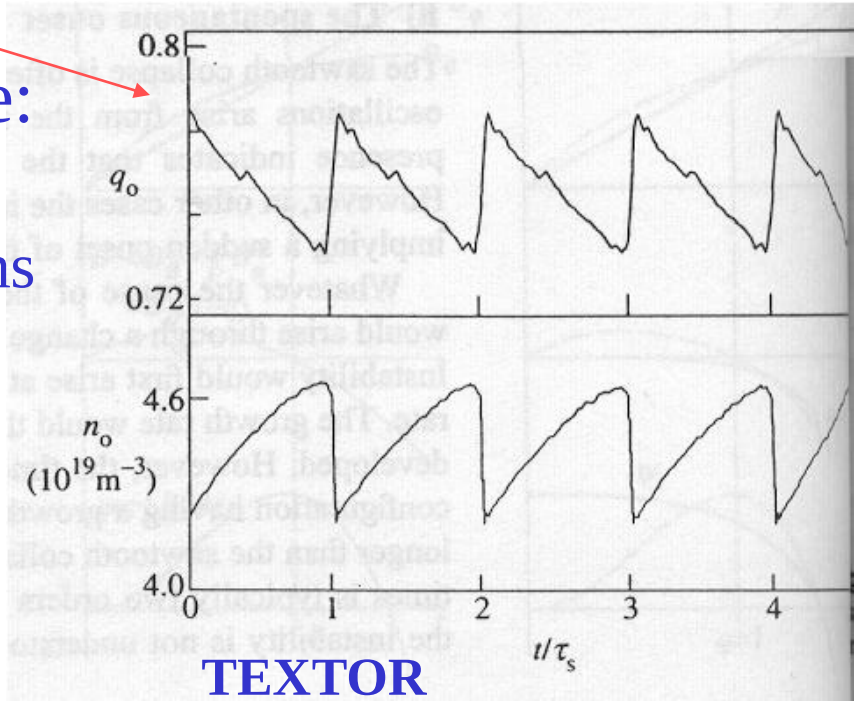

# Disruptions

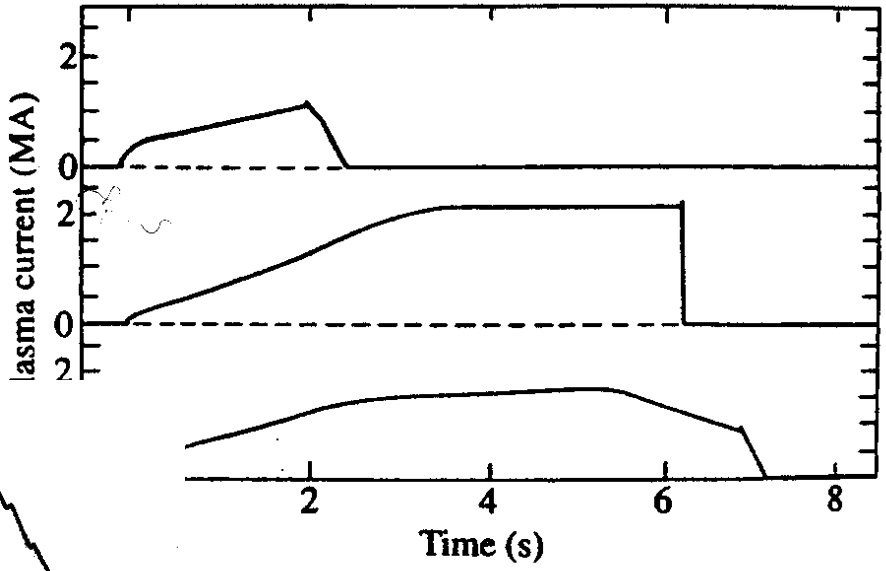


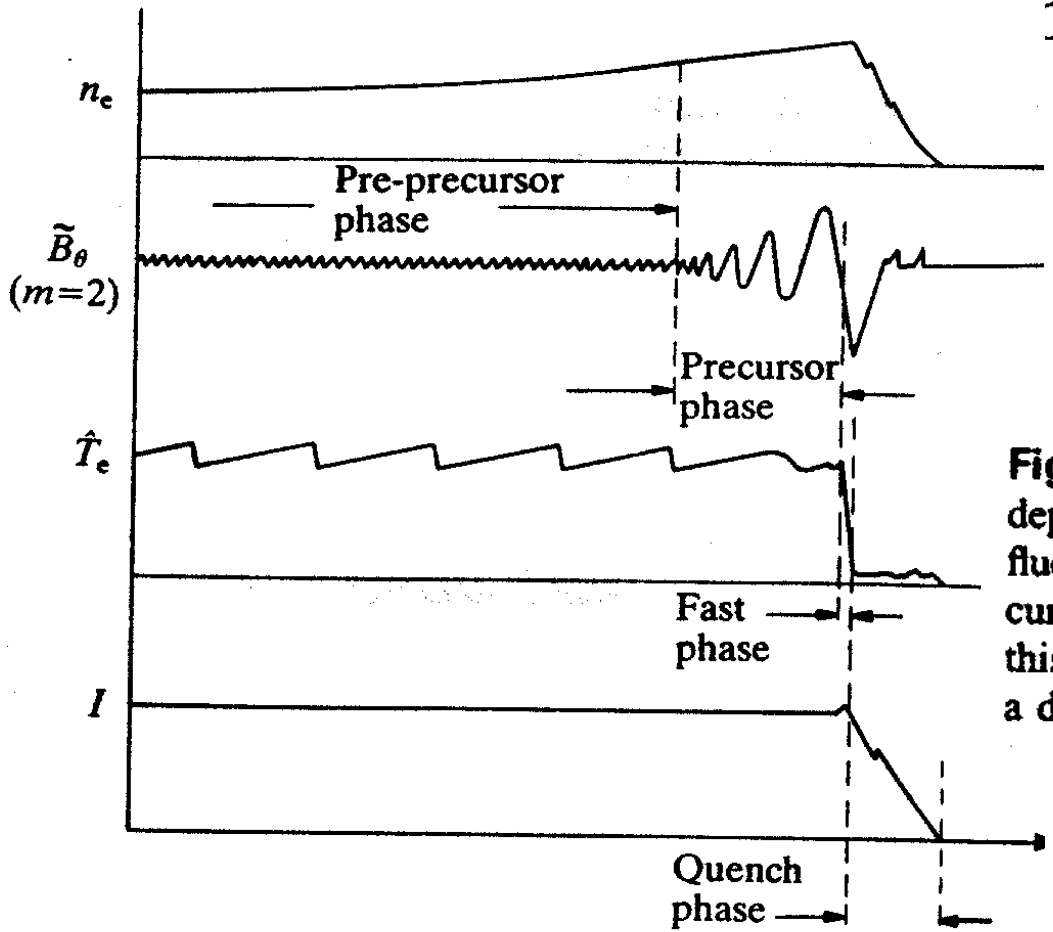


**Fig. 7.7.2** Showing typical time dependence of the $m = 2$ magnetic fluctuations, central temperature, and plasma current during the period of a disruption. In this example the disruption is precipitated by a density increase as shown.

# Causes of Disruptions

- Low-q disruptions
- Density limit disruptions

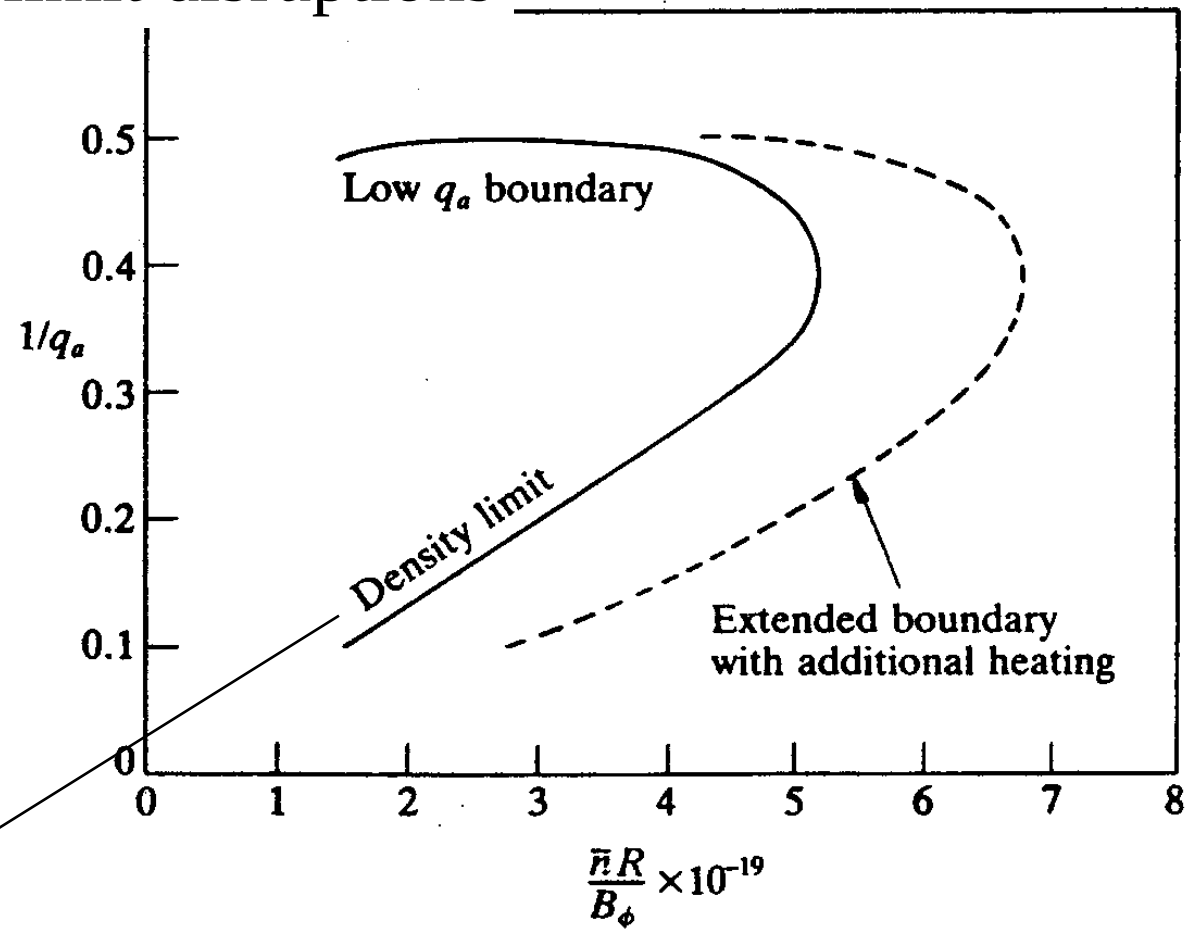


Murakami

Greenwald density limit $\bar{n}(10^{20}\,m^{-3}) < I(MA)/\pi a^2$

# Physics of Disruptions

- Tearing mode instability
- Non-linear growth of the tearing mode : mode locking
- The fast phase (Thermal quench)
- Current decay (Current quench)
- Runaway electron current
- Vacuum vessel current (Halo currents)

- Mode locking
- Error field instability
- Vertical disruption event(VDE)
- Ergodicity

# Mode Locking

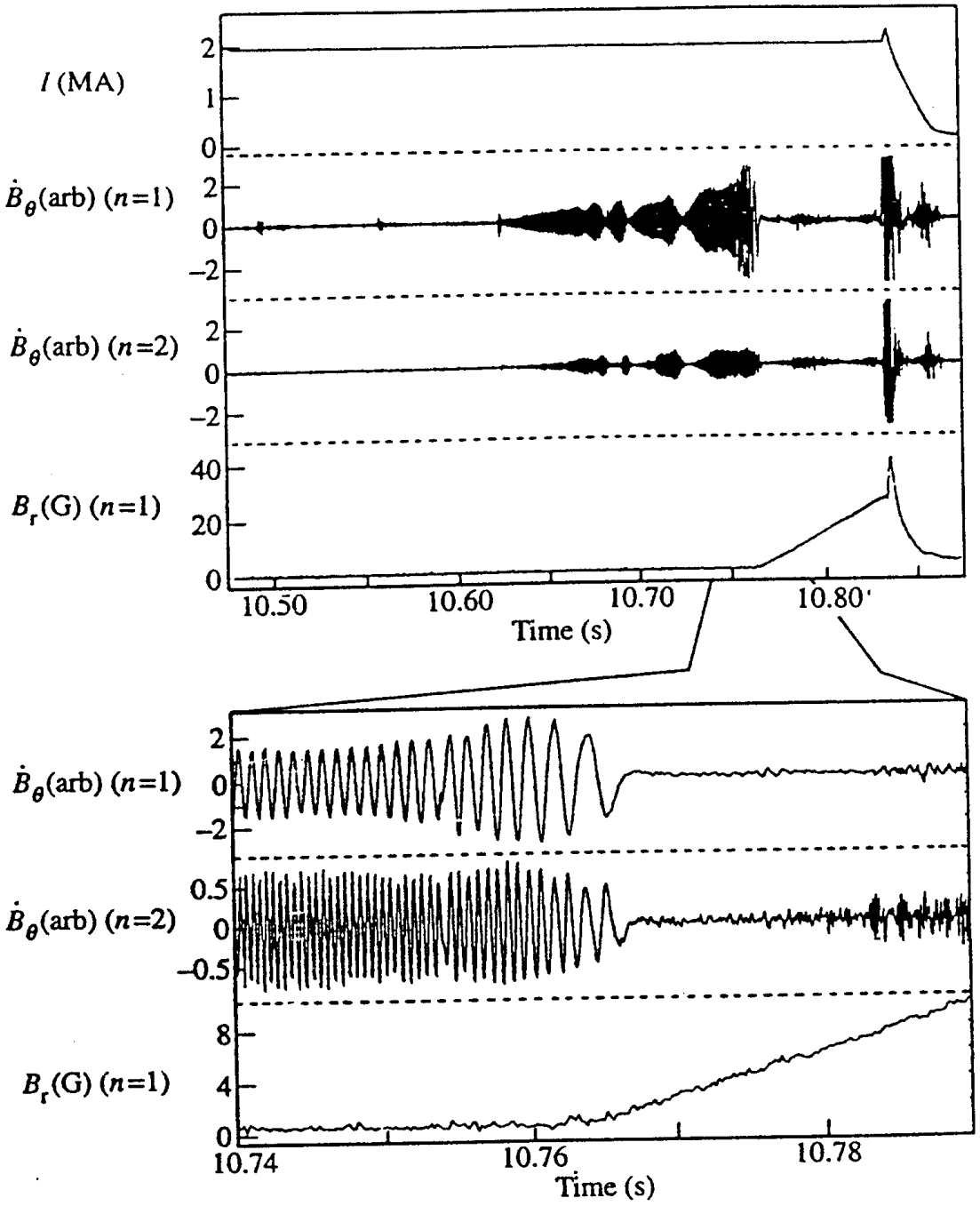


**ig. 7.9.3** An example of the growth of hd instabilities in a disruption, with xpanded traces around the time of mode- xking. The bottom trace gives the time ntegrated $\dot{B}_r$ signal, showing the continued nstability growth following mode-locking. Wesson J.A. *et al.*, *Nuclear Fusion*, 29, 641 1989).)

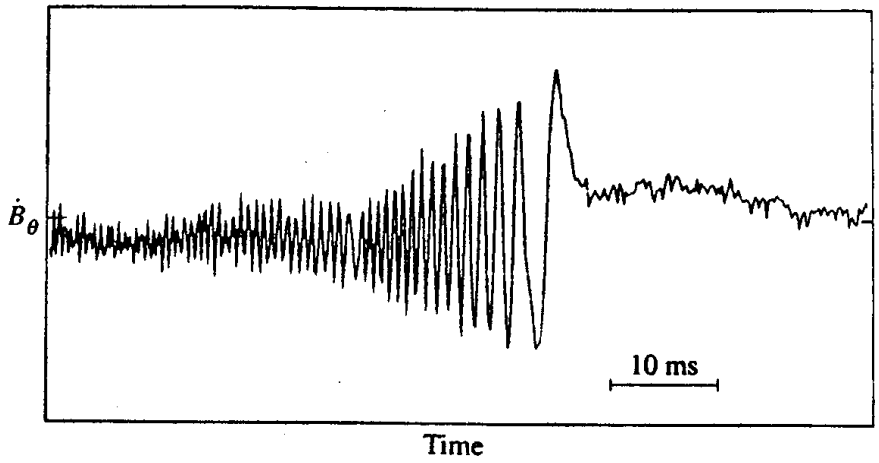


**Fig. 7.10.1** The magnetic signal $\dot{B}_\theta$ shows the frequency and growth of an $n = 1$ tearing mode. The reduction in frequency corresponds to a fall of the propagation speed, and the removal of the gross oscillation indicates the final mode locking (JET).

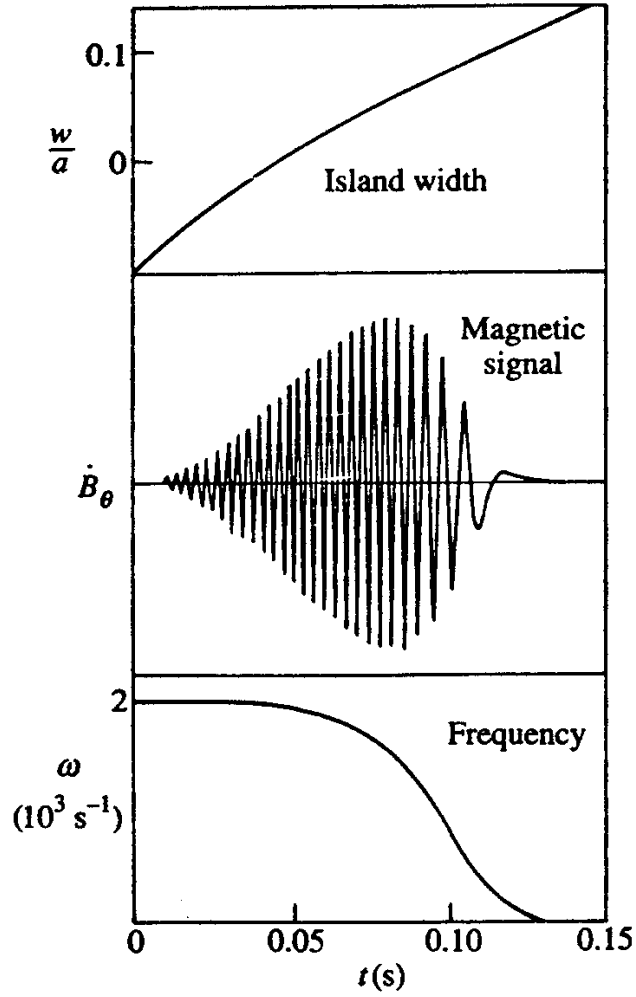


**Fig. 7.10.2** Self-consistently calculated growth and mode-locking for an $m = 2$ tearing mode (Nave, M.F.F., and Wesson, J.A., *Nuclear Fusion* **30**, 2575 (1990).)

# Thermal and Current Quench

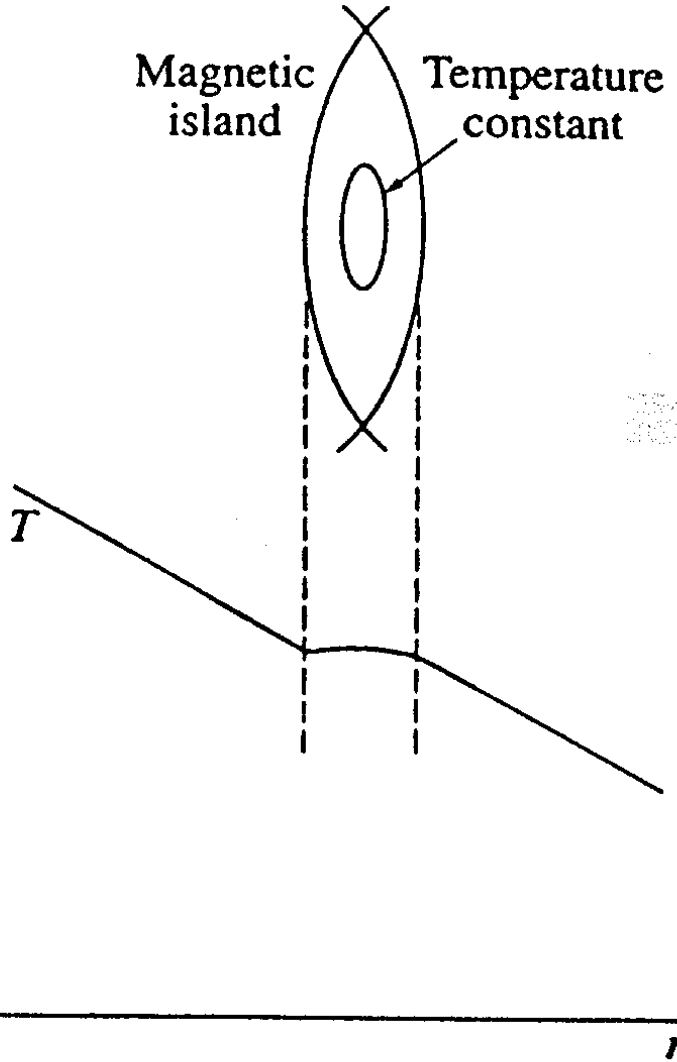


**Fig. 7.9.4** The temperature across the midplane of a magnetic island is flattened through the equalization of the temperature around the interior flux surfaces.

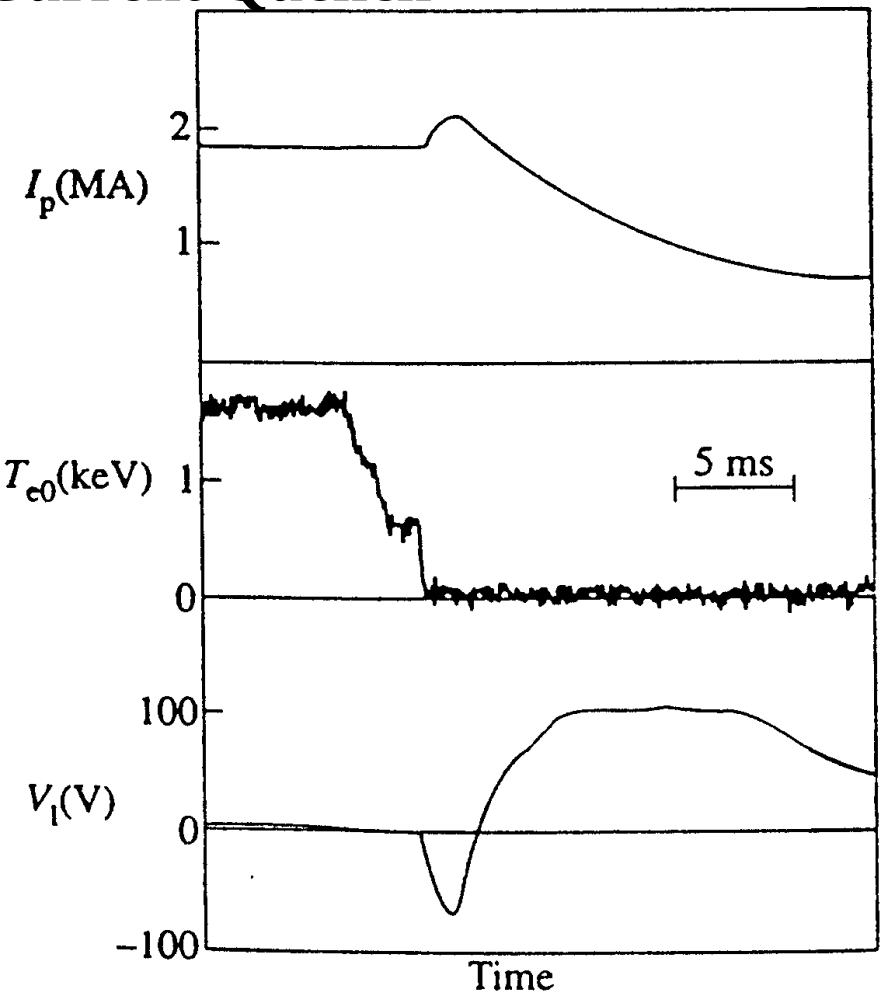


**Fig. 7.9.5** At the time of disruption, indicated by the fall in $T_e$, there is an increase in plasma current and an associated negative voltage spike. (Wesson, J.A., Ward, D.J. and Rosenbluth, M.N., *Nuclear Fusion* 30, 1011 (1990).)

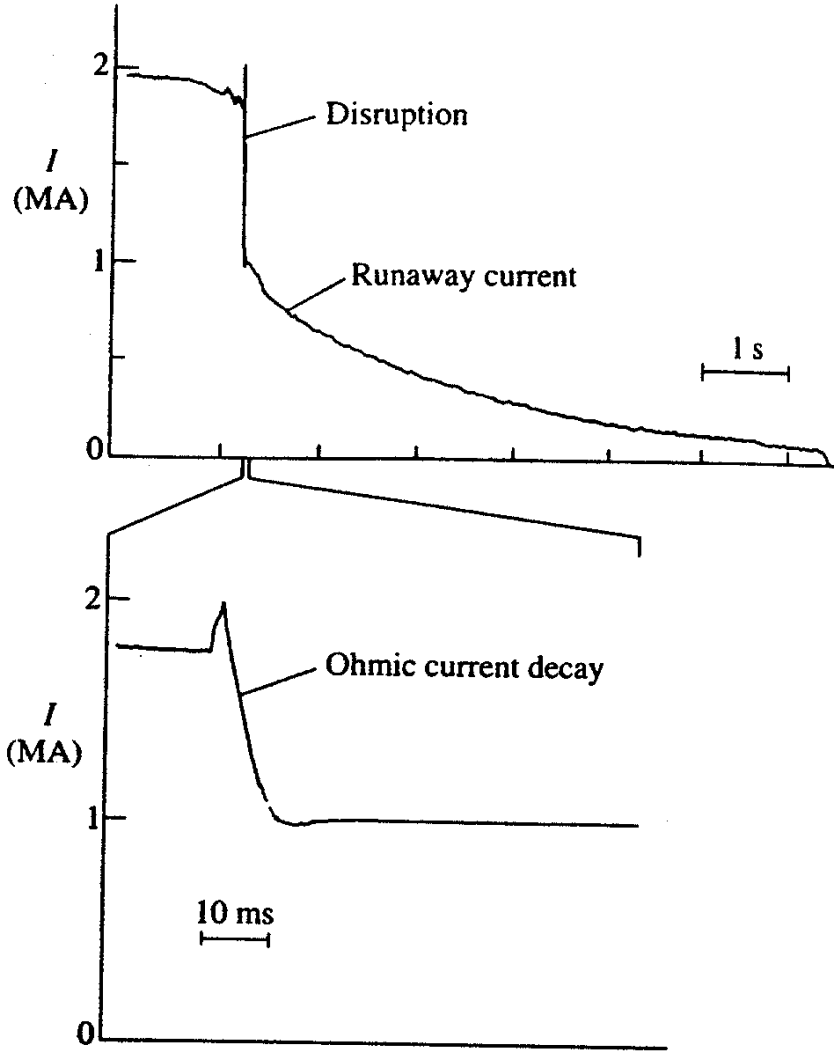


**Fig. 7.9.7** Runaway electron current formed at a disruption together with an expanded trace showing the decay of the ohmic current (JET).

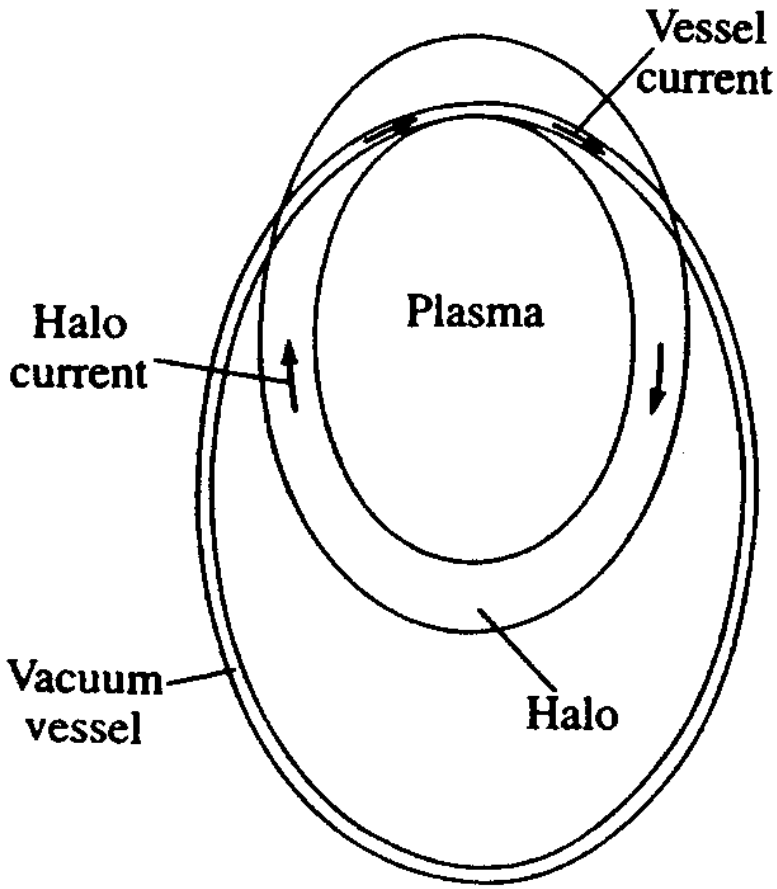


**Fig. 7.12.1** Showing the intersection of the plasma with the vacuum vessel in a vertical instability, resulting in a halo which carries current to the vessel.

# Other Instabilities

- Fishbone instability
- Toroidal Alfven eigenmodes (TAE)
- ELM (edge localized mode)
- MARFE (Radiation instability, not MHD)
- Operational overview

# Fishbone Instability

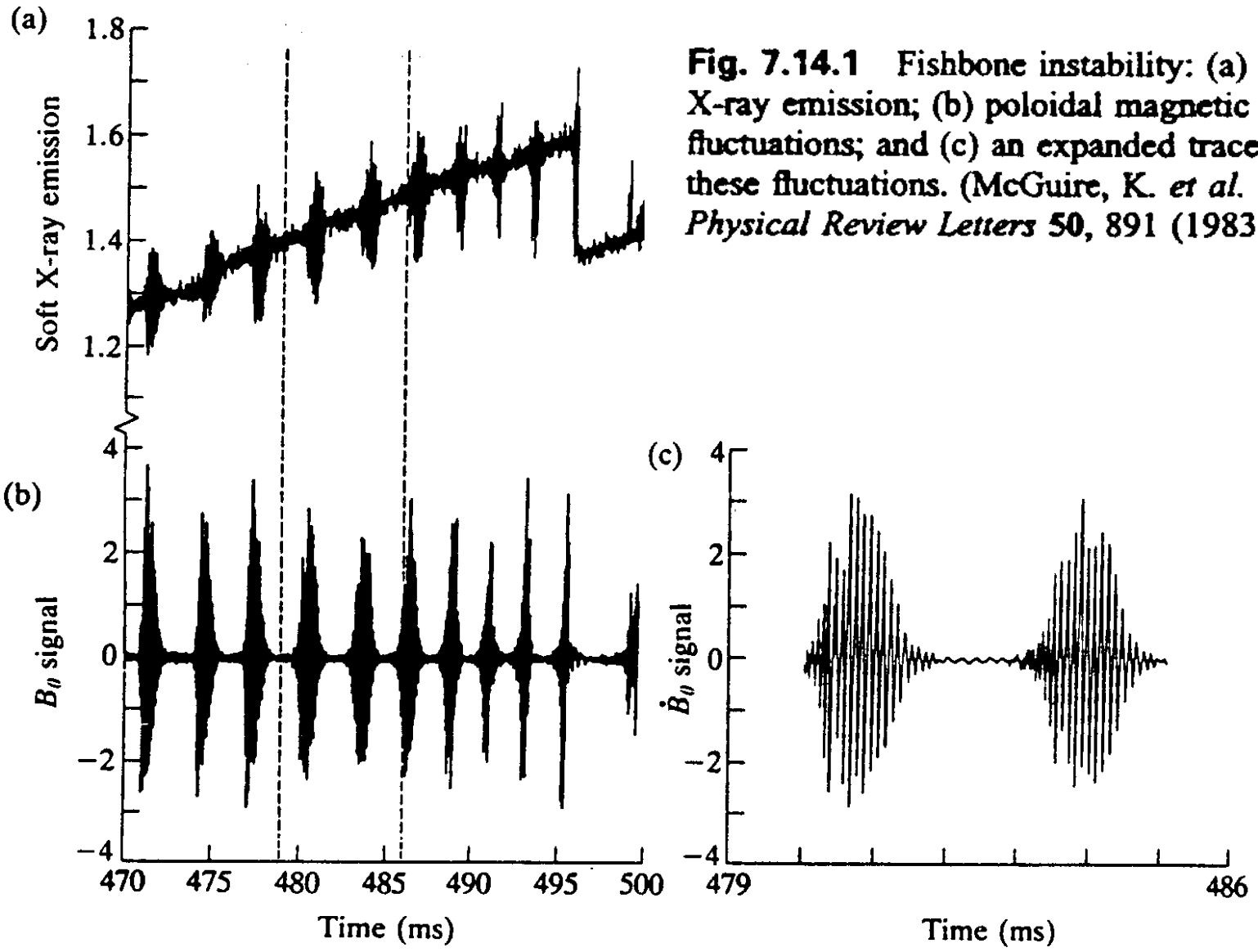


**Fig. 7.14.1** Fishbone instability: (a) soft X-ray emission; (b) poloidal magnetic field fluctuations; and (c) an expanded trace of these fluctuations. (McGuire, K. *et al.* *Physical Review Letters* **50**, 891 (1983).)

# Fishbone Instability: Stability Boundary

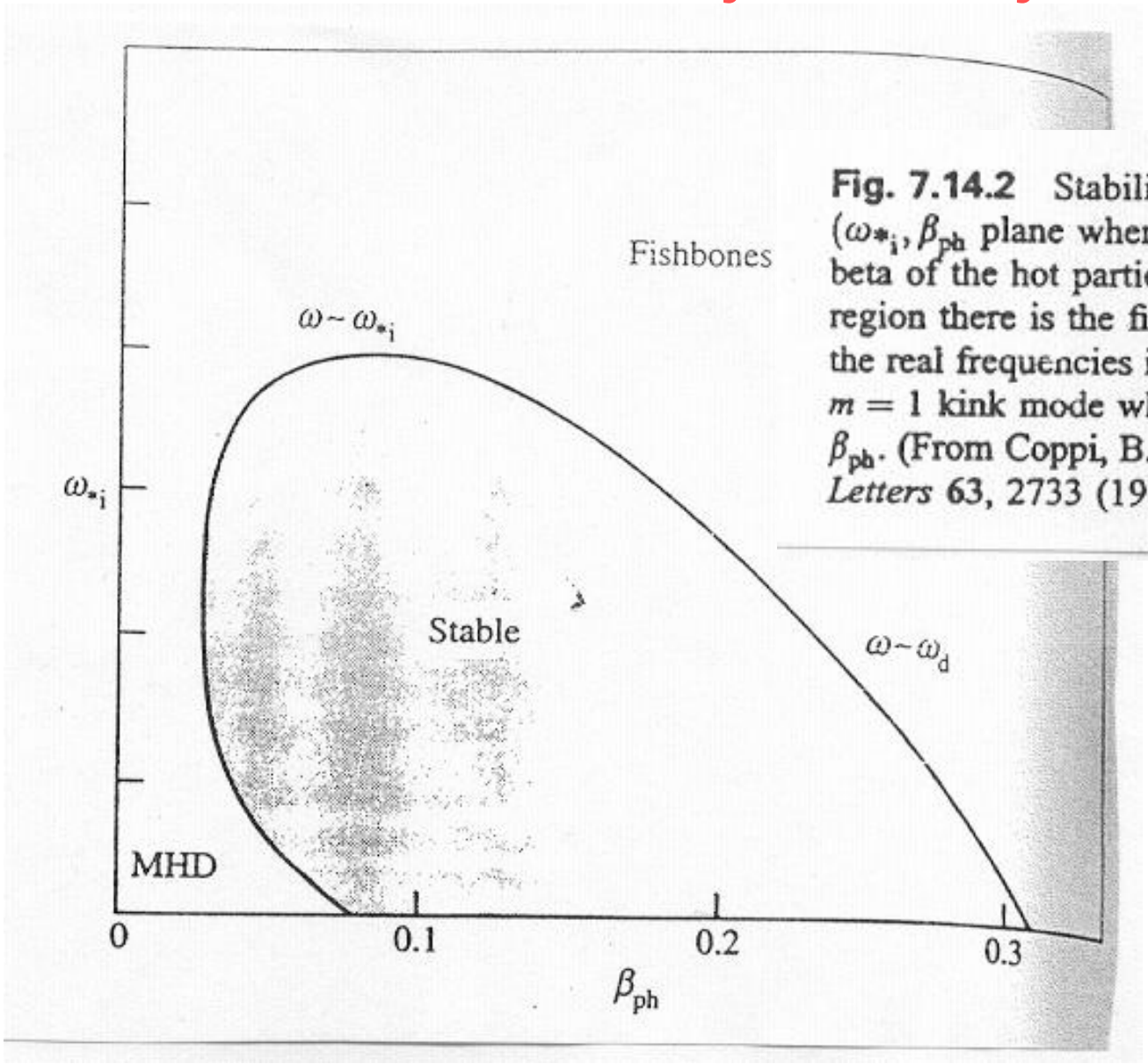


**Fig. 7.14.2** Stability diagram in the $(\omega_{*_i}, \beta_{ph}$ plane where $\beta_{ph}$ is the poloidal beta of the hot particles. Outside the stable region there is the fishbone instability, with the real frequencies indicated, and the MHD $m = 1$ kink mode which appears at small $\beta_{ph}$. (From Coppi, B. *et al.*, *Physical Review Letters* 63, 2733 (1989).)

# Toroidal Alfven Eigenmodes (TAE)

- MHD wave equation of shear effect (large aspect ratio)

$$\frac{d}{dr}\left[(\rho\omega^2 - F^2)r^3\frac{d\xi}{dr}\right] - (m^2-1)[\rho\omega^2 - F^2]r\xi + \omega^2 r^2\frac{d\rho}{dr}\xi = 0$$

$$F = (m - nq)B_\theta/\mu_0^{1/2}r. \qquad m - nq = \pm\frac{\omega r}{B_\theta/(\mu_0\rho)^{1/2}}.$$

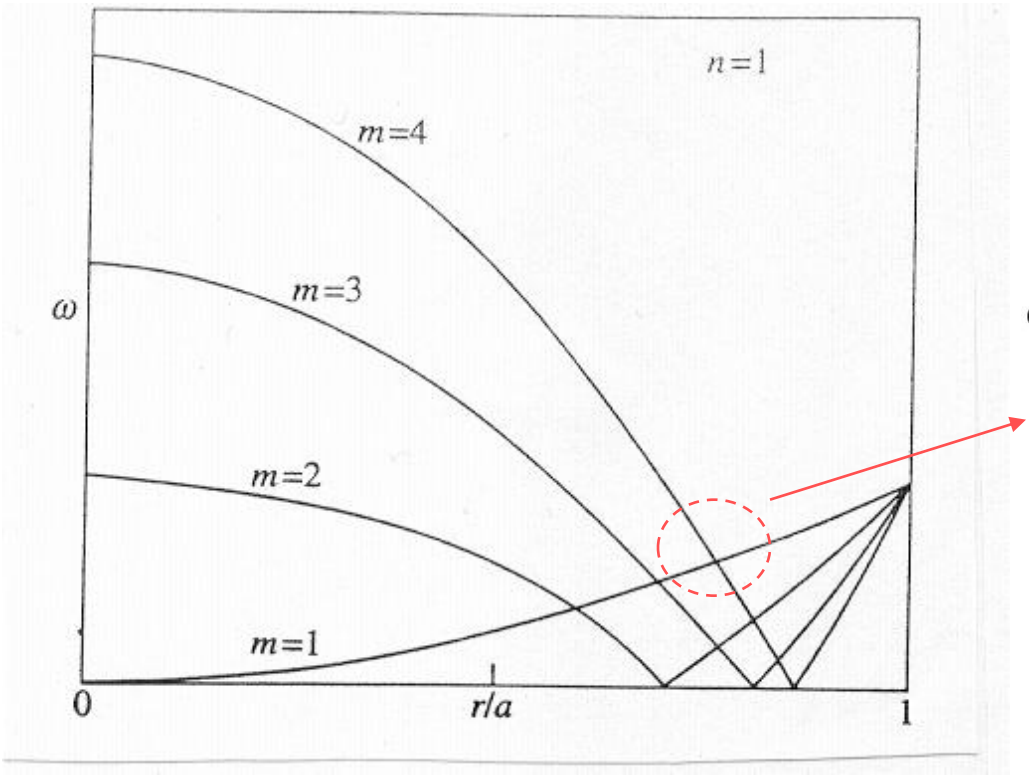


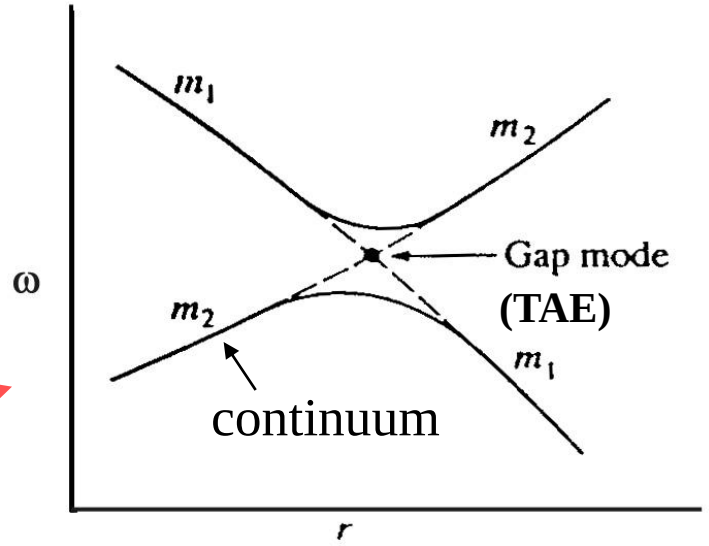

# Instability growth rate γ

$$\frac{\gamma}{\omega_0} \simeq \frac{9}{4} + \beta_z \left(\frac{\omega_{*\alpha}}{\omega_0} - \frac{1}{2}\right) F\left(\frac{V_A}{V_\alpha}\right) - D \quad \text{(Damping)}$$

$F(x)=x(1+2x^2+2x^4)\exp(-x^2)$; predominantly associated with $V_\alpha$ around or above $V_A$

- Without damping, TAE is unstable to all m's.
- Stability depends on magnitude and m dependence of damping.
- Finite orbit effects limit the increase of destabilizing term with m
- Small m's, typically 2-6 are most unstable.

## Four main contributions to damping

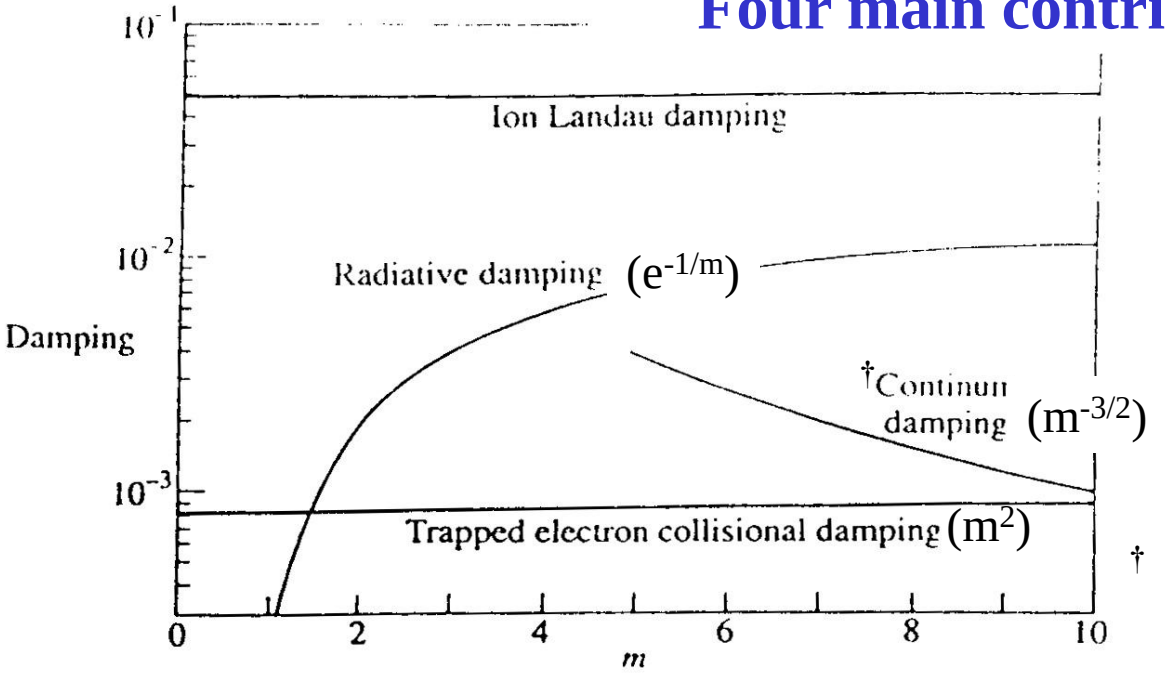


† Coupling to continuum damping is predominate at low m.

# ELM
# (edge localized mode)

**Fig. 7.17.2** Discharges with and without ELMs, showing the increase in electron density and impurity accumulation associated with the ELM-free case. Note that the iron emission line signals are amplified in the case with ELMs. (ASDEX Team, *Nuclear Fusion* **29**, 1959 (1989).)

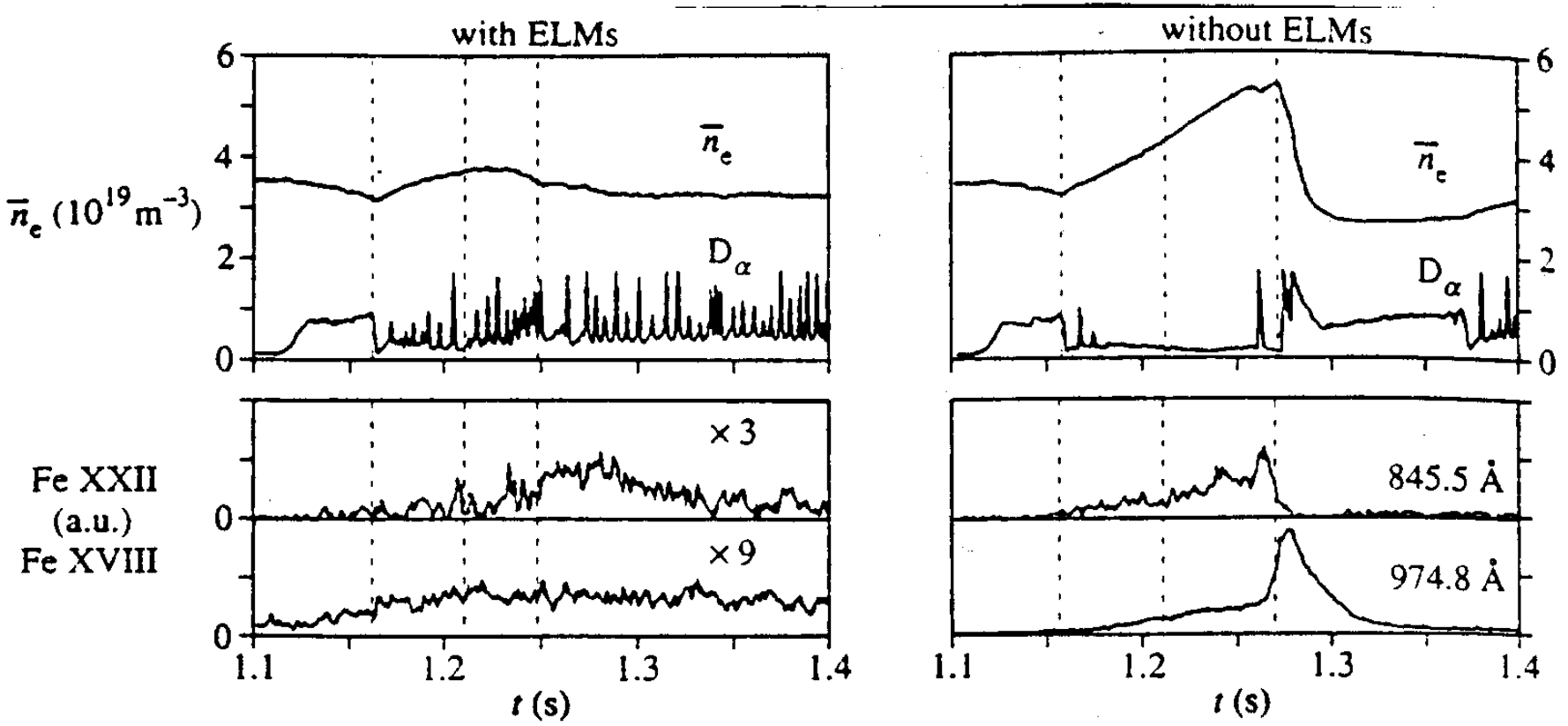

# Types of ELMs

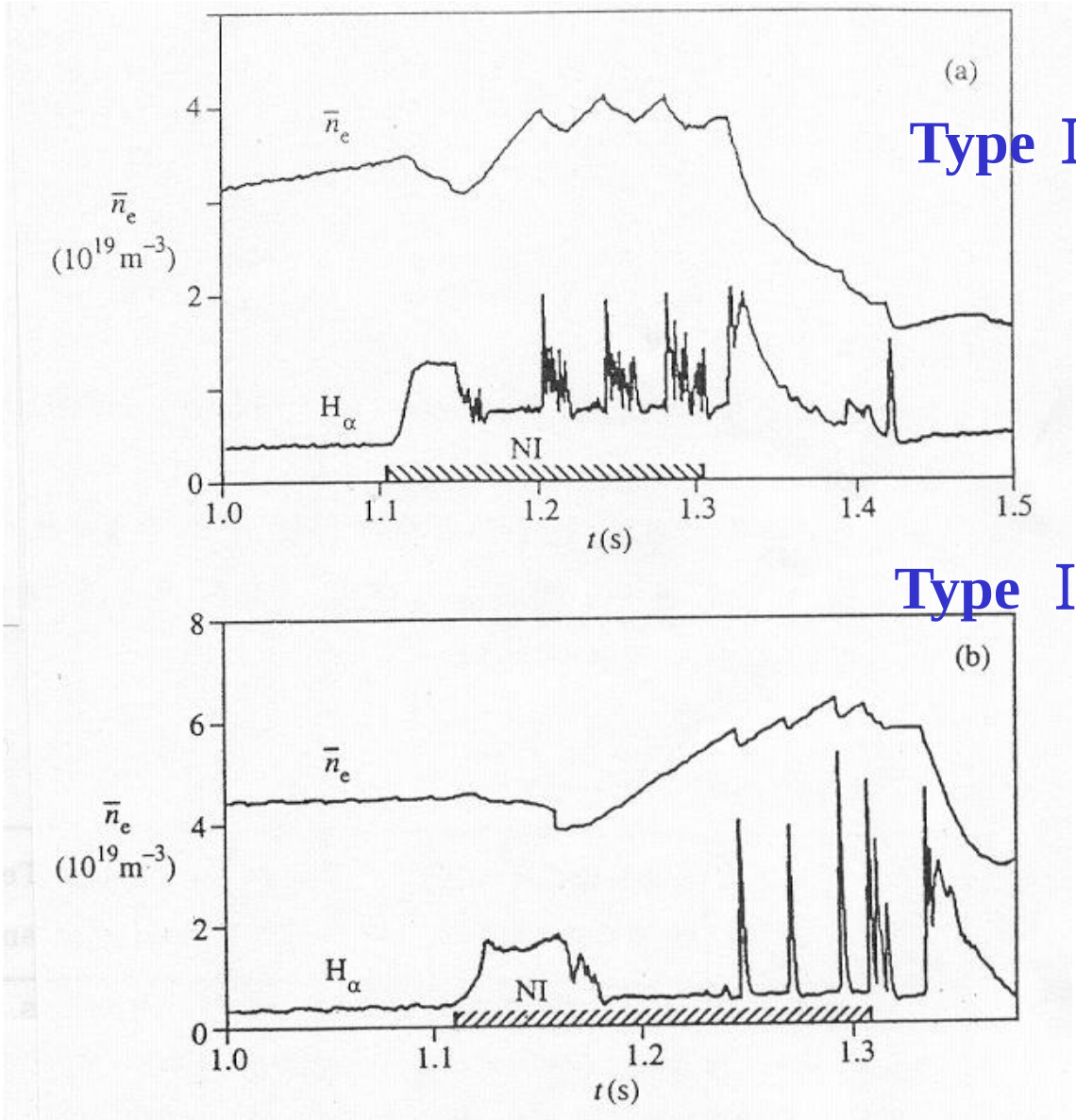


**Type Ⅱ ELMs (Grassy ELMs)**

**Type Ⅰ ELMs (Giant ELMs)**

# MARFEs
# (Multifaceted Asymmetric Radiation from the Edge)

- Plasma locally cooled by radiation in circumstances where the cooling itself leads to increased radiation and hence further cooling
- Radiation instability of MARFE occurs on the inner side of tokamak or the X-points of diverted plasmas

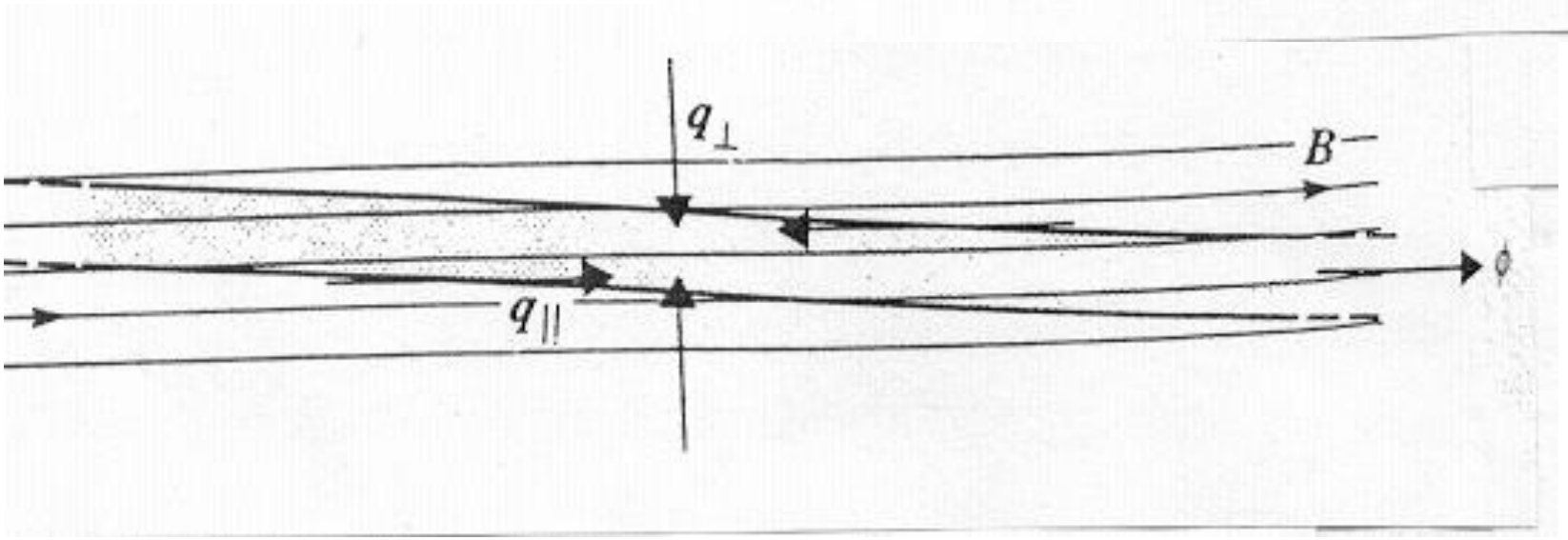


**Fig. 7.16.1** The MARFE region, shown shaded, is cooled by radiation and heated by the stabilizing perpendicular and parallel heat fluxes.

# Stability Diagram

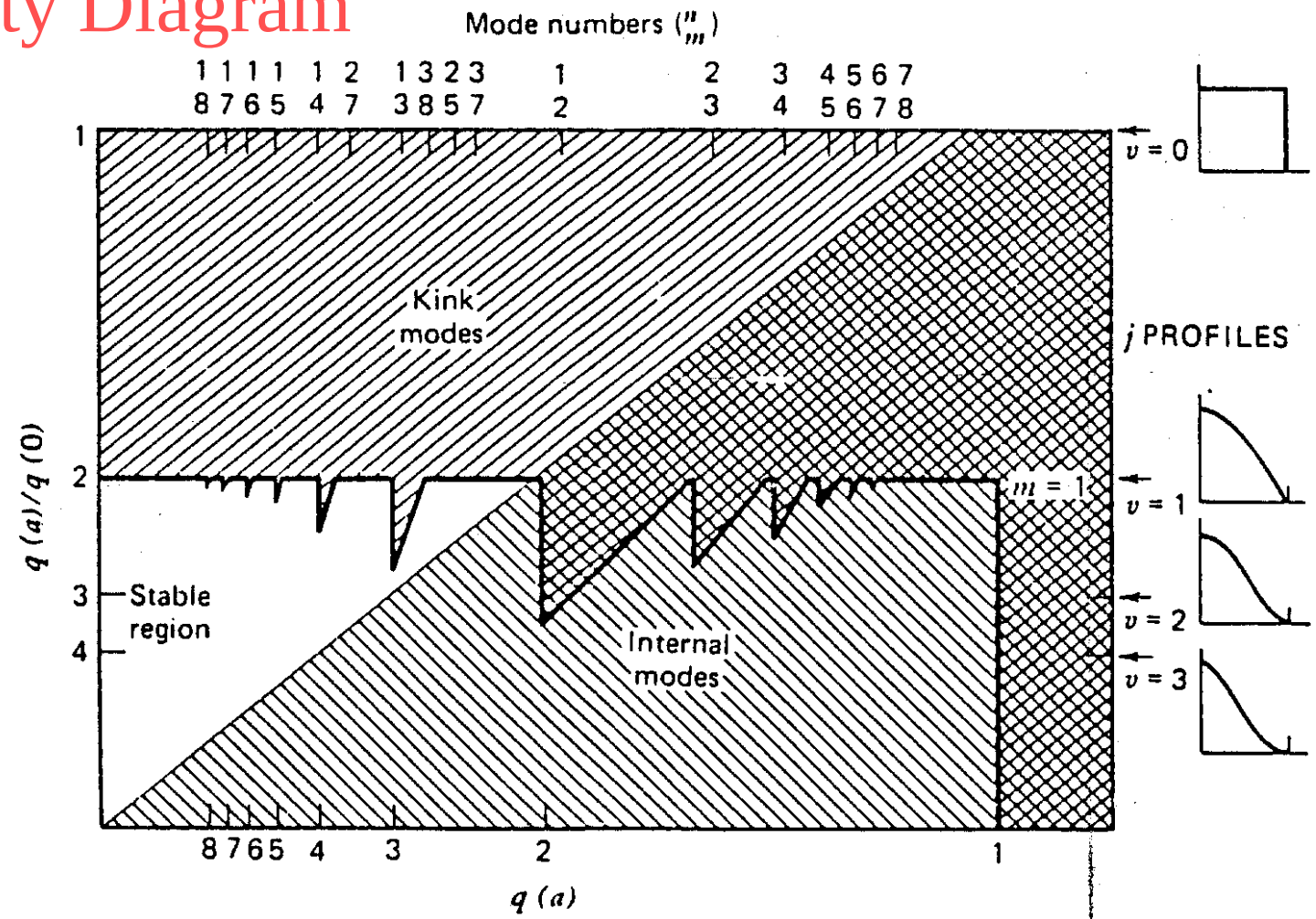


**FIGURE 5.7.** Stability diagram for ideal kink and internal modes of a large-aspect-ratio circular cross-section tokamak. The current distribution is $j_\phi(r) = j_\phi(0)[1 - r/a)^2]^\nu$. Complete stability against kink modes may be obtained for any $q(a) > 1$ by sufficient peaking of the current profile (larger value of $\nu$). The maximum stable current for this model is obtained with a parabolic current distribution with $q(0) = 1$ and $q(a) = 2$. (Data from J.A. Wesson [17].)

# Operational Overview

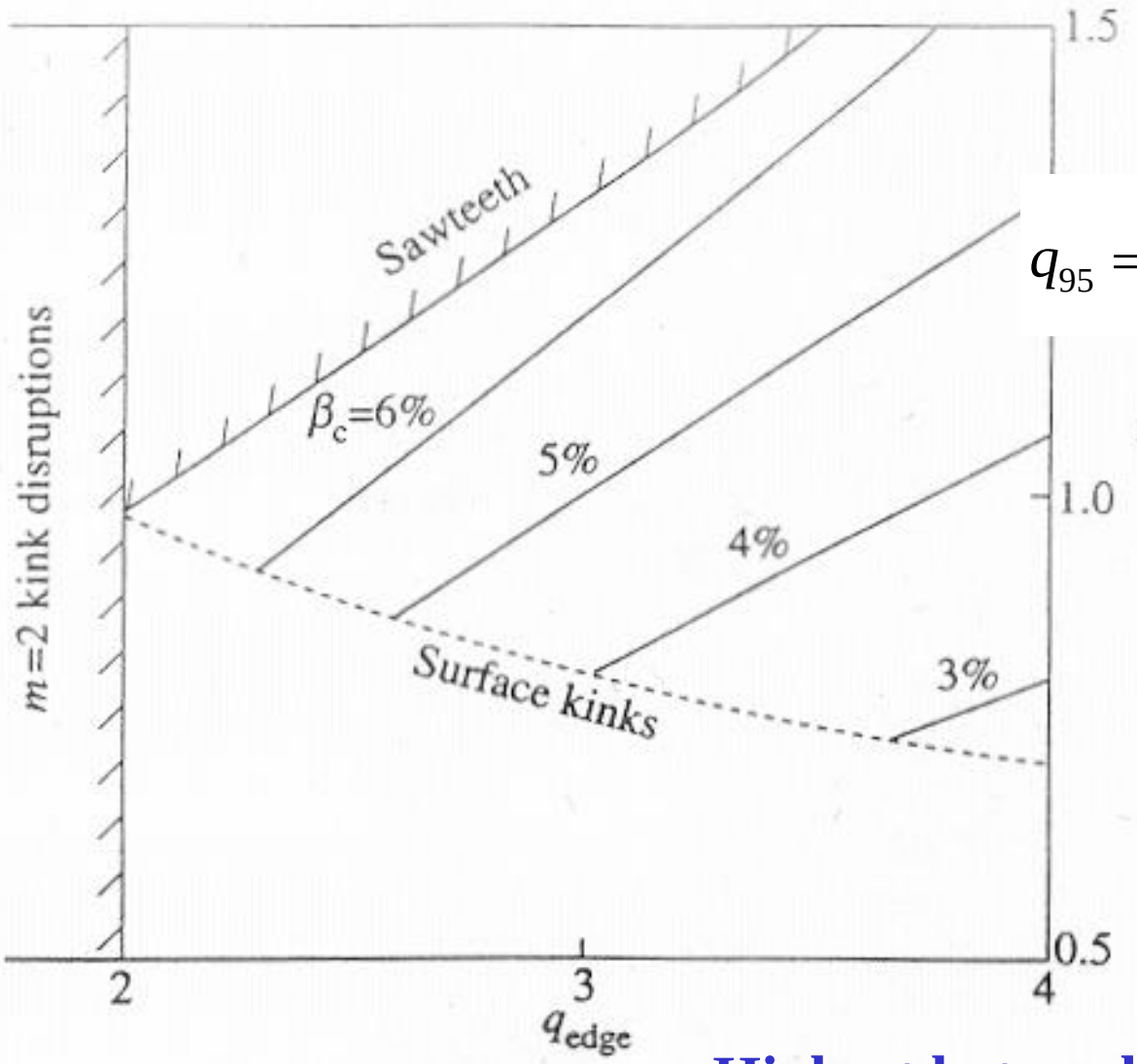


$$\beta_c[\%] = 4 l_i \frac{I[MA]}{aB_\phi}$$

$$q_{95} = \frac{5a^2 B}{2RI}\left(1+\frac{b^2}{a^2}\right)\left(1+\frac{2}{3}\frac{a^2}{R^2}\right)$$

$$R/a = 3 \quad b/a = 5/3$$

$$\beta_c[\%] = 15 \frac{l_i}{q_{95}}$$

**Highest beta achieved : 12.5% (DIII-D)**

# Micro-Instabilities

Finite Larmor radius and kinetic dissipation effects,
where wavelength comparable to ion gyro radius
--> fine scale plasma turbulence
--> anomalous plasma transport in tokamaks

Different roles due to different mass
: drive or damp instabilities

- Dissipative microinstability : caused by dissipation either from collisions or from Landau resonance
- Reactive microinstability : ion temperature gradient mode

# Simple Model for Micro-Instabilities

- Toroidal geometry : large aspect ratio, circular cross section, low β tokamak equilibrium
  - independent poloidal and toroidal mode numbers
  - curvature drifts couple the poloidal harmonics
- Slab model when curvature drifts are not important

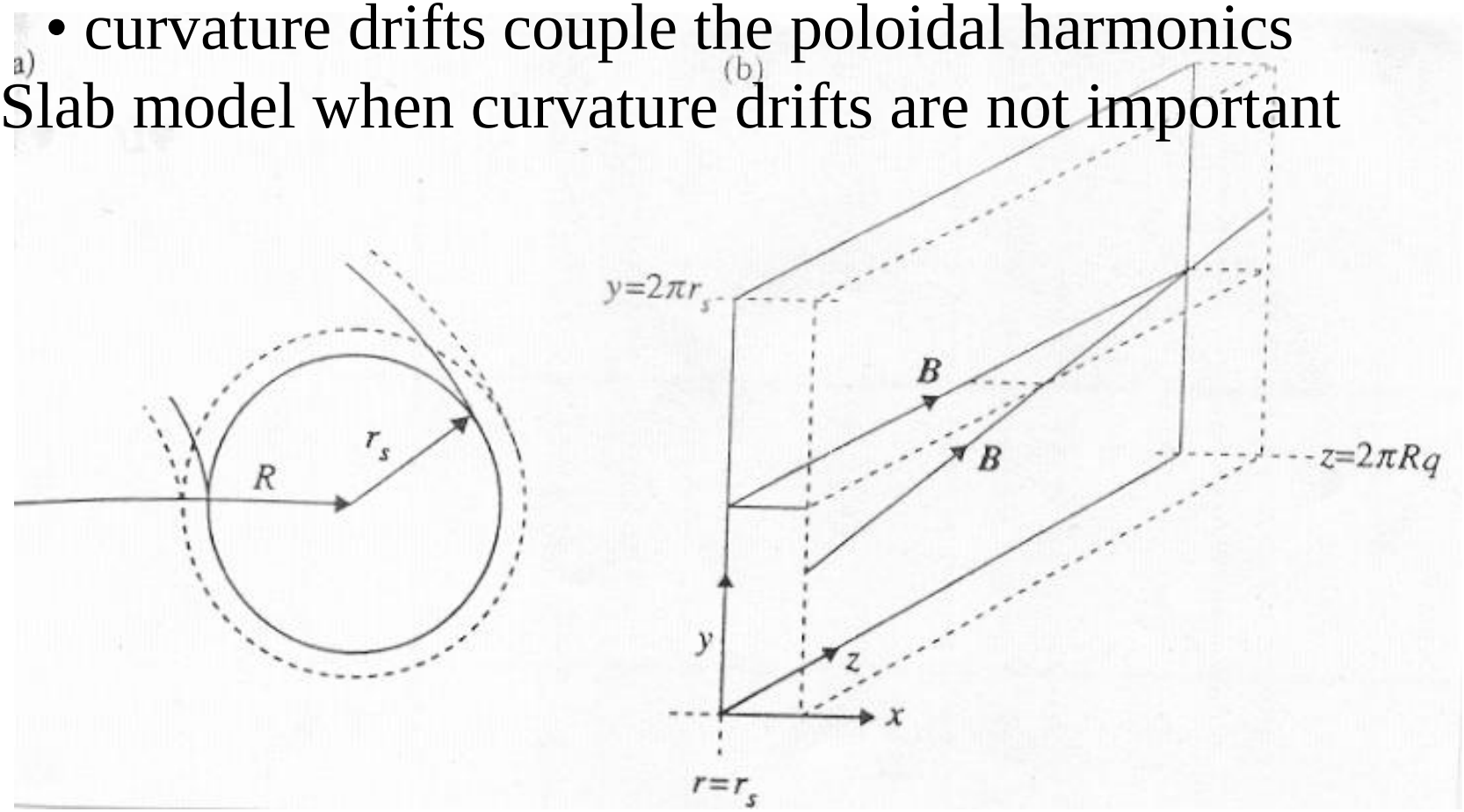

# Microinstabilities

Plasma waves and their associated instabilities

- Electron drift wave : ‘Universal’, trapped electron
- Sound wave : Ion temperature gradient
- Alfven wave :  Micro-tearing

- Electrostatic instabilities : drift wave instabilities
  - Passing particle instabilities
  - Trapped particle instabilities
- Electromagnetic instabilities : Micro-tearing modes

# Electron Drift Wave

Force balance $-ne\vec{E}_{//} - \nabla_{//} p_e = 0$

linearize $\tilde{n}_e / n_e = e\varphi / T_e$

⟶ ExB drift wave

from diamagnetic drift $\vec{v}_{dj} = \vec{B} \times \nabla p_j / n_j B^2$

$$\frac{\partial n_i}{\partial t} = -\nabla \cdot n_i \vec{v}_{di} \qquad i\omega \tilde{n}_i = \tilde{v}_{ex} \frac{dn}{dx} = -\frac{1}{B} \frac{\partial \tilde{\varphi}}{\partial y} \frac{dn}{dx}$$

**electron diamagnetic frequency**

$$\omega = \omega_{*e} = -\frac{k_y T_e}{eBn} \frac{dn}{dr}$$

**Electron drift mode**

- **destabilized by electron disspations either by collisions or Landau damping**
- **stabilized by shear damping**
- **destabilized by trapped electrons**

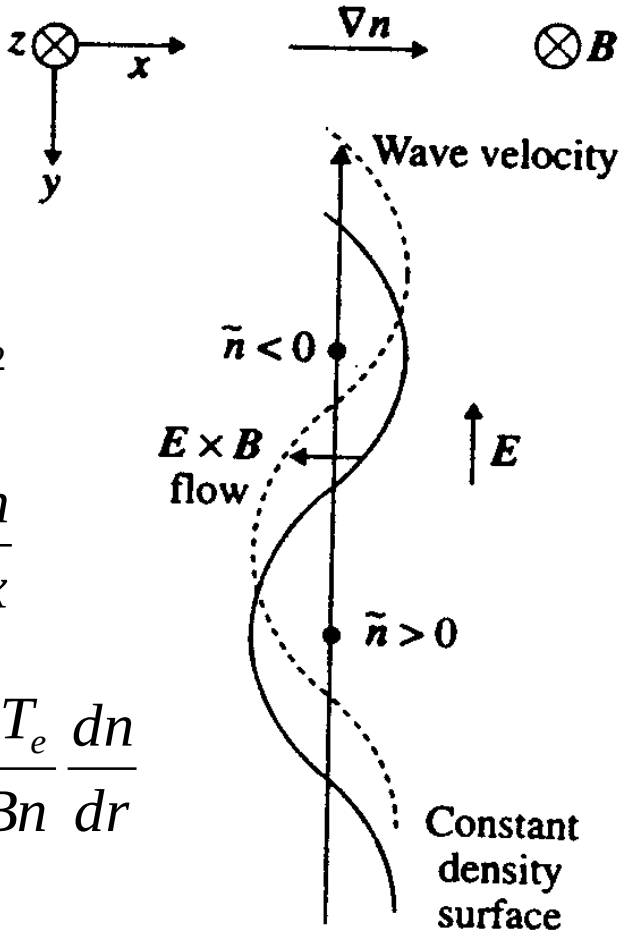


**Fig. 8.2.1** Movement of the constant density surface due to the $E \times B$ motion in an electron drift wave, represented by the full curve at an initial time and the dashed curve at a later time.

**universal instability**

# Passing Particle Instabilities

- Electron drift mode
- Ion temperature gradient (ITG) mode : $\eta_i$ mode
- $\eta_e$ mode

**Dispersion relation from gyro-kinetic equation**

Negligible trapped particle effects $\omega >> \omega_{bj}$ $k_{//} v_{Te} >> \omega >> k_{//} v_{Ti}$

$\tilde{n}_e / n_e = e\varphi / T_e$ Boltzman relation

$\omega_{di} = 2\varepsilon_n \omega_{*e} << \omega$ Slow ion magnetic curvature drift

$\varepsilon_n = L_n / R$ with the density scale length $L_n = (d \ln n / dr)^{-1}$

Perturbed ion distribution function with finite ion Larmor radius effects

$$f_i = -\frac{e\tilde{\varphi}}{T_i} f_M + g \exp[\frac{ik_\perp v_\perp}{\omega_{ci}} \sin\alpha_g]$$

gyro-kinetic equation

$$v_{//} \frac{\partial g}{\partial l} - i(\omega - \vec{k}\cdot\vec{v}_d) g - i\frac{e\tilde{\varphi}}{m_i} J_o(z)[\frac{k_\theta}{\omega_{ci}} \frac{df_M}{dr} + \omega \frac{df_M}{dK}] = 0$$

# Passing Particle Instabilities

With equilibrium drift velocity of grad B and curvature, G-K eqn

$$-v_{//}\frac{\partial g}{\partial l}+i(\omega-\bar{\omega}_{di})g=i\frac{e\tilde{\varphi}}{T_i}J_o(z)(\omega-\omega_{*i}^{T})f_M \qquad \bar{\omega}_{di}=\vec{k}\cdot\vec{v}_d$$

$$\eta_i=nT_i'/T_in' \qquad \omega_{*i}^{T}=\omega_{*i}[1+(\frac{v^2}{2v_{Ti}^2}-\frac{3}{2})\eta_i]$$

$$\longrightarrow \quad \{\rho_i^2\frac{\partial^2}{\partial x^2}-(\frac{\varepsilon_n}{b^{1/2}\tau q\Omega})^2(\frac{\partial}{\partial\theta}+ik_\theta sx)^2$$

$$-\frac{2\varepsilon_n}{\tau\Omega}(\cos\theta+\frac{i\sin\theta}{k_\theta}\frac{\partial}{\partial x})-(\frac{\Omega-1}{\tau\Omega+(1+\eta_i)}+b)\}\tilde{\varphi}=0$$

for $\eta_i>>1$ • for weak toroidal coupling $\omega\sim(k_{//}^2v_{Ti}^2\omega_{*i}\eta_i)^{1/3}$

slab branch of $\eta_i$ mode evolves from sound wave

$\omega\sim(i\varepsilon_n s\eta_i/q)^{1/2}\omega_{*i}$ for a sheared slab

• for strong toroidal coupling

$\omega\sim(\eta_i\omega_{*i}\omega_{di})^{1/2}$ toroidal branch of $\eta_i$ mode

for $\Omega=\omega/\omega_{*e}\sim 1$

• slab branch of electron drift mode $\omega\sim\omega_{*e}$

# Energy Flow for the Electron Drift Mode

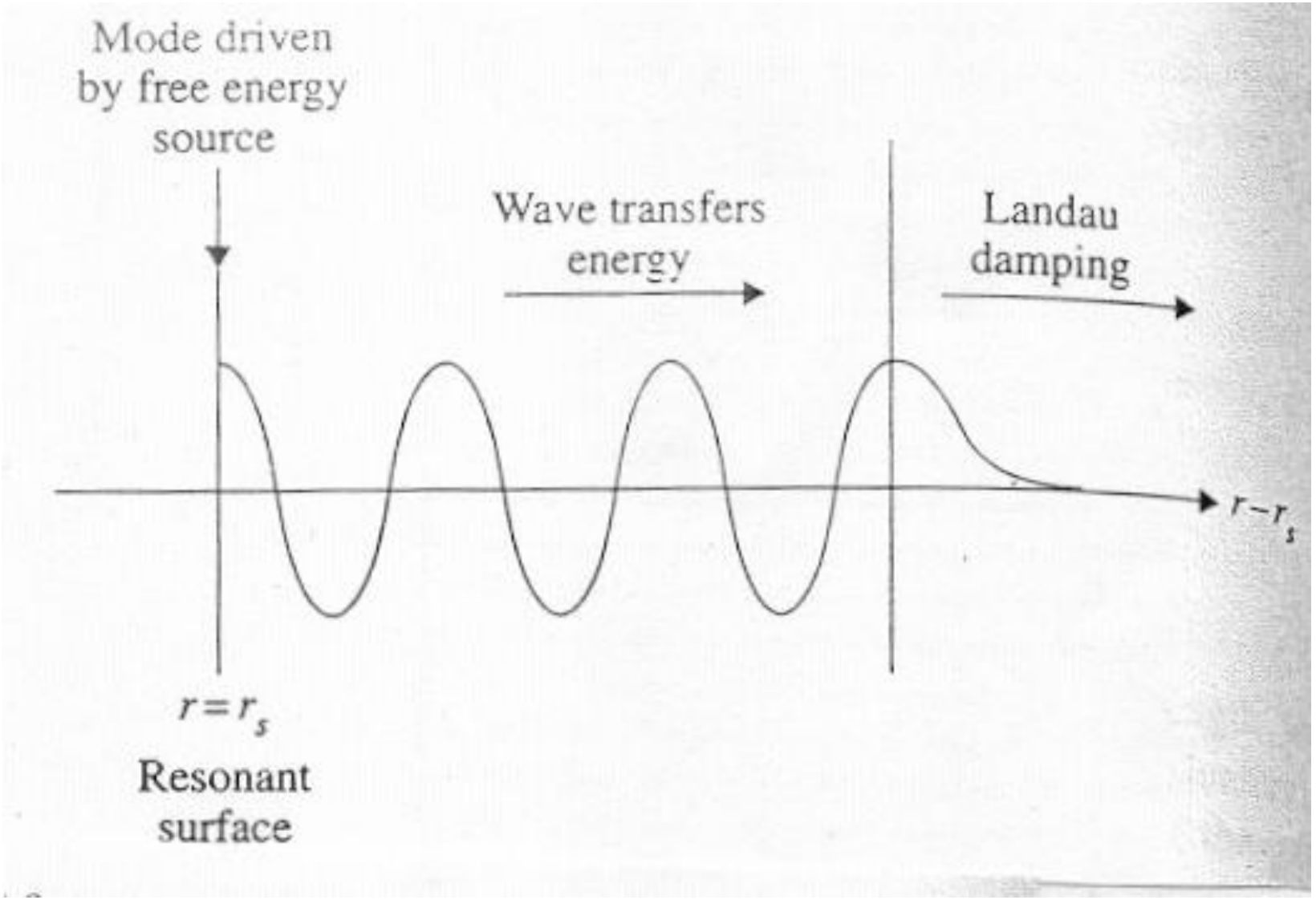

# Electron Drift Mode

Potential hill and
strong shear damping

Local well and
less effective shear damping

Electron drift wave is generally more unstable in a toroidal plasma than in the slab

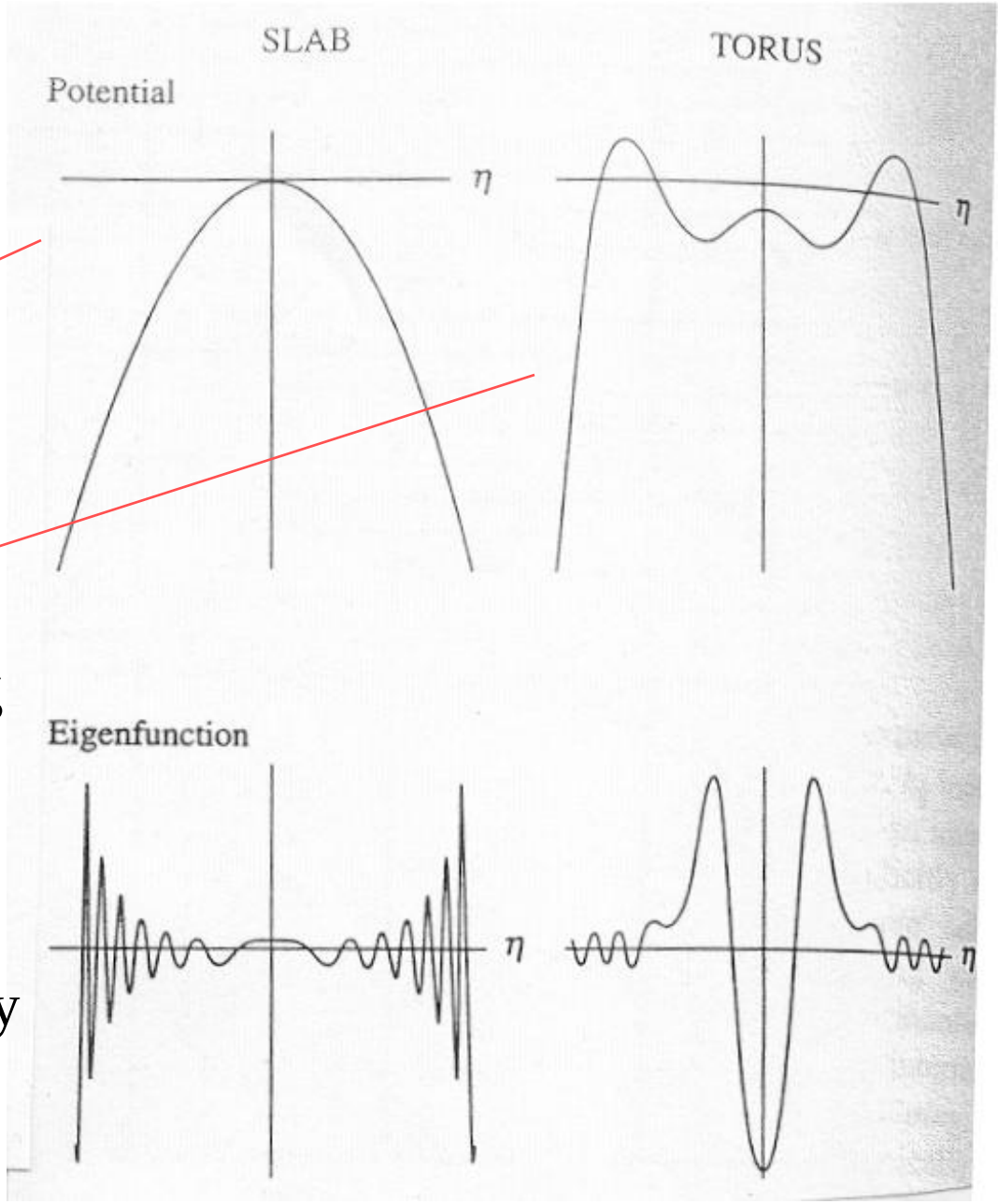

# $\eta_i$ or ITG mode

Slab and toroidal branches

Confined mode structure with a potential well --> suppress shear damping

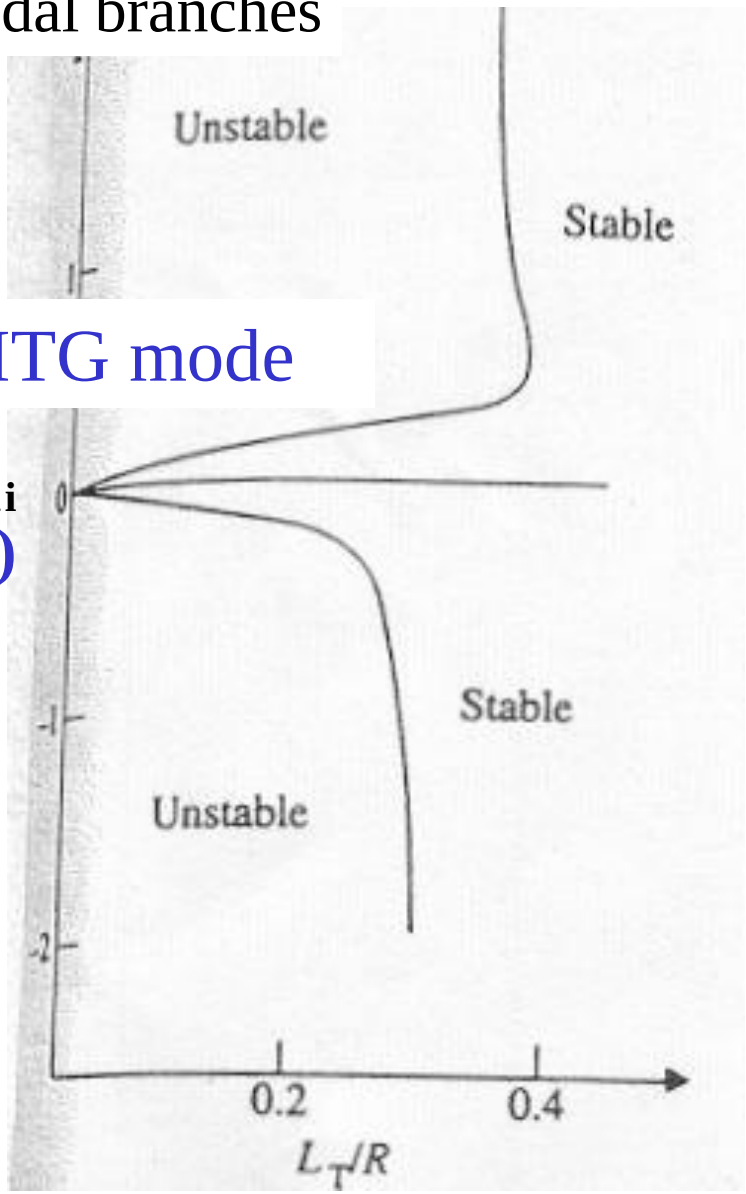


## Stability diagram for the toroidal ITG mode

**Growth rate depends on the value of $\eta_i$ ($\eta_i$ mode)**

$$\eta_i < \eta_{ic} \sim 1 \quad \text{stable}$$

$$\eta_{ic} = \begin{cases} 1.2 & \varepsilon_n < \varepsilon_{nc} \\ \frac{4}{3}(1+\tau^{-1})(1+2s/q)\varepsilon_n & \varepsilon_n > \varepsilon_{nc} \end{cases}$$

$$\varepsilon_{nc} = \frac{0.9}{(1+\tau^{-1})(1+2s/q)}$$

**For flat density, ion temperature gradient determine the instability (ITG mode)**

# Trapped Particle Instabilities

- Collisionless trapped particle mode
- Dissipative trapped particle mode : collision dependent, dangerous

**Physical mechanism of collisionless trapped particle mode** :
trapped particles are trapped between magnetic mirrors and spend most time in the bad curvature region --> flute-like modes

- charge polarization due to the curvature drift of the trapped particles
- local electric fields from polarization drive small scale ExB flows
- enhance the initial perturbations and lead to instability

From drift kinetic equation,

$$\omega^2 = \overline{\omega}_{de}(\overline{\omega}_{de} + \sqrt{2\varepsilon}\omega_{*e})$$

$\sqrt{2\varepsilon}R/L_n > 1$ : unstable for $\overline{\omega}_{de} < 0$

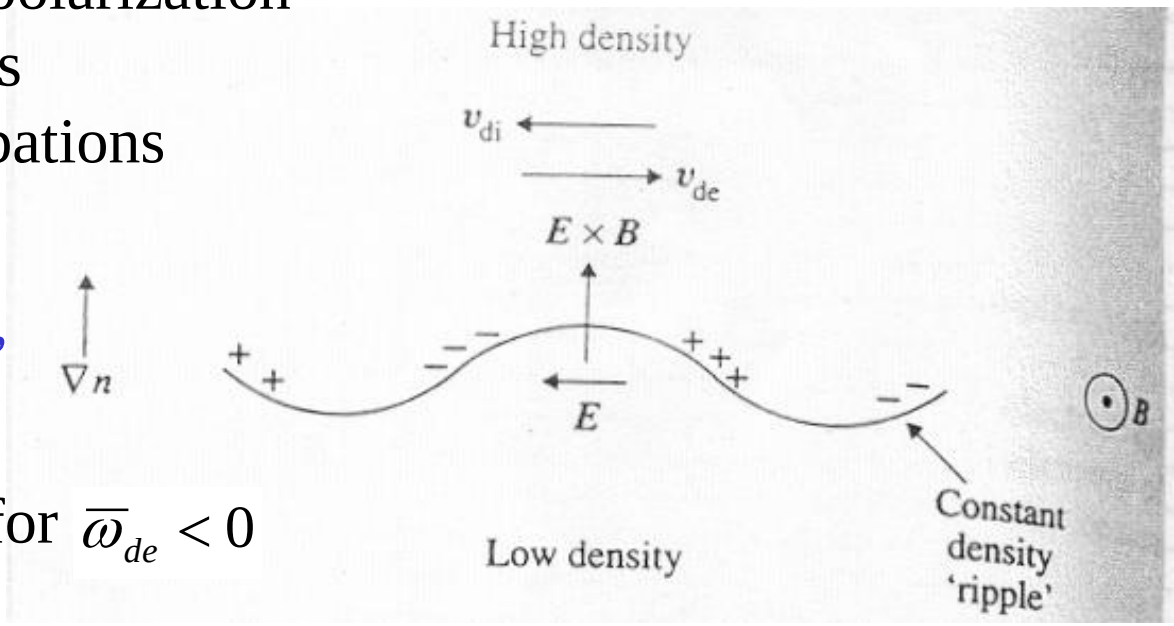

# Dissipative Trapped Particle Instabilities

• Effective collision frequency be the same order as the relevant drift frequency : trapped particle may be scattered into passing, etc

• trapped ion mode : dissipative version of collisionless mode, stabilizing ion collisions and destabilizing electron collisions

• dissipative trapped electron mode : stability only by trapped electrons i.e. the trapped electron collisions and an electron temperature gradient

• collision frequency not too high, i.e. $\nu_j < \varepsilon\omega_{bj}$

**Growth rate for the trapped ion mode**

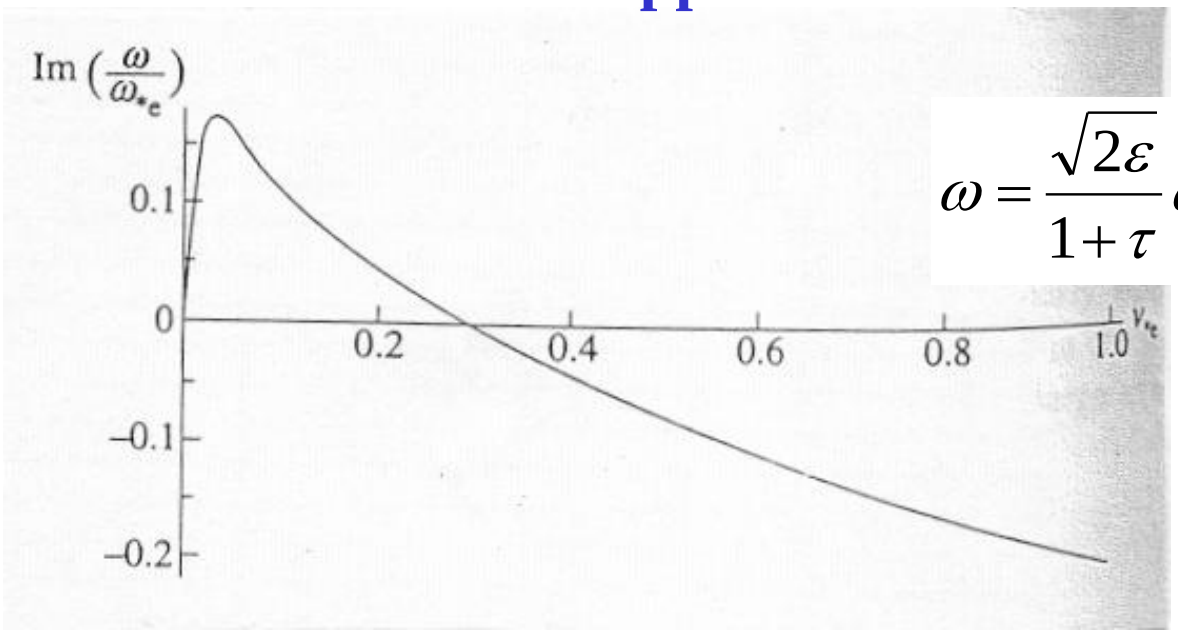


Stabilizing ion

$$\omega = \frac{\sqrt{2\varepsilon}}{1+\tau}\omega_{*e} - i\frac{\nu_i}{\varepsilon} + i\frac{\varepsilon^2}{(1+\tau)^2}\frac{\omega_{*e}^2}{\nu_e}$$

Destabilizing electron

# Micro Tearing Modes

Short wavelength with high poloidal mode number $\Delta' \cong -2m/r < 0$ Stable?

Two effects result in growth of magnetic perturbation to a saturated island

- nonlinear effect of island structure can modify equilibrium and particle drifts
- kinetic effects : electron temperature gradient in a sufficiently collisional plasma

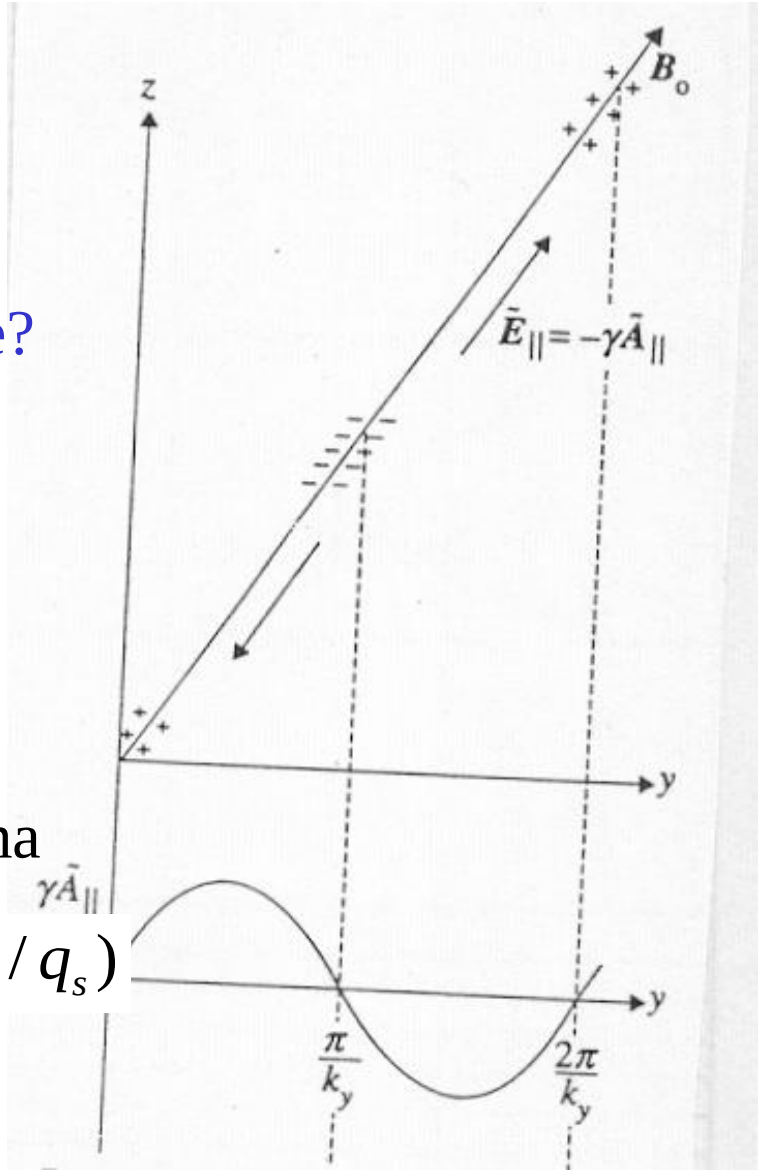


$$\frac{\partial^2 A_{//}}{\partial x^2} = -\mu_o j_{//} \qquad A_{//} = -\tilde{\psi} e^{-i\xi} e^{\gamma t} \qquad \xi = m(\theta - \phi/q_s)$$

$$B_r = (im/r) A_{//}$$

$$E_{//} = -\gamma A_{//} \qquad E_{//} = -\gamma A_{//} - ik_{//}\varphi$$

$$\begin{cases} v_{//} > \omega / k_{//} & \text{Electron 'short out'} \quad i\gamma A_{//} \cong k_{//}\varphi \\ \text{Current only flows for} \quad \omega / k_{//} v_{//} > 1 & k_{//} = (m/r)x/L_s \end{cases}$$

# Linear Micro Tearing Modes

$$\Delta' = \frac{1}{A_{//}^{out}}\left[\left.\frac{\partial A_{//}^{out}}{\partial x}\right|_{r=r_s^+} - \left.\frac{\partial A_{//}^{out}}{\partial x}\right|_{r=r_s^-}\right]$$

$$= \frac{-\mu_o j_{//} d}{A_{//}^{out}} = \frac{-2m}{r}$$

$$\frac{\partial^2 A_{//}}{\partial x^2} = -\mu_o j_{//} \qquad A_{//}^{out} \sim r^{\pm m}$$

In 'semi-collisional' regime

$$n v_{//} = D_e k_{//} n = (v_{Te}^2 / \nu_e) k_{//} n$$

$$k v_{//} = k_{//}^2 v_{Te}^2 / \nu_e = k_y^2 d^2 v_{Te}^2 / L_s^2 \nu_e = \gamma$$

$$j_{//} = E_{//} / \eta = -\gamma A_{//} / \eta$$

Growth rate

$$\gamma \sim \gamma_o^{2/3} \nu_e^{1/3} \qquad \gamma_o \sim \frac{k_y v_{Te} \Delta'}{L_s}\left(\frac{c}{\omega_{pe}}\right)^2$$

**Growth rate calculated numerically**

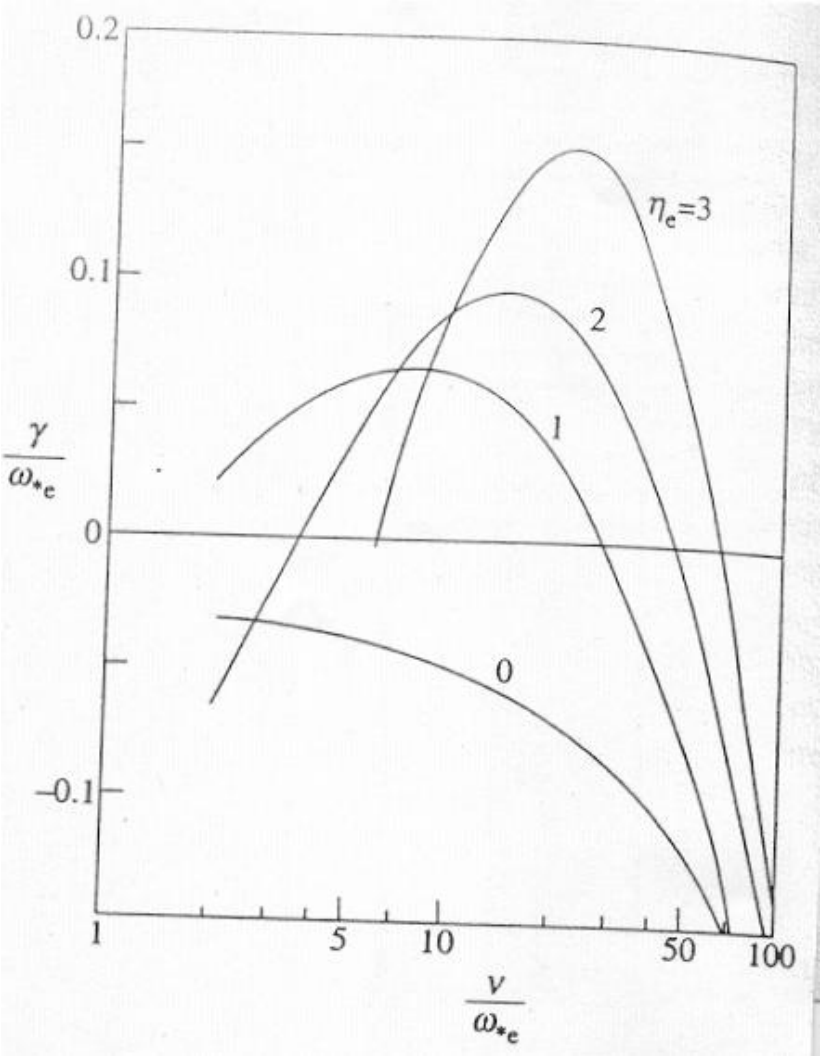


Collisionless growth rate

# Growth Rate for Micro Tearing Modes

An approximate analytical form for the growth rate in the ‘semi-collisional’ regime

$$\frac{\gamma}{\omega_{*e}} = \left[\frac{2\Gamma(17/4)}{\sqrt{\pi}\Gamma(11/4)}\right]\frac{\eta_e(1+5\eta_e/4)}{\nu_e/\omega_{*e}}$$

$$+\left[\frac{3}{8\sqrt{2}\pi^{1/4}\Gamma(11/4)}\right]\frac{\Delta'}{\rho_e}\left(\frac{c}{\omega_{pe}}\right)^2\left(\frac{L_n}{L_s}\right)\frac{(\nu_e/\omega_{*e})^{1/2}}{(1+5\eta_e/4)^{1/2}}$$

## non-Maxwellian distributions

If an electron beam is injected into a plasma, the beam represents a bump on the high-energy tail of the electron velocity distribution function as shown in Fig. 8E1. The region where $(\partial f/\partial v)>0$ is highly unstable to generation and amplification of electron plasma waves with $k \sim \omega/v_b$, $\omega \simeq \omega_{pe}$.

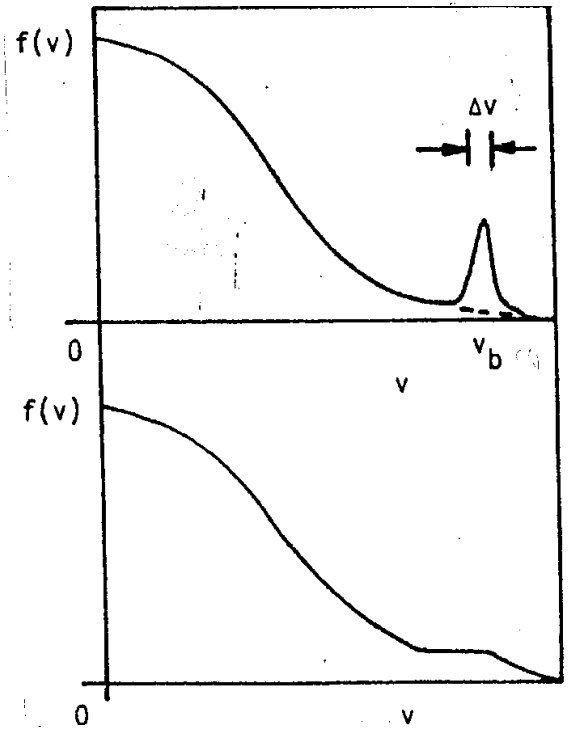


*Fig. 8E1. A one-dimensional Maxwellian electron velocity distribution (top) with a bump due to an injected electron beam, and the formation of a plateau (bottom).*

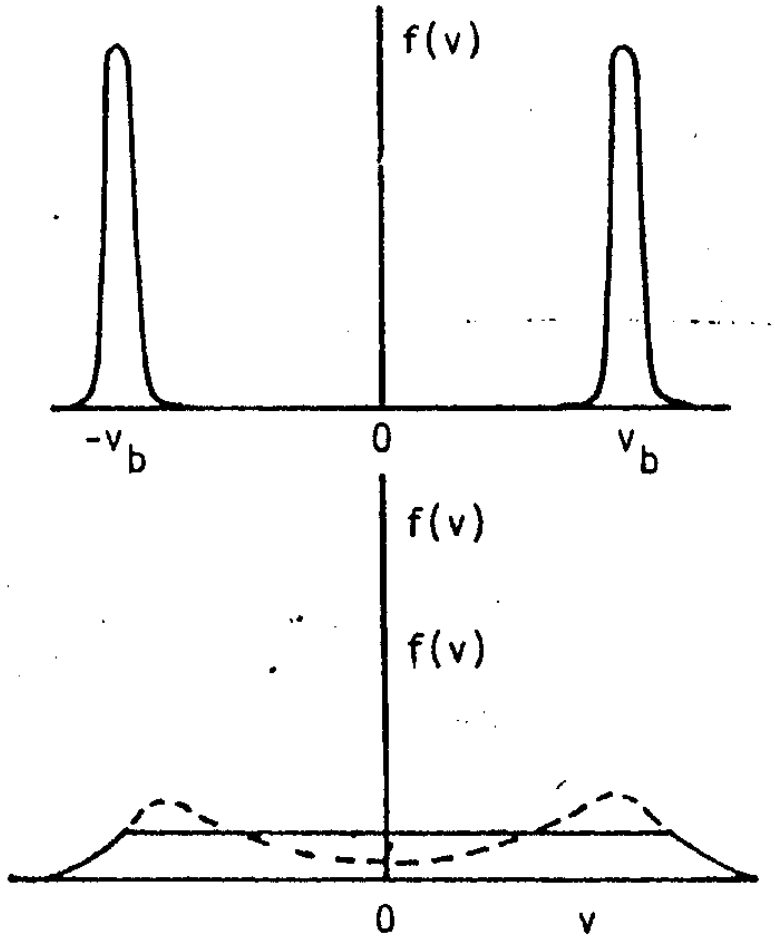


*Fig. 8E2. The two-stream instability. Initial condition (top), intermediate stage (bottom, dashed curve), plateau (bottom, smooth curve).*

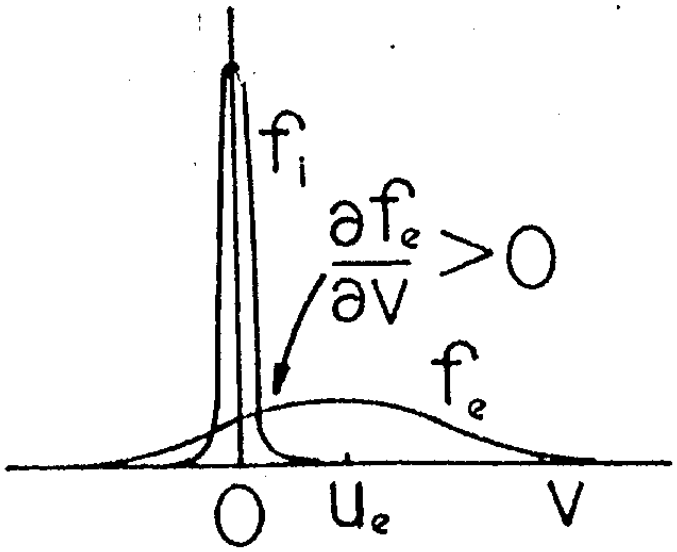


*Fig. 8E3. Ion and electron velocity distribution functions for case in which ion acoustic instability may occur.*

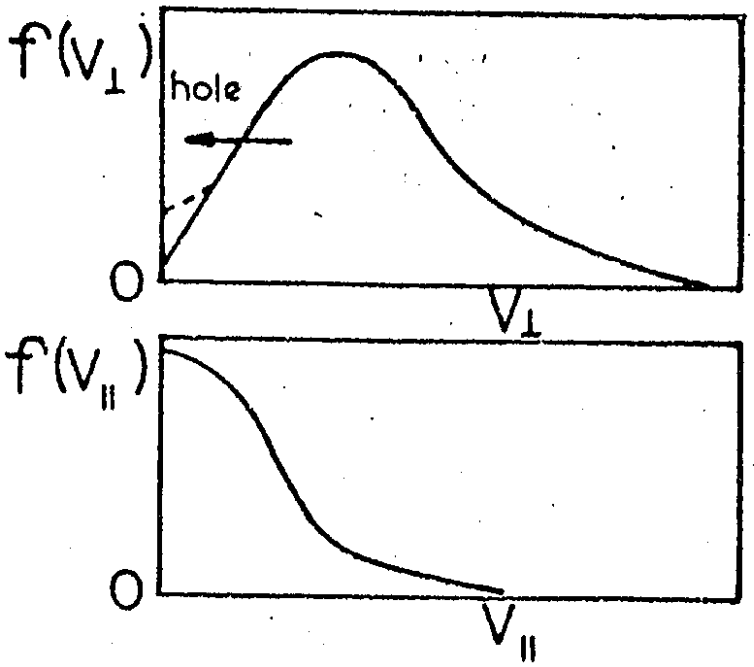


*Fig. 8E4. A "mirror loss cone" distribution.*